ผลของอนุภาคนาโนซิลิกาดัดแปรต่อสมบัติเชิงกลของยางธรรมชาติ

นายอดิศักดิ์ ชัยธานี

วิทยานิพนธ์นี้เป็นส่วนหนึ่งของการศึกษาตามหลักสูตรปริญญาวิทยาศาสตรดุษฎีบัณฑิต
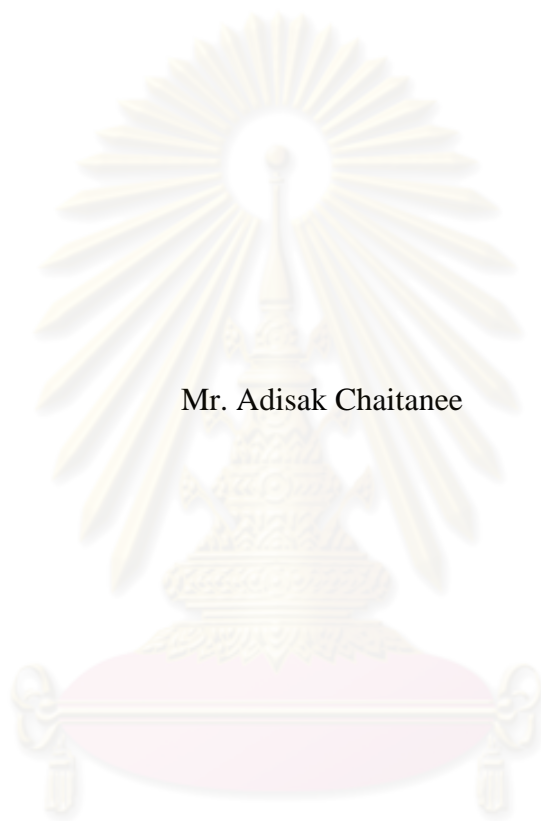สาขาวิชาเคมี   ภาควิชาเคมี
คณะวิทยาศาสตร์ จุฬาลงกรณ์มหาวิทยาลัย
ปีการศึกษา 2553

EFFECTS OF MODIFIED SILICA NANOPARTICLES ON MECHANICAL
PROPERTIES OF NATURAL RUBBER

Mr. Adisak Chaitanee

A Dissertation Submitted in Partial Fulfillment of the Requirements
for the Degree of Doctor of Philosophy Program in Chemistry
Department of Chemistry
Faculty of Science
Chulalongkorn University
Academic Year 2010
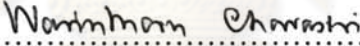
Thesis Title   EFFECTS OF MODIFIED SILICA NANOPARTICLES
                      ON MECHANICAL PROPERTIES OF NATURAL
                      RUBBER
By   Mr. Adisak Chaitanee
Field of Study   Chemistry
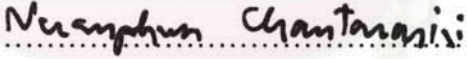Thesis Advisor   Assistant Professor Warinthorn Chavasiri, Ph.D.

Accepted by the Faculty of Science, Chulalongkorn University in Partial
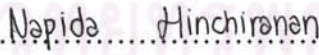Fulfillment of the Requirements for the Doctoral Degree

.....................................Dean of the Faculty of Science
(Professor Supot Hannongbua, Dr.rer.nat.)

THESIS COMMITTEE

.... Chairman
(Associate Professor Sirirat Kokpol, Ph.D.)

.... Thesis Advisor
(Assistant Professor Warinthorn Chavasiri, Ph.D.)

.... Examiner
(Associate Professor Nuanphun Chantarasiri, Ph.D.)

.... Examiner
(Assistant Professor Napida Hinchiranan, Ph.D.)

.... External Examiner
(Associate Professor Ittipol Jangchud, Ph.D.)

4973859823   : MAJOR CHEMISTRY
KEYWORDS :   NATURAL RUBBER / SILICA NANOPARTICLES / GRINDING

ADISAK CHAITANEE: EFFECTS OF MODIFIED SILICA NANOPARTICLES ON MECHANICAL PROPERTIES OF NATURAL RUBBER. ADVISOR: ASST.PROF. WARINTHORN CHAVASIRI, Ph.D., 148 pp.

A new material, silica-filled rubber nanocomposite can be prepared from acid coagulation of the mixture of nanosilica slurry and natural rubber latex. By employing wet grinding process of conventional silica with grinding machine, nanosilica slurry can be formed. This efficient preparation method produces nanosilica slurry within a short time and in very large amount per batch. The selected modifying agents were silane coupling agents, polymer with low molecular weight and derivatives of polyethylene glycol. The effects of type and amount of treating agents on mechanical properties such as tensile strength, tear strength, elongation at break and abrasion resistance of natural rubber/silica nanocomposites were investigated. These coupling agents provided the dispersibility of silica nanoparticles in natural rubber. The silane coupling agents could form strong chemical bond with silanol groups of silica nanoparticles and double bonds in natural rubber. Moreover, the larger amount of treating agents in natural rubber/silica nanocomposite affected curing behavior by reducing both scorch time and cure time. Furthermore, the natural rubber/silica nanocomposites prepared from this method can decrease air pollution by using small amount or absence of silica powder in mixing process to prepare rubber compounding.

Department : _____Chemistry_____   Student's Signature _Adisak Chaitanee_

Field of Study : _____Chemistry_____   Advisor's Signature _W. Chavasiri_

Academic Year : _____2010_____

อดิศักดิ์ ชัยธานี : ผลของอนุภาคนาโนซิลิกาดัดแปรต่อสมบัติเชิงกลของยางธรรมชาติ. (EFFECTS OF MODIFIED SILICA NANOPARTICLES ON MECHANICAL PROPERTIES OF NATURAL RUBBER) อ. ที่ปรึกษาวิทยานิพนธ์หลัก: ผศ.ดร. วรินทร ชวศิริ, 148 หน้า.

ได้เตรียมวัสดุนาโนเชิงประกอบชนิดใหม่จากกระบวนการจับตัวด้วยกรดของของ ผสมอนุภาคนาโนซิลิกาแขวนลอยกับยางธรรมชาติเลเท็กซ์ อนุภาคนาโนซิลิกาแขวนลอย เตรียมจากกระบวนการบดแบบเปียกของอนุภาคซิลิกาที่มีขายทั่วไปด้วยเครื่องบดอนุภาค วิธีนี้ เป็นวิธีที่มีประสิทธิภาพในการเตรียมนาโนซิลิกาแขวนลอย ใช้เวลาสั้นและสามารถเตรียมได้ ในปริมาณมาก สารดัดแปรพื้นผิวอนุภาคนาโนซิลิกาที่ใช้ ได้แก่ สารคู่ควบไซเลน พอลิเมอร์ที่ มีน้ำหนักโมเลกุลต่ำและอนุพันธ์ของพอลิเอทิลีนไกลคอล เพื่อศึกษาผลกระทบต่อสมบัติ เชิงกลของวัสดุนาโนเชิงประกอบของอนุภาคนาโนซิลิกากับยางธรรมชาติ เช่น ความต้านทาน ต่อแรงดึง ความต้านทานต่อแรงเฉือน ความยืดสูงสุด ณ จุดขาด และความต้านทานการขัดถู เป็นต้น ได้ศึกษาชนิดและปริมาณของสารดัดแปรพื้นผิว พบว่าสามารถช่วยปรับปรุงการ กระจายตัวของอนุภาคนาโนซิลิกาในยางธรรมชาติ โดยเฉพาะสารคู่ควบไซเลนสามารถสร้าง พันธะเคมีที่แข็งแรงกับหมู่ไซลานอลของอนุภาคนาโนซิลิกาและพันธะคู่ในโมเลกุลของยาง ธรรมชาติจึงส่งผลให้ได้สมบัติเชิงกลของยางธรรมชาติดีที่สุด และยังพบว่าเมื่อเพิ่มปริมาณสาร ดัดแปรพื้นผิว ส่งผลให้เวลาในการบ่มยางสั้นลง นอกจากนั้นวัสดุนาโนเชิงประกอบของ อนุภาคนาโนซิลิกากับยางธรรมชาติซึ่งเตรียมด้วยวิธีนี้ยังช่วยลดมลภาวะทางอากาศโดยลด ปริมาณการใช้ผงซิลิกาในการเตรียมยางคอมพาวนด์

ภาควิชา...........เคมี...........ลายมือชื่อนิสิต..

สาขาวิชา...........เคมี...........ลายมือชื่อ อ.ที่ปรึกษาวิทยานิพนธ์หลัก.........................

ปีการศึกษา ....2553............

ACKNOWLEDGEMENTS

CONTENTS

ศูนย์วิทยทรัพยากร

จุฬาลงกรณ์มหาวิทยาลัย

LIST OF TABLES

ศูนย์วิทยทรัพยากร

จุฬาลงกรณ์มหาวิทยาลัย

LIST OF FIGURES

LIST OF ABBREVIATIONS

ca.	Approximately
dN/m	Decinewton per meter
$^{\circ}$C	Degree Celsius
$^{\circ}$C/min	Degree Celsius per minute
g	Gram (s)
g/cm^3	Gram (s) per cubic centimeter
Kg	Kilogram (s)
L	Liter (s)
MPa	Megapascals
μm	Micrometer (s)
m/s	Millimeter per second
mg	Milligram (s)
min	Minute (s)
mm	Millimeter
mm/min	Millimeter (s) per minute
mm^3	Cubic millimeter
ms	Millisecond (s)
N/mm	Newton per millimeter
nm	Nanometer (s)
phr	Parts by weight per one hundred grams of rubber
%	Percent

xx

%wt	Percent by weight
rpm	Round per minute (s)
sec	Second (s)
E′	Storage modulus
A	Abrasion loss
ASTM	American society for testing and materials
AMEO	3-Aminopropyl triethoxysilane
BA	Butyl acrylate
BET	Brunauer-Emmett-Teller
BR	Butadiene rubber or polybutadiene
CBS	*N*-Cyclohexyl-2-benzothiazolesulfenamide
CR	Chloroprene rubber or polychloroprene
CRI	Crystallization rate index
DBP	Dibutylphthalate
DI	Deionized water
DIN	Deutsches institut für normung
DMAs	Dynamic mechanical analysis
DRC	Dry rubber content
Eb	Elongation at break
Glyeo	3-Glycidyloxypropyl triethoxysilane
IR	Isoprene rubber or polyisoprene
JIS	Japanese industrial standards
M300	Modulus at 300% elongation
MAA	Methacrylic acid

MDR	Moving die rheometer
MEMO	3-Methacryloxypropyl triethoxysilane
MH	Maximum torque
ML	Minimum torque
MTMO	3-Mercaptopropyl trimethoxysilane
NMR	Nuclear magnetic resonance
NR	Natural rubber
NRL	Natural rubber latex
PEG	Polyethylene glycol
PMMA	Poly(methyl methacrylate)
PPG	Polypropylene glycol
PS-*b*-PMMA	Polystyene-*block*-poly(methyl methacrylate) copolymer
PVC	Polyvinylchloride
PVDF	Poly(vinylidene fluoride)
SBR	Styrene butadiene rubber
SEM	Scanning electron microscopy
Si-69	*Bis*-(3-triethoxysilylpropyl)tetrasulfide
SIC	Strain induced crystallization
SiC	Silicon carbide
SMA	Styrene maleic anhydride copolymer
SSA	Specific surface area
t_c90	Optimum cure time
t_s2	Scorch time
tan δ	Loss tangent

TEM	Transmission electron microscopy
TEOS	Tetraethoxysilane
TMTD	Tetramethylthiuram disulfide
TS	Tensile at break
UV	Ultraviolet
WAXD	Wide angle X-ray diffraction
wt	Weight (s)

CHAPTER I

INTRODUCTION

1.1 Background

In rubber industry, the reinforcing fillers are introduced into rubber matrix to improve the mechanical properties of rubber for example carbon black, silica, Kaolin clay, Talc and calcium carbonate [1]. The primary reinforcing filler for many rubber compounds is carbon black and, secondary, silica powder. Carbon black is used for black rubber products while silica is popular in color rubber products. In the last decade, silica particle has been intensively used for reinforcing rubber compounds, especially in outsole product. In addition, many products utilize silica particles together with carbon black. The silica particles contain the silanol groups on their surface including isolated, vicinal and geminol silanol groups. The structures of silica particles and silanol groups are shown in Figure 1.1, whereas elastomers for example natural rubber (NR), isoprene rubber (IR), butadiene rubber (BR), chloroprene rubber (CR) and styrene butadiene rubber (SBR) are non polar materials, Figure 1.2.

Isolated silanol   Vicinal silanol   Geminal silanol
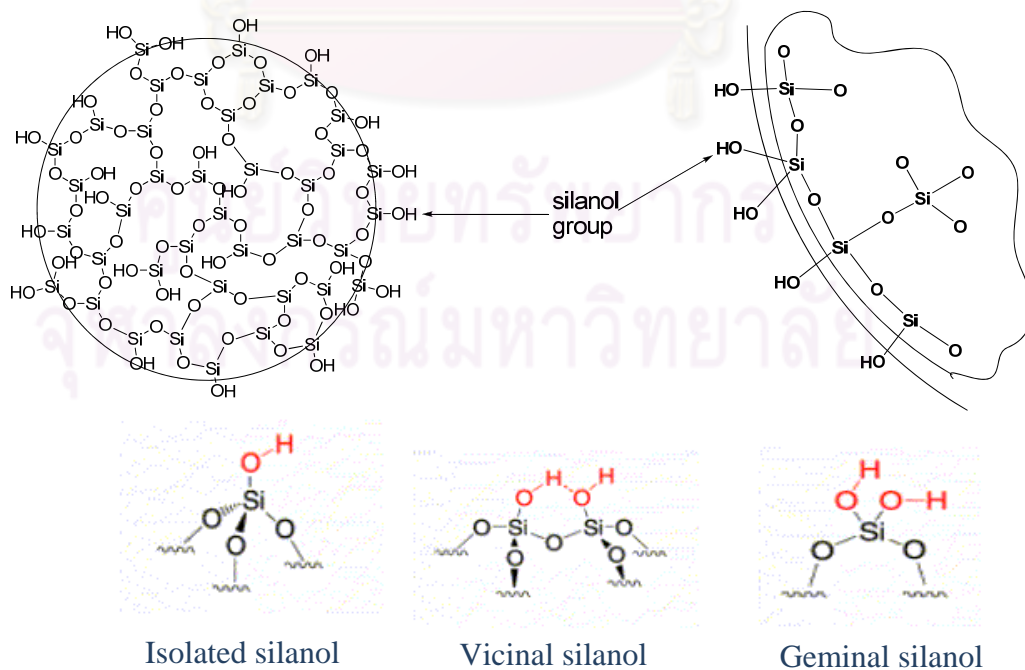
Figure 1.1 The structure of silica particles and their silanol groups
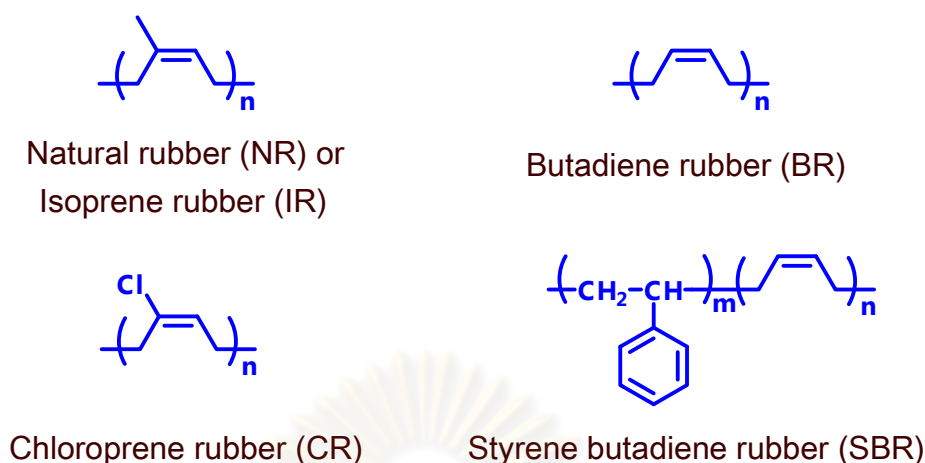
Figure 1.2 Structures of lipophilic rubbers.

Therefore, a major problem of silica reinforced rubber is the incompatibleness between hydrophilic silica and lipophilic rubbers. Silica surface silanols produce a low degree of silica-elastomer bonding, well known as filler-rubber or filler-elastomer interaction, which leads to low abrasion resistance, high elongation, low modulus and excessive heat build-up in silica-filled rubber compounds [2, 3]. Moreover, in a sulfur cross-linking system, a portion of soluble could be trapped by the reactive silica surface silanol, resulting in, the low cure states (reduced cross-linking density) and retarded the vulcanization reaction. Silica's cluster structure related to high viscosity during processing and higher hardness after curing [3]. The attempt to reduce silica surface energy and improve silica dispersion, many methods were examined to solve this problem such as using silane coupling agent, pretreated silica surface as reinforcing filler and sol-gel process to generate silica particle in the rubber matrix.

1.1.1 Using silane coupling agent

This method is suitable for conventional mixing process because the silane coupling agents can be added directly during the mixing process [4-6]. Silane coupling agent can act as the compatibilizer between hydrophilic silica and lipophilic rubber during the mixing process. It also improves the dispersing and reinforcing efficiency of silica reinforced rubber. Furthermore, silane coupling agent could precipitate in both sulfur and peroxide cross-linking reactions. The molecules of silane coupling agents consist of two functional active sites, the accessible hydrolysis

alkoxy groups and the organo-functional groups. The first one acts as reacting chemical with the silanol groups on silica surface to form stable siloxane linkages whereas the second one, which is relatively non-polar, is more compatible with rubber and also can participate with the vulcanizing agent to form chemical bonds with rubber chains.

1.1.2 Using pretreated silica surface as reinforcing filler

Pretreated silica surface with coupling agent such as fatty acid, silane coupling agent and polymeric coupling agent were used as reinforcing filler. The coupling agents were introduced to silica surface before mixing with rubber. This method provided low silica surface energy, resulting in, comfortable to introduce silica particles into rubber matrix [7-9].

1.1.3 Using sol-gel process to generate silica particle in the rubber matrix

The sol-gel process was performed to generate silica particle in the rubber matrix, well known as *in situ* process, in term of nanotechnology called "bottom-up process". The silica particles were synthesized on the basis of hydrolysis and condensation of tetraethoxysilane (TEOS) [10], Figure 1.3, within rubber matrix including styrene butadiene rubber (SBR) [11], isoprene rubber (IR) [12], natural rubber (NR) [13-16] and butadiene rubber (BR) [17]. In this method, silica particles were generated in the rubber matrix with small size, low aggregated form and good silica dispersion.

1.2 Theory and related works

1.2.1 Preparation of silica nanoparticles

In 2003, Mende and coworkers [18] reported the preparation of fused corundum (Al_2O_3) nanoparticles by using wet comminution process in stirred media mills. It was found that the ground product suspension was affected by pH, grinding media materials, grinding media sizes and electrostatic stabilization on the grinding process.

Hydrolysis $-Si-OEt$ + H_2O ⇌ $-Si-OH$ + $EtOH$

$-Si-OEt$ + OH^- ⇌ $-Si-OH$ + EtO^-

$\updownarrow$ H_2O

OH^- + $EtOH$

Alcohol Condensation $-Si-OEt$ + $HO-Si-$ ⇌ $-Si-O-Si-$ + $EtOH$

Water Condensation $-Si-OH$ + $HO-Si-$ ⇌ $-Si-O-Si-$ + H_2O

Overall reaction $EtO-Si(OEt)-OEt$ + $2H_2O$ ⇌ SiO_2 + $4EtOH$
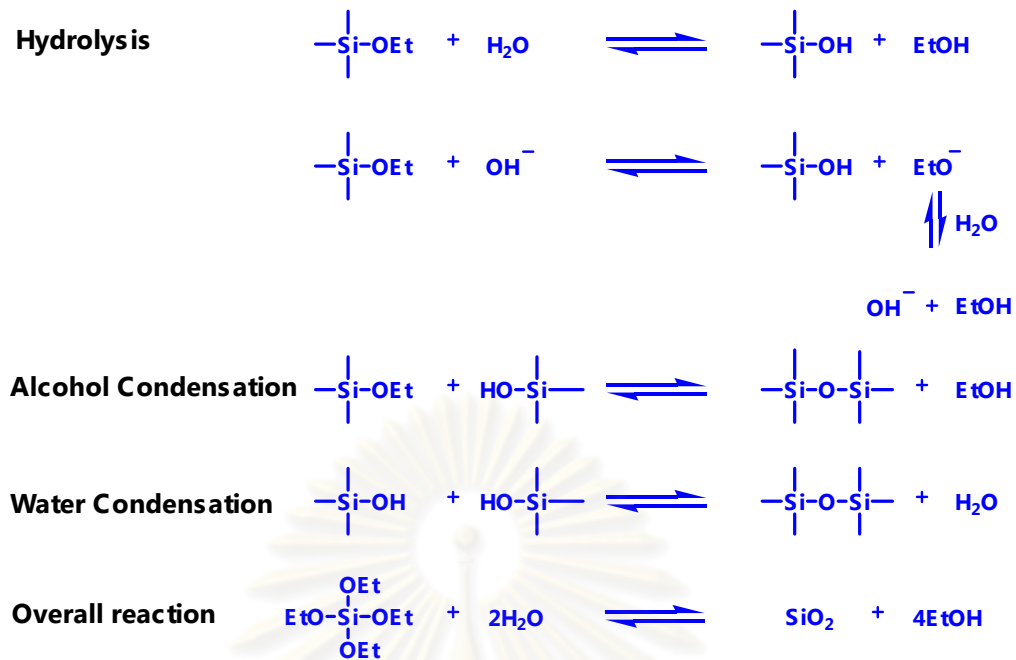
Figure 1.3 The mechanism to synthesize silica particle by sol-gel process [10].

In 2005, Stenger and coworkers [19] studied the comminution of alumina (Al_2O_3) and tin oxide (SnO_2) in stirred media mills. It was reported that the grinding media diameter, solid mass fraction and the stirrer tip speed were effect to comminution results.

In 2006, Wang and Forssberg [20] published the experimental results of the mechanical production of silica and carbonate and comparative study of two types of stirred bead mills, horizontal and vertical stir bead mills, Figure 1.4.

In 2007, Pérez-Rodríguez and coworkers [21] reported the comparative study of sonication and grinding on the comminution efficiency of pyrophyllite. The comparative study was focused on the particle size, particle size distribution, morphology and crystallization of comminution results.

In 2010, Chen and coworkers [22] published the preparation of villus-like polymethyl methacrylate/silica hybrids (PMMA/SiO_2 hybrids) via surface modification and wet grinding. It is evident that, a wet milling process was successfully utilized to comminute the aggregated silica powder to obtain a good colloidal stability.
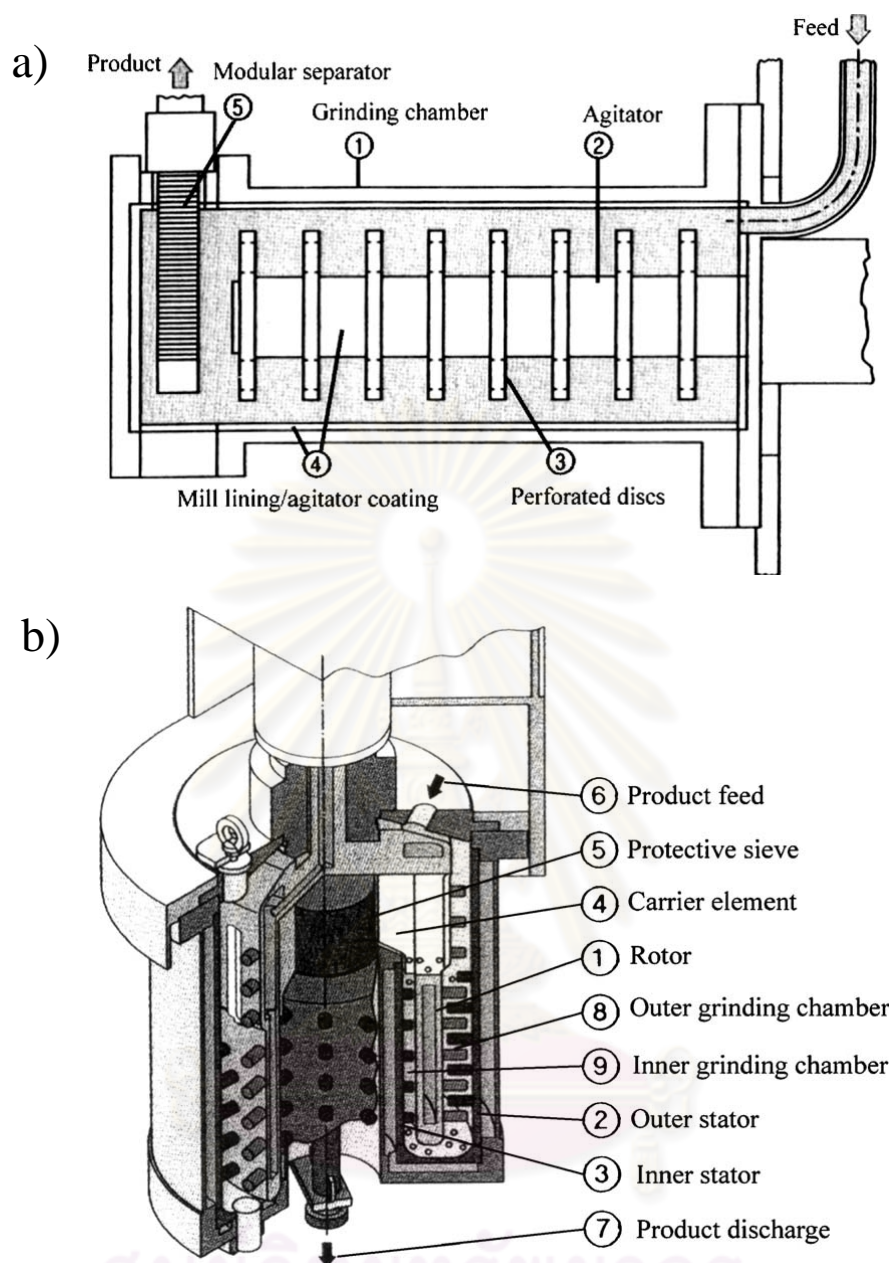
Figure 1.4 The stirred bead mills a) horizontal and b) vertical [20].

1.2.2 Surface modification of silica nanoparticles

In 2003, Bauer and coworkers [23] prepared the modified silica by using silane coupling agent. The surface modification of silica nanoparticles with silane coupling agent was refluxed in acetone for 2 hours and catalyzed by maleic anhydride. The modified silica dried and mixed with 1,6-hexandiol diacrylate and aliphatic urethane hexaacrylate. Then, the mixer was coated on plastic surface and polymerized by UV or electron beam to generate thin film coated plastic surface. The modified silica could improve scratch performance and abrasion resistance of thin film product.

In 2003, Park and Cho [24] studied the effect of surface modified silica nanoparticles on the properties of SBR. Silane coupling agents were used in this study including γ-amino propyl triethoxysilane, γ-chloropropyl trimethoxysilane and γ-methacryloxypropyl trimethoxysilane. It was found that the modified silica improved crosslink density, thermal stability, and mechanical properties of the SBR/silica composites, especially, γ-methacryloxypropyl trimethoxysilane showed superior crosslink density and thermal stability in these systems.

In 2003, Weng and Wei [25] modified titanium oxide (TiO$_2$) surface with cetyl trimethylammonium chloride and 3-methacryloyloxypropyl trimethoxysilane. Then, modified TiO$_2$ was introduced to polystyene-*block*-polymethyl methacrylate (PS-*b*-PMMA). It revealed that glass transition temperature (T$_g$) of PS-*b*-PMMA/TiO$_2$ was raised up.

In 2004, Sun and coworkers [26] studied the modification of silica nanoparticles by using silane coupling agent in DI water (5%) and methanol (95%) solution at 90°C. the modified silica nanoparticles was mixed with epoxy resin. Resulting in, the thermal stability of was increased. In addition, the contact angle of water of epoxy/silica nanocomposites was also raised up.

In 2005, Wada and coworkers [27] studied the effect of silane coupling agent in the thin film of acrylic resin/silica nanocomposites. A thin film that treated with silane coupling agent had better optical and hydrophilic properties than another that not treated with silane coupling agent.

In 2006, Sun and coworkers [28] prepared the surface modification of silica nanoparticles with γ-methylacryloxypropyl trimethoxysilane. Then it was blended with polyvinylchloride (PVC). The higher impact and tensile strength could be obtained from PVC/silica nanocomposites which present silane coupling agent.

In 2007, Guo and coworkers [29] investigated the preparation of copper oxide (CuO) nanoparticle filled vinyl-ester resin nanocomposites by using methacryloxypropyl trimethoxysilane as a surface modifying agent. It was found that the nanocomposite had better thermal stability and mechanical properties.

In 2007, Hong and coworkers [30] improved the tensile strength of PMMA/silica nanocomposites by using γ-methylacryloxypropyl trimethoxysilane as a modifying agent. The PMMA/silica nanocomposites were prepared by bulk polymerization of PMMA and modified silica nanoparticle.

In 2007, Song and coworkers [31] prepared the nanocomposite of poly(vinylidene fluoride) (PVDF) and three type of silica nanoparticles including amino silane treated, alkyl silane treated and untreated silica nanoparticles. The nanocomosite of PVDF mixed with amino silane modified silica had better thermal stability than that of PVDF mixed with alkyl silane treated and untreated silica.

In 2007, Zou and coworkers [32] prepared the nanocomposite via *in-situ* solution polymerization of butyl acrylate (BA) and methacrylic acid (MAA) with γ-methylacryloxypropyl trimethoxysilane treated silica nanoparticles. In was revealed that the thermal stability, water resistance, transparency and shear strength were enhanced.

From the literature reviews, it had not been seen that, the nanosilica-filled rubber was prepared by employing the nanosilica that generated via top-down process. The top-down process is one method to prepare nanomaterials by comminuting process such as attrition, milling, etching and etc. the other one, bottom-up process is the method to generate nanomaterials by synthesis or build-up a material from atom-by-atom, molecule-by-molecule, or cluster-by-cluster by employing chemical vapor deposition, electro-deposition, chemical reactions and etc. [33, 34]. Figure 1.4 displayed the comparison between bottom-up and top-down process to prepared nanoparticles.

This research was interested in the preparation of silica nanoparticles using stirred bead mill machine, well known as wet grinding process and a one type of top-down process. This process could produce small particle size, high stable and good dispersion of metal oxide nanoparticles in water media such as alumina, tin oxide, silica and titania [17-20, 35]. In addition, the particle size of grinding product was affected by grinding media size, it follows that, the smaller the used grinding media, the better is the comminution result. Moreover, styrene maleic anhydride (SMA) derivatives, silane coupling agent and polyethylene derivatives were investigated to

modify silica surface. Then, the untreated or treated silica slurry was mixed with natural rubber latex (NRL) having 20% dry rubber content (DRC) and coagulated by using 2.5% formic acid. The experimental designs were selected for screening their effects on the curing behavior and the mechanical properties of both uncured and cured NR/silica nanocomposites.
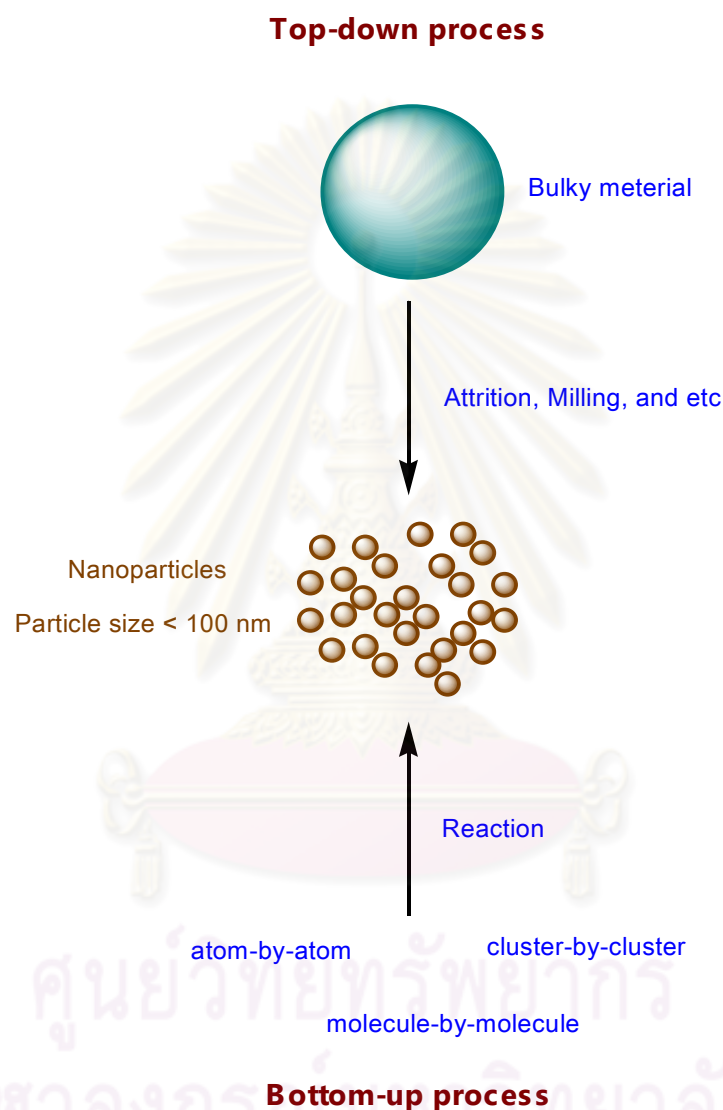
Figure 1.5 The comparison between bottom-up and top-down process to prepare nanoparticles.

1.3 The goals of this research

1.3.1 Preparation of nanosilica slurry by using mechanical grinding machine.

1.3.2 Modification of nanosilica surfaces by employing styrene maleic anhydride (SMA) derivatives, silane coupling agent and polyethylene derivatives.

1.3.3 Preparation of NR/silica nanocomposites by using acid coagulation process of the mixture of natural rubber latex and nanosilica slurry.

1.3.4 Study the mechanical properties and morphology of NR/silica nanocomposites.

1.4 The scope of this research

This research was focused on study of the effect of surface modifying silica nanoparticles on the mechanical properties of NR/silica composites. SMA, silane coupling agent and polyethylene derivatives were selected to employ as modifying agents.

1.4.1 Styrene maleic anhydride (SMA) and derivatives

SMA was widely used to improve thermal and mechanical properties in thermoplastic materials [36, 37]. Moreover, SMA could act as compatibilizer of immiscible thermoplastic blends [38-40]. Meanwhile the SMA was rare applied to elastomers. The major reason, SMA had glass transition temperature higher than processing temperature of rubber compounding. Resulting in, SMA could not melt and disperse in rubber matrix. In this study, the water soluble SMA was employed as treating agent on silica surface. The SMA that used in this study including styrene maleic anhydride copolymer (SMA 1000F), styrene maleic anhydride amic acid (SMA 1000MA), styrene maleic anhydride ester acid (SMA 1440F), styrene maleimide resin (SMA 1000I) and styrene maleimide methyl chloride quat (SMA 7052P) and their structures are shown in Figure 1.6.

The hypothesis of interaction between SMA molecules and silica surface are displayed in Figure 1.7. SMA 1000F molecules coated on silica surface and stabilized by hydrogen bonding between oxygen atoms in maleic anhydride rings and hydrogen atoms of silica silanol groups. For SMA 1000MA, silica surface was concealed by SMA 1000MA molecules via hydrogen bonding. Hydrogen atoms of silica silanol groups were formed hydrogen bonding with oxygen and nitrogen atoms on SMA 1000MA molecules. In addition, nitrogen atoms could be trap hydrogen atoms of silica silanol groups to generate ion pair interaction between maleimidium ion in SMA 1000MA molecules and oxide ions on silica surface. In the presence of SMA

1440F, the interaction between SMA 1440F molecules and silica particles were stabilized by hydrogen bonding between oxygen atoms and hydrogen atoms in both silica silanol groups and SMA 1440F molecules. For SMA 1000I, its nitrogen atoms could be form hydrogen bonding with hydrogen atom of silica silanol groups. Moreover, its nitrogen atom could also be trap hydrogen atoms of silica silanol groups to create ion pair interaction between alkyl ammonium and maleimidium ions in SMA 1000I molecules and oxide ions on silica surface. Similar to SMA 1000I, the interaction between SMA 7052P molecules and silica particles were stabilized by hydrogen bonding between its nitrogen atoms and hydrogen atoms of silica silanol groups. Furthermore, the cations on SMA 7052P molecules were balanced with oxide ions that generated from silica silanol groups by releasing hydrogen atom.
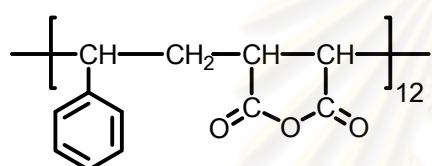
Styrene maleic anhydride copolymer
(SMA 1000F)
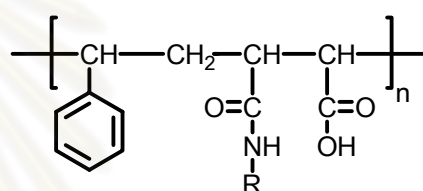
Styrene maleic anhydride amic acid
(SMA 1000MA)
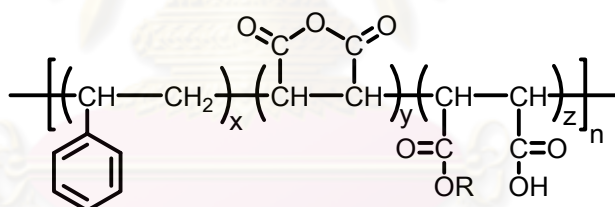
Styrene maleic anhydride ester acid
(SMA 1440F)
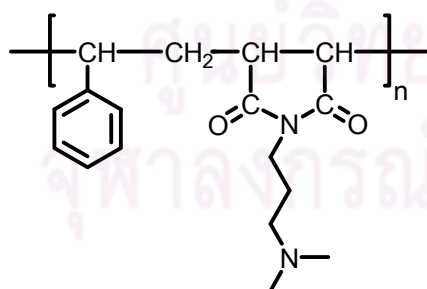
Styrene maleimide resin
(SMA 1000I)
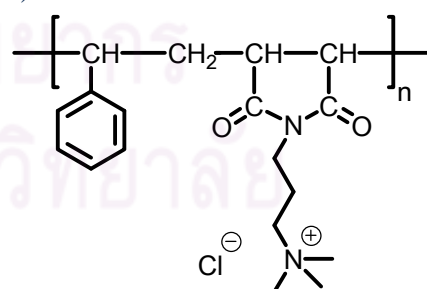
Styrene maleimide methyl chloride
(SMA 7052P)

Figure 1.6 The molecular structures of SMA and its derivatives.
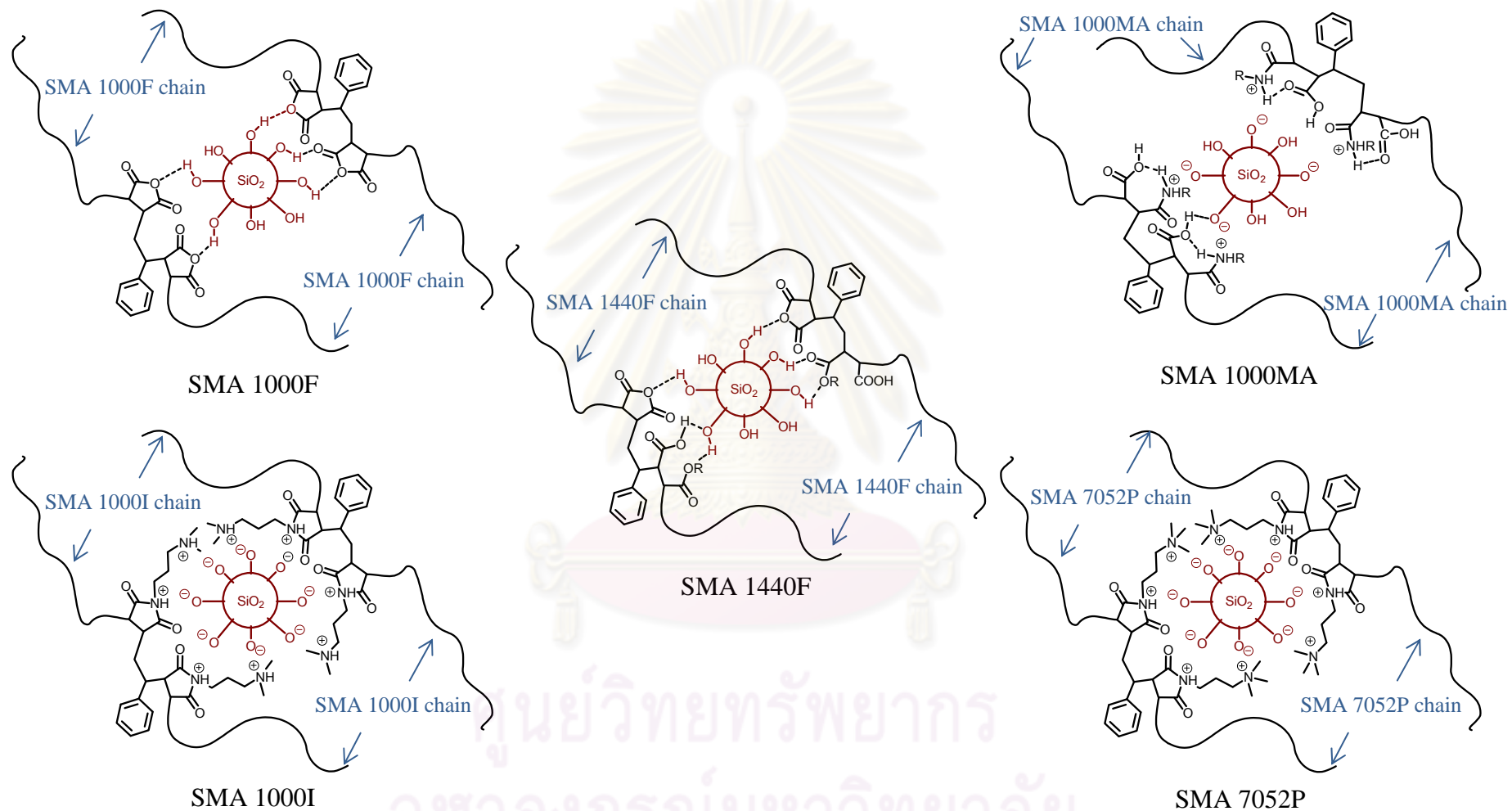
Figure 1.7 The hypothesis of interaction between SMA molecules and silica particles.
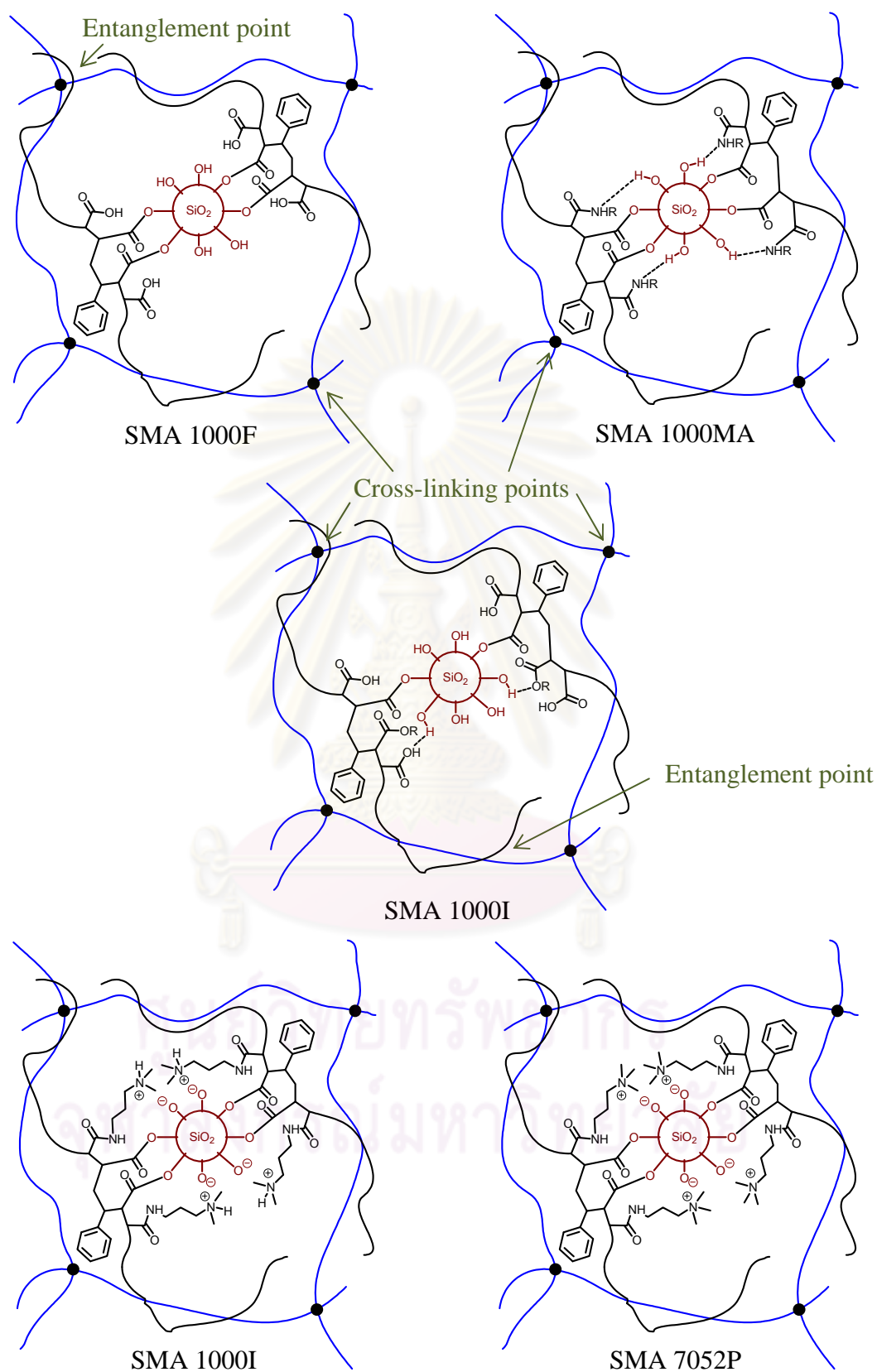
Figure 1.8 The hypothesis of interaction between NR molecules, silica particles and SMA molecules after vulcanizing.

When the NR/silica nanocomposites were cured vulcanizing agents under heat pressing, the hydrogen bonding and ion pair interaction undisturbed from heat, in addition, the silanol groups might be reacted with maleic anhydride to generate strong chemical bonds such as ester bond, Figure 1.8. In addition, the entanglement between SMA and NR molecules would be appearing.

Three experimental systems were interested to study the effect of SMA and derivatives on mechanical properties of NR and SMA 7052P was selected to employ as studying model.

The first one was the comparative study of silica reinforced NR on mechanical properties with variable silica loading such as 10, 20 and 30 phr. Three types of silica were investigated including conventional silica, untreated nanosilica and SMA 7052P treated nanosilca at 1%wt of silica.

The second one was studied the effect of SMA 7052P loading on mechanical properties of NR. The SMA 7052P loading was varied at 0, 0.1, 1, 2 and 3%wt of silica and silica loading was controlled at 30 phr.

The last one was studied the effect of SMA types on mechanical properties of NR. Five SMA types were investigated for example SMA 1000F, SMA 1000MA, SMA 1440F, SMA 1000I and SMA 7052P. The difference among SMA types was their functional groups on SMA molecules. The SMA and silica loading were fixed at 1%wt of silica and 30 phr, respectively.

1.4.2 Silane coupling agents

Silane coupling agents were common used as treating agent to improve the properties of rubber compounding, especially, when silica particle was presented as reinforcing filler [4-9, 41, 42]. This research was interested to study the effect of silane coupling agent treated nanosilica on mechanical properties of NR. The silane coupling agents were selected to investigate in this research comprised of 3-glycidyloxypropyl triethoxysilane (Glyeo), 3-methacrylo-xypropyl triethoxysilane (MEMO), *bis*-(3-triethoxysilylpropyl)tetrasulfide (Si-69), 3-mercaptopropyl triethoxysilane (MTMO), and 3-aminopropyl triethoxysilane (AMEO), Figure 1.9.
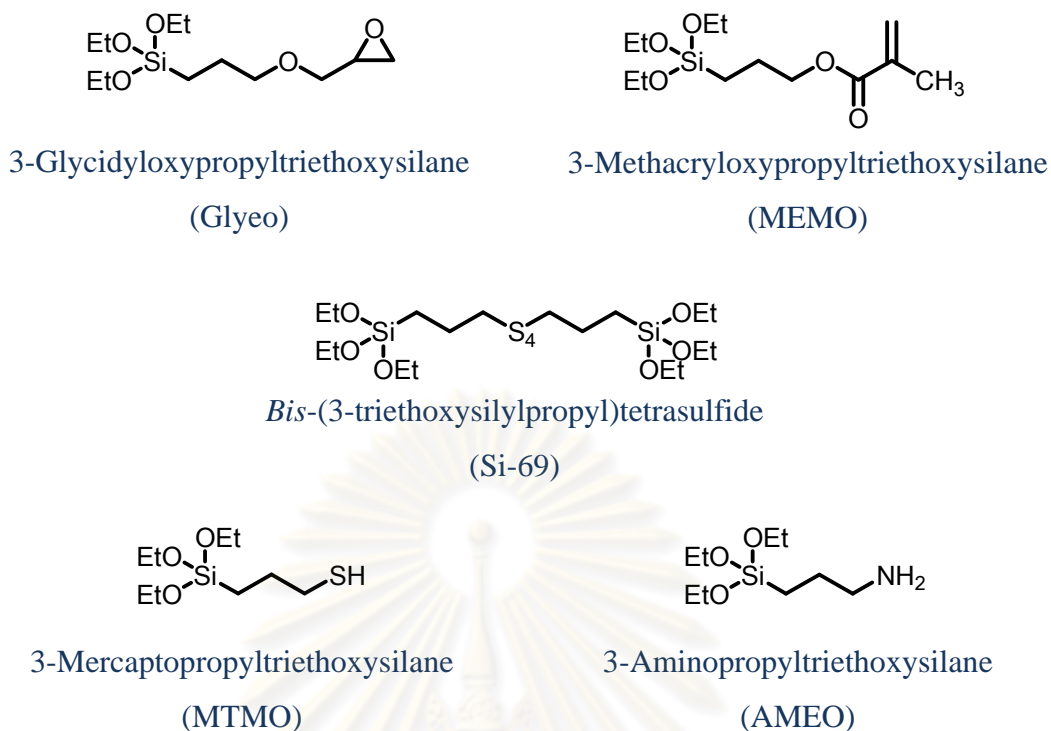
Figure 1.9 The molecular structures of silane coupling agents.

The structure of silane coupling agents composed of reactive alkoxy siloxane and organo functional groups. The former could hydrolyze by the silanol groups on silica surface to form stable siloxane linkages whereas the later is reactive functional groups which precipitated in vulcanizing reaction to form chemical bond with rubbers molecules. Figure 1.10 displayed the assumption of the siloxane linkages between silane coupling agents and silica particle.

The silane coupling agents could act as bridges linkages between rubber molecules and silica particle in silica reinforced NR vulcanizates, Figure 1.11. The organo functional on their molecules could precipitate in vulcanizing reaction and react with rubber molecules to form covalent bond. Therefore, the presence of silane coupling agents could be improve the filler-rubber interaction between silica particles and rubber matrix in vulcanized rubber. In addition, the presence of silane coupling agents could be reduce silica surface energy and might be develop silica dispersion.

Glyeo

MTMO

Si-69

MEMO

AMEO
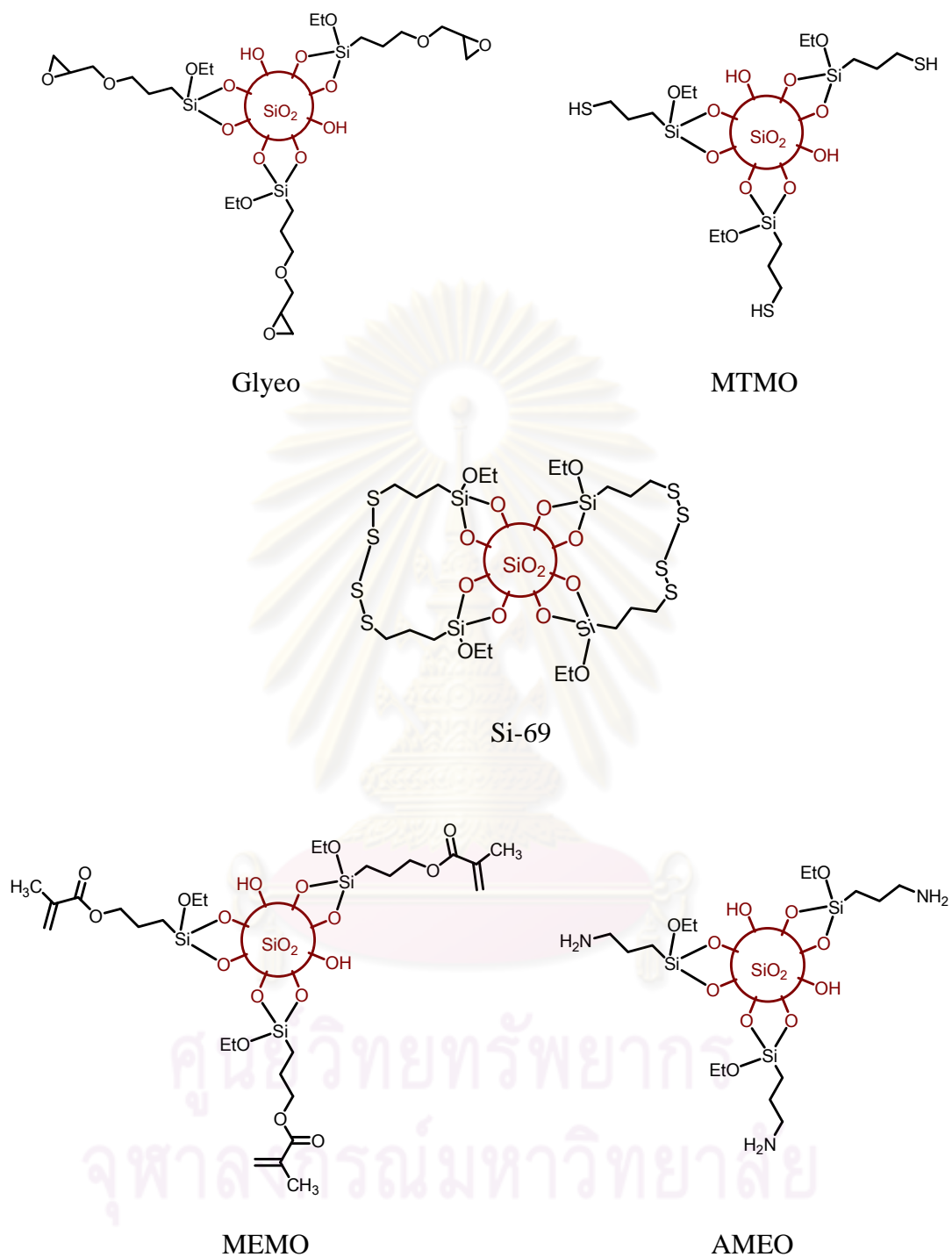
Figure 1.10 The assumption of the siloxane linkages between silane coupling agents and silica particle.
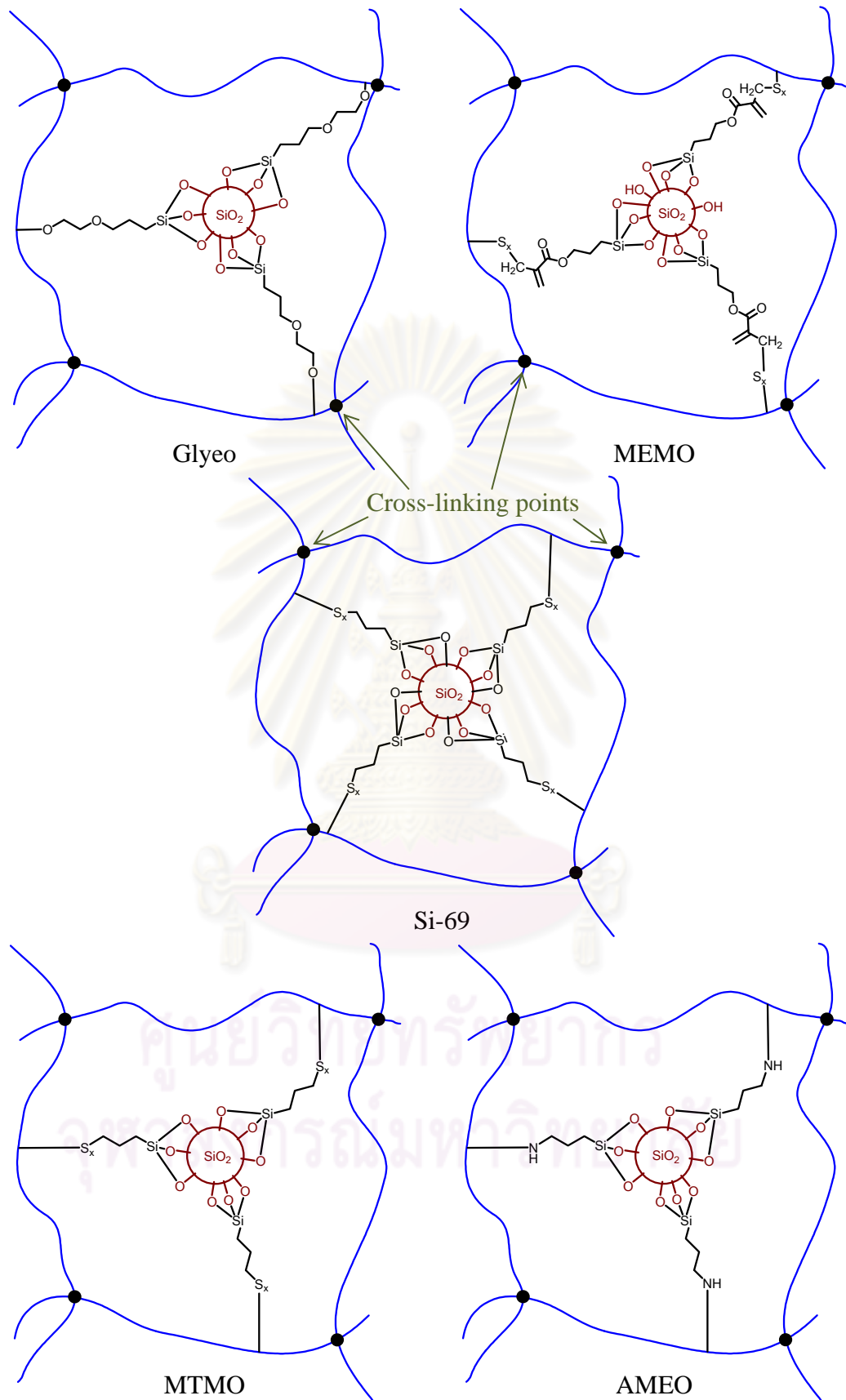
Figure 1.11 The assumption of silane coupling agents as bridge linkages between silica particles and rubber molecules.

The treating efficiency of silane coupling agents was investigated by varying the treating time and treating temperature and using Si-69 as a treating agent. The former was surveyed at 15, 30, 45 and 60 min with constant treating temperature at 60ºC. The later was explored at 60, 70, 75, 80 and 90ºC with controlled treating time at 30 min. After that, four experimental designs were selected to investigate the effect of silane coupling agents on mechanical properties of NR. Si-69 was chosen as the study model.

The first one, the comparative study of silica reinforced NR on mechanical properties with variable silica loading such as 10, 20 and 30 phr, three types of silica were investigated in this study including conventional silica, untreated nanosilica and Si-69 treated nanosilca at 10%wt of silica.

The second one, study the effect of Si-69 loading on mechanical properties of NR, the Si-69 loading was surveyed at 0, 1, 3, 5, 10 and 15%wt of silica and silica loading was fixed at 30 phr. In addition, the study the effect of couple treating agent on mechanical properties of NR was investigated by using SMA 7052P and Si-69 at silica loading 30 phr. SMA 7052P loading was controlled at 1%wt of silica while Si-69 content was varied at 0, 1, 3, 5, 10 and 15%wt of silica.

The third one, study the effect of Si-69 and PEG 4000 ratio on mechanical properties of NR, the Si-69 and PEG 4000 ratios were varied at 0:10, 1:9, 3:7, 5:5 and 10:0 by weight or %wt of silica when silica content was controlled at 30 phr.

The last one, study the effect of silane types on mechanical properties of NR, five silane coupling agents were investigated for example Si-69, MEMO, MTMO, Glyeo and AMEO. The difference among silane coupling agents was functional group on their molecules such as tetrasulfide, methacrylate, thiol, epoxide and amine. The silane coupling agents and silica loading were fixed at 10%wt of silica and 20 phr, respectively. Moreover, the study the effect of couple treating agent on mechanical properties of NR was also surveyed by using SMA 7052P and silane coupling agents at silica loading 20 phr. SMA 7052P loading was fixed at 1%wt of silica while silane coupling agents loading was served at 10%wt of silica with variable types including Si-69, MEMO, MTMO, Glyeo and AMEO.

1.4.3 Polyethylene glycol (PEG) and polypropylene glycol (PPG) derivatives

In generally, PEG was applied to the rubber compound when silica particle was used as reinforcing filler. The propose of adding PEG to the rubber compound is to prevent the trapping of soluble zinc on the silica surface, that is, the cause of the retarded vulcanizing reaction. In this study, PEG and PPG derivatives were acted as modifying agent. Figure 1.12 displayed the molecular structures of PEG and PPG derivatives.

2-(2-Ethoxyethoxy)ethyl acrylate (SR256)

Methoxypolyethylene glycol monomethacrylate SR550

Polyethylene glycol (400) dimethacrylate (SR603)

Polypropylene glycol (400) dimethacrylate (SR604)
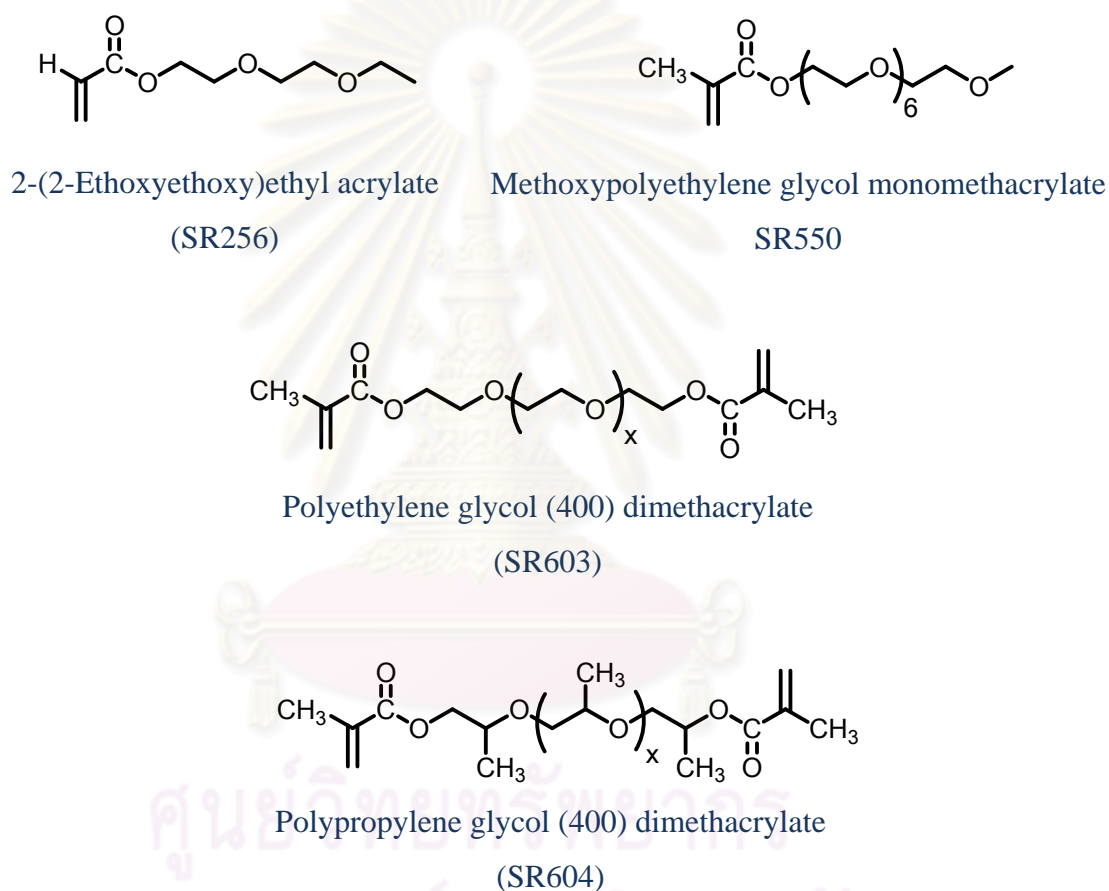
Figure 1.12 Molecular structures of polyethylene glycol derivatives and poly-propylene glycol derivative.

The oxygen atom on molecular backbone of PEG and PPG derivatives could form hydrogen bonding with hydrogen atom of silanol groups on silica surface. Figure 1.13 exhibited the PEG and PPG derivatives treated silica surface with the presence of hydrogen bonding. Moreover, the containing methacrylate groups on their molecules, thus, this functional group could precipitate in vulcanizing reaction to

form stable covalent bonds with rubber molecules. Corresponding to silane coupling agents, PEG and PPG derivatives could be act as bridge linkage between silica particles and rubber molecules in vulcanized rubber, Figure 1.14.
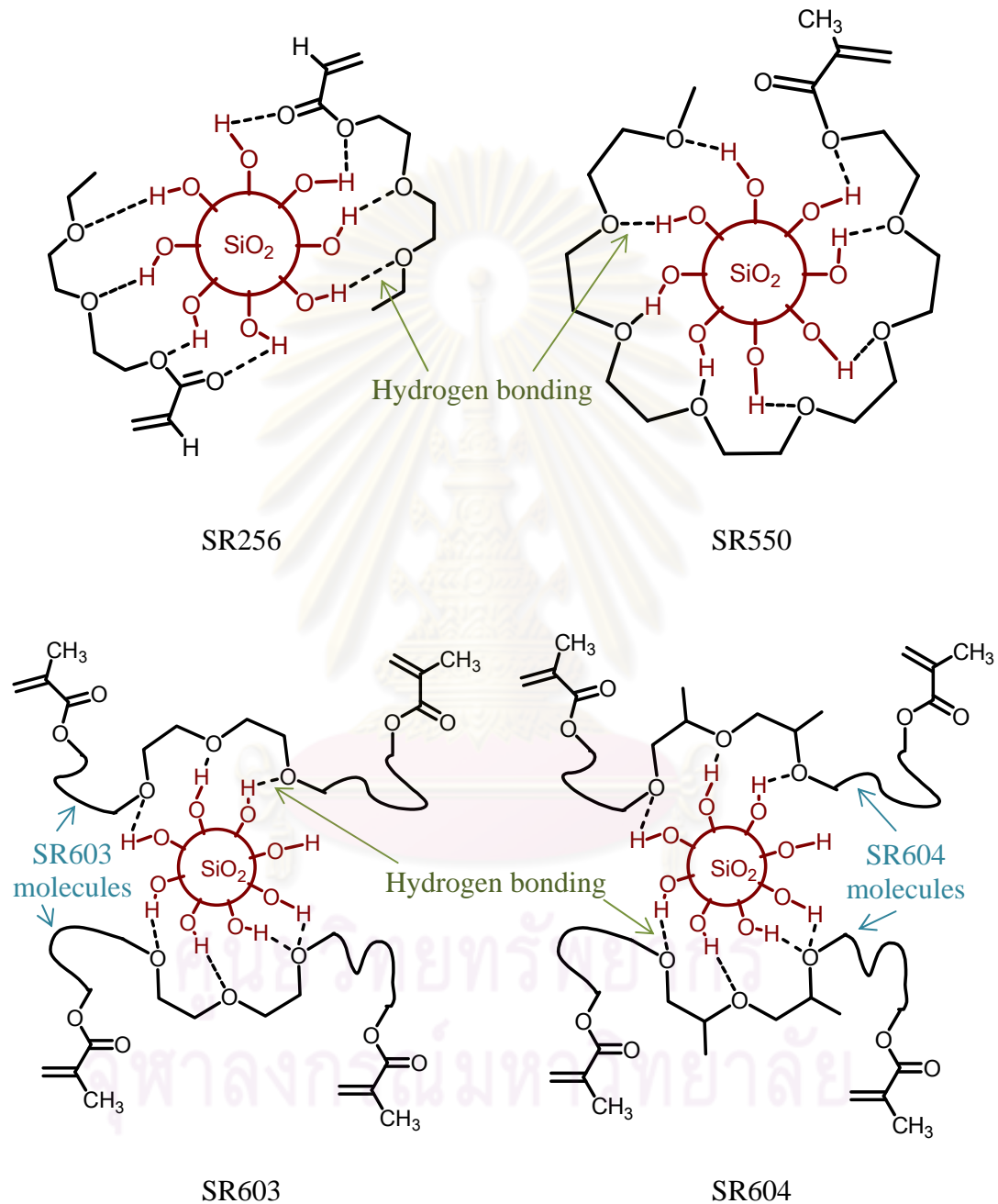
Figure 1.13 The PEG and PPG derivatives treated silica surface with the presence of hydrogen bonding.
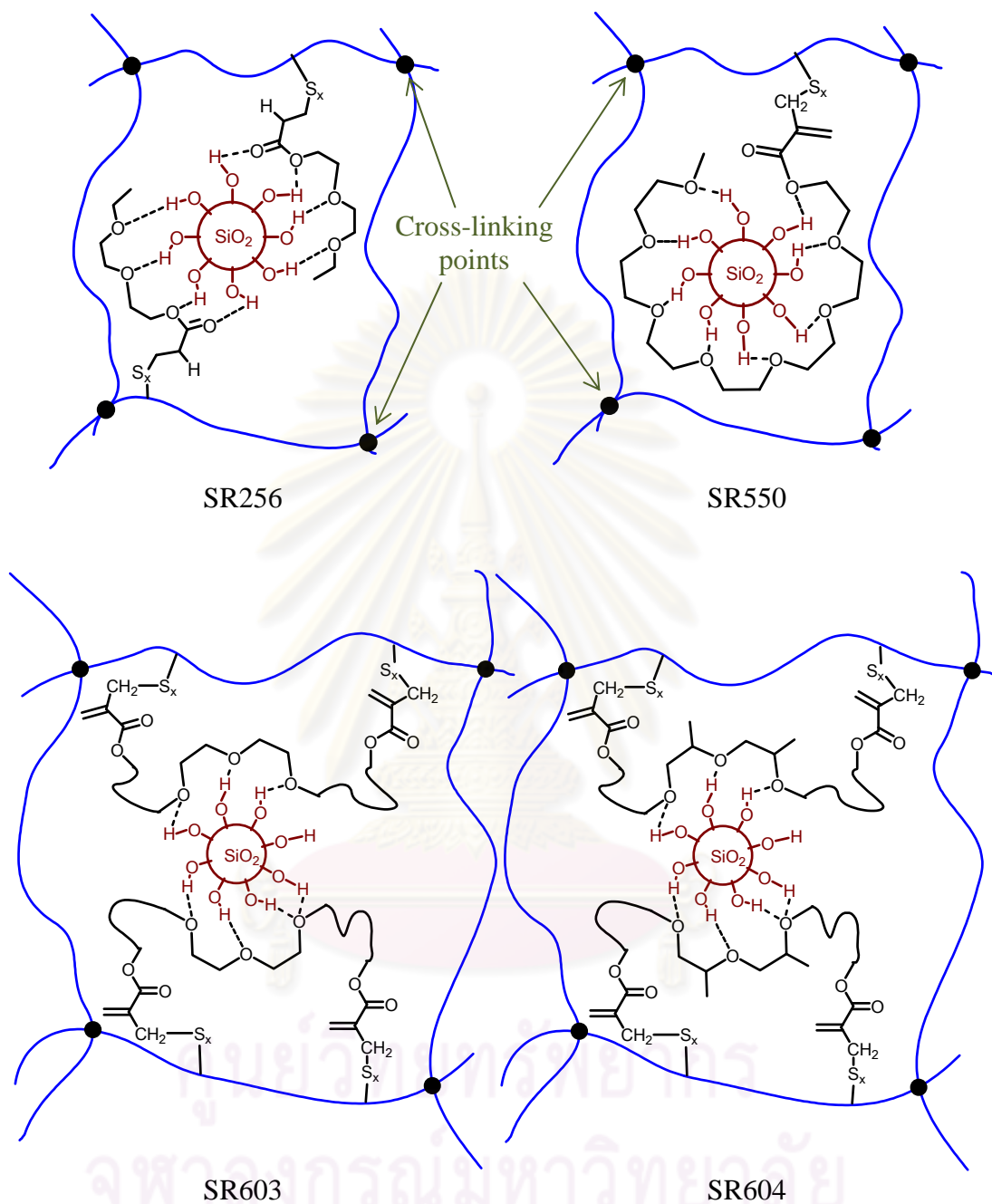
Figure 1.14 The PEG and PPG derivatives as bridge linkages between silica particles and rubber molecules.

In this section, four experimental designs were investigated the effect of PEG and PPG derivatives on mechanical properties of NR. SR550 was selected to employ as studying model.

The first one, three types of silica including conventional silica, untreated nanosilica and SR550 treated nanosilca at 10%wt of silica were investigated the comparative study of silica reinforced NR on mechanical properties with variable silica loading such as 10, 20 and 30 phr.

The second one, study the effect of SR550 loading on mechanical properties of NR, the SR550 loading was investigated at 0, 1, 3, 5, 10 and 15%wt of silica and silica loading was fixed at 30 phr. Furthermore, the couple treating agents between SMA 7052P and SR550 were studied their effect on mechanical properties of NR at silica loading 30 phr. SMA 7052P loading was controlled at 1%wt of silica while SR550 content was varied at 0, 1, 3, 5, 10 and 15%wt of silica.

The third one, study the effect of SR550 and PEG 4000 ratio on mechanical properties of NR, the SR550 and PEG 4000 ratios were studied at 0:10, 1:9, 3:7, 5:5 and 10:0 by weight or %wt of silica with silica content 30 phr.

The last one, study the effect of the types of PEG and PPG derivatives on mechanical properties of NR, four types of PEG and PPG derivatives were investigated including SR256, SR550, SR603 and SR604. The differences among s PEG and PPG derivatives were functional group on their molecules, amounts of functional group, length of their molecular chains and type of their molecular chains. The PEG and PPG derivatives and silica loading were fixed at 10%wt of silica and 30 phr, respectively. In addition, the study the effect of couple treating agent on mechanical properties of NR was also investigated by using SMA 7052P and PEG and PPG derivatives at silica loading 30 phr. SMA 7052P loading was fixed at 1%wt of silica while PEG and PPG derivatives loading was served at 10%wt of silica with variable types including SR256, SR550, SR603 and SR604.

1.5 The benefits could be achieve from this research

This research greatly wished to prepare master batch of NR/silica nanocomposites which provided the good performance. This master batch could reduce the air pollution from silica powder during mixing process and comfort to handle and prepare rubber compounds. Moreover, the master batch of NR/silica nanocomposites could enhance the valuable of NR and NRL.

CHAPTER II

EXPERIMENTAL

2.1 Materials

2.1.1 Chemicals

Concentrated natural rubber latex (NRL), high ammonia, with pH 11.06 and dry rubber content (DRC) 60.19% by weight was furnished by Pan Asia Biotechnology Co., Ltd., Thailand and used as rubber matrix.

Silica powder (WL180) received from Degussa Wellink Silica (Nanping) Co., Ltd., China and utilized as reinforcing filler and raw material to prepare nanosilica slurry. The specific surface area (BET) is 170-230 m^2/g. Absorption value (DBP) is 2.10-2.50 cm^3/g.

2.1.2 Vulcanizing agents

Zinc oxide (ZnO white seal) was provided by Utide Enterprise Co., Ltd., Thailand and used as an activator in vulcanization reaction.

Fatty acid co-activator, stearic acid, was supplied by Imperial Industry Co., Ltd., Thailand.

Polyethylene glycol (Monopol PEG 4000) furnished by Dongnam Chemical Co., Ltd., South Korea.

Primary accelerator, *N*-cyclohexyl-2-benzothiazolesulfenamide (Santocure pellet CBS "CZ"), satisfied by Flexsys (Monsanto), Belgium.

Secondary accelerator, tetramethylthiuram disulfide (Perkacit TMTD), received from Flexsys (Monsanto), Germany.

Sulfur powder was contributed by the Siam Chemicals Public Co., Ltd., Thailand and used as cross-linking agent.

2.1.3 Treating agents

2.1.3.1 Styrene maleic anhydride (SMA) copolymer and its derivatives

The styrene maleic anhydride copolymer and its derivatives were supported by Sartomer Company, Inc. Pennsylvania, USA and their structures are shown in Figure 1.6 including

- Styrene maleic anhydride copolymer (SMA 1000F) is a low molecular weight copolymer with an approximately 1:1 mole ratio of styrene and maleic anhydride.

- Styrene maleimide resin (SMA 1000I) is the aminization product of SMA 1000F and dimethylaminopropylamine.

- Styrene maleic anhydride amic acid (SMA 1000MA) is the product of ring opening reaction of SMA 1000F by amine.

- Styrene maleic anhydride ester acid (SMA 1440F) is a partial esterification of SMA 1000F with alcohol.

- Styrene maleimide methyl chloride quat (SMA 7052P) is salt form of methylation product of SMA 1000I and methyl chloride.

2.1.3.2 Silane coupling agents

All silane coupling agents including *Bis*-(3-triethoxysilylpropyl) tetrasulfide (Si-69), 3-methacryloxypropyl triethoxysilane (MEMO), 3-mercapto-propyl trimethoxysilane (MTMO), 3-glycidyloxypropyl triethoxysilane (Glyeo) and 3-aminopropyltriethoxysilane (AMEO) were supported by Evonik Degussa GmbH, Germany., and their structure are exhibited in Figure 1.9.

2.1.3.3 Polyethylene glycol (PEG) and polypropylene glycol (PPG) derivatives

All polyethylene glycol derivatives were supported by Sartomer Company, Inc. Pennsylvania, USA. For example, 2-(2-ethoxyethoxy)ethyl acrylate or SR-256,

methoxypolyethylene glycol (350) monomethacrylate or SR-550, polyethylene glycol (400) dimethacrylate or SR-603 and polypropylene glycol (400) dimethacrylate or SR-604, and their structures are demonstrated in Figure 1.12.

2.2 Instrument

The mill used in this research is the high performance mill system ZETA[®] type *LabStar* (manufactured by NETZSCH-Feinmahltechnik GmbH, Germany). This mill comprises of preparation part (storage tank and stirrer), pump, grinding part and controller part. The grinding part consist of a motor, grinding disks (ZrO_2), a grinding chamber (SiC), cooling jacket and grinding media (ZrO_2 bead, 0.5 mm). The net grinding chamber volume of the mill is 0.6 L. The small beads used as the grinding media in the grinding chamber are fluidized by the interaction with the movement of grinding disks which driving by motor. The grinding machine was operated in circulation mode with contained grinding media at 90% by volume of grinding chamber; circulation speed is 175 rpm and stirrer tip speed 6-8 m/s. The stirred bead mill diagram is shown in Figure 2.1.
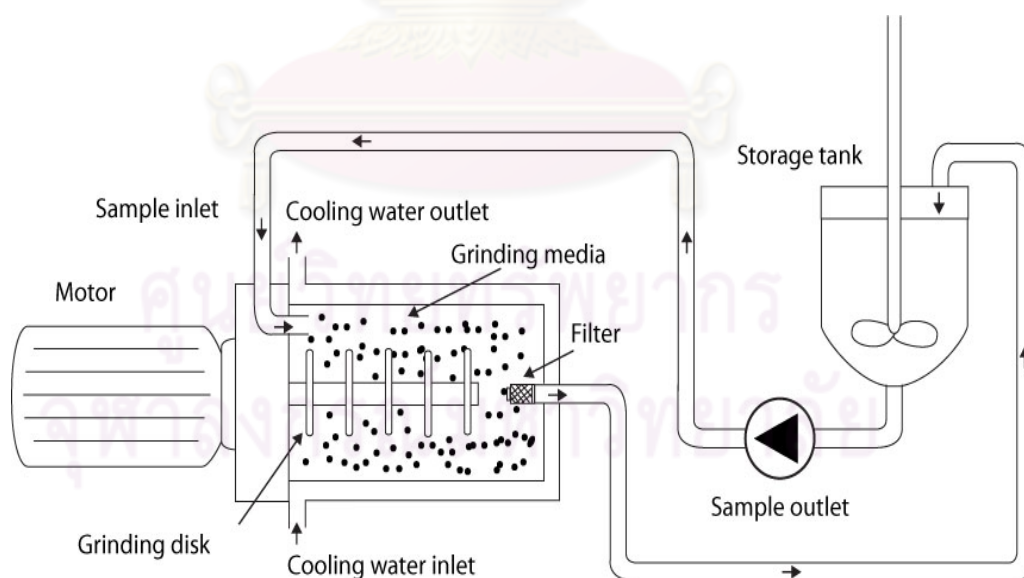
Figure 2.1 Schematic of the stirred bead mill.

2.3 Sample preparation

2.3.1 Preparation of silica nanoparticles

2.3.1.1   Untreated nanosilica slurry

Nine hundred grams of conventional silica, WL180, were carefully added into 3.6 L of deionized (DI) water in the storage tank. Then, the silica slurry was pumped to grinding chamber that contain the motive grinding media. The grinding media are fluidized by the interaction with the movement of grinding disks which driving by motor. The temperature of grinding chamber was controlled at 60ºC by cooling water. The silica slurry was grinded and circulated for 90 min. The nanosilica slurry was cooled down and adjusted to 15% by weight before used.

2.3.1.2   Treated nanosilica slurry

- **SMA treating agents**

After cooling down, the aqueous solution of SMA was added into the untreated nanosilica slurry with various amounts and types. The concentration of SMA treated nanosilica slurries were controlled at 15% by weight before mixing with NRL.

- **Silane coupling agent**

The Si-69 was selected to study the optimum condition of treating reaction and the treating conditions were investigated in treating temperatures and treating times. According to preparation of untreated nanosilica slurry, after an hour of grinding time was taken, 90 g of Si-69, 10% by weight of silica, was slowly added into the silica slurry. Then, the mixture was continuously grinded at 60ºC and circulated for 30 min. The optimum condition was applied to prepare the silane treated nanosilica slurry with variables Si-69 loadings and silane types. The silane treated nanosilica slurries were also adjusted to 15% by weight with DI water before used.

- **Polyethylene glycol (PEG) and polypropylene glycol (PPG) derivatives**

Regarding to the condition for preparing silane treated nanosilica slurry (grinding temperature 60ºC and grinding time 30 min after added treating agents), it was applied to prepare PEG and PPG derivatives treated nanosilica slurry with variables types and amounts. The treated nanosilica slurries were also controlled at 15% by weight with DI water before used.

2.3.2 Preparation of NR/silica nanocomposites

Concentrated NRL, 60%DRC, was deammonized at room temperature over night by using overhead mechanical stirrer with speed at 200 rpm. Then, 300 g of concentrated NRL was diluted to 20%DRC with DI water and stirred for 15 min, the pH of diluted NRL was 8.5. After that, the desired amount of untreated or treated silica slurry, pH 6.0, was poured into diluted NRL and continuously stirred for 15 min. The pH of mixture was 7.5. Then, the droplet of 2.5% formic acid was added to the mixture as a coagulating agent. The coagulation product was washed with water in creeper roller machine to remove access formic acid and achieve sheet rubber, and then, dried at 60ºC for 24 hours or until constant weight to achieve NR/silica nanocomposites with approximately 10, 20 and 30 phr silica content.

2.3.3 Preparation of uncured sample sheet

Seven grams of neat NR or NR/silica nanocomposites without vulcanizing agents were molded into a square sheet of ca. 1 mm thickness by pressing at 155°C for 7 min to obtain uncured sample sheets with approximate size $7 \times 7 \times$ thickness *ca.* 1 mm^3 of neat NR and NR/silica nanocomposites.

2.3.4 The compounding of NR/silica nanocomposites

The NR/silica nanocomposites were mixed with vulcanizing agents by using a brabender mixer (Brabender Plasticorder-PL2000). The mixing condition was fixed as follows, fill factor is 0.7, initial mixing chamber temperature is 50°C and rotor speed is 40 rpm. The amounts of curing ingredients are exhibited in Table 2.1. The

ingredients "ZnO, stearic acid and PEG 4000" were mixed with NR/silica nanocomposites which the total mixing time was 12 min. After cool down to room temperature, the compound was further mixed for 1 min. Then, the curatives "CBS, TMTD and sulfur" were added and mixed for more three minutes. Before compressing, the compounds were sheeted out using a two-roll mill and kept at room temperature. Square sheet of vulcanized NR/silica nanocomposites were prepared by compressing of rubber compound into square-shape at 155°C for 7 min to receive square sheet mold with approximate size $120 \times 150 \times$ thickness ca. 2 mm^3.

Table 2.1 The recipe for vulcanization reaction of NR/silica nanocomposites[a]

Vulcanizing agents	Amount (phr[b])
ZnO whit seal	5
Stearic acid	1
Monopol PEG 4000[c]	3
Santocure pellet CBS "CZ "[d]	1.5
Perkacit TMTD pdr-d[e]	0.4
Sulfur powder	1.5

[a] Vulcanizing conditions: 155ºC, 7 min under pressure.

[b] Parts by weight per one hundred grams of dry rubber.

[c] Polyethylene glycol.

[d] *N*-cyclohexyl-2-benzothiazolesulfenamide.

[e] Tetramethylthiuram disulfide.

2.4 Characterization

2.4.1 Particle size of silica nanopaticles

The particle size of silica slurry was determined by static light scattering (Horiba, LA-950), the nanosilica slurry was taken and immediately measured during grinding process. Particle size of nanosilica slurry was confirmed by employing transmission electron microscope, TEM (JEOL, JEM 2010), the nanosilica slurry was adjusted to 10%wt and dropped into carbon grid, then, the sample was dried under vacuum over night before measurement.

2.4.2 Silica content

The small pieces of NR/silica nanocomposites (approximately 50 mg) were taking placed into aluminium oxide cup. Then the temperature was raised under atmosphere to 850°C and held for 30 min in an oven (Carbolite GM 11/7). The silica content was computed by

$$\text{Silica content (phr)} = 100[W_2/(W_1-W_2)] \qquad (1)$$

Where W_1 was the weight of NR/silica nanocomposites and W_2 was the residual ash weight of NR/silica nanocomposites.

2.4.3 Silica dispersion

The dispersion of silica in NR vulcanizates was determined by using scanning electron microscope, SEM (JEOL, JSM-6400). The samples were cryogenically fissured under liquid nitrogen then sputter-coated with gold and the photographs were taken.

2.4.4 Simultaneous time-resolved wide angle X-ray diffraction (WAXD) and tensile measurement

WAXD measurement during stretching with selected uncured samples was carried out at BL-40XU beam line in SPring-8, Harima, Japan. A custom-made tensile tester (ISUT-2201, Aiesu Giken, Co., Kyoto) was placed on the beam line and WAXD patterns were recorded during stretching at a speed of 100 mm/min at room temperature. The wavelength of the X-ray was 0.0832 nm and the camera length was 113 mm. The two-dimensional WAXD patterns were recorded using a CCD camera (HAMAMATSU ORCAII-ER C4742-98-24ER). Intensity of the incident X-ray was attenuated using a rotating slit equipped by the beam line and the incident beam was irradiated at every 3 sec for 70 ms in order to avoid radiation damage of the specimens. This fast measurement of WAXD is possible at SPring-8, which enabled

us to carry out the *in situ* elucidation of strain-induced crystallization (SIC) of uncured NR/silica nanocomposites under the tensile strain.

2.4.5 Dynamic mechanical analysis (DMA)

Dynamic mechanical properties were also evaluated for uncured samples using a Rheospectolar DVE-4 instrument (Rheology Co., Kyoto) at a frequency of 10 Hz and the temperature range of -150 to 150°C at a heating rate of 2°C/min. Storage modulus (E′) and loss tangent (tan δ) were measured as a function of temperature. The tensile mode was used, and the applied static force was automatically controlled. The size of the specimen was $20 \times 5 \times$ thickness *ca.* 1 mm^3, and the dynamic strain was ±10 μm.

2.4.6 Rheology measurement

Rheology behavior was appreciated to study the filler-rubber interaction. The specimen was cut into circular sheet with diameter 8 mm. The specimen was subjected into the rheometer and measured at 25°C.

2.4.7 Determination of curing behavior

The rubber compounds were weighed approximately 6 g and measured at 155ºC for 12 min in a moving die rheometer (MDR, Ektron, EKT-2000P) for determining vulcanization characterization including scorch time (t_s2), cure time (t_c90), minimum torque (ML), maximum (MH) and cure rate index (CRI). The cure rate index was determined by employing equation 2 [43]. The curing behavior of the rubber compound was demonstrated by using MDR based on ASTM D5289.

$$\text{Cure rate index} = 100/(\text{Cure time} - \text{Scorch time}) \qquad (2)$$

2.4.8 Mechanical tests

The tensile strength (TS), elongation at break (Eb), tensile at 300% elongation or 300% modulus (M300) and tear strength of vulcanized NR/silica nanocomposites were examined by using the universal testing machine (Tech Pro, TensiTECH). The

specimens were cut and tested at 24°C. For the tensile testing, the samples were cut into dumbbell shaped and tested in accordance with JIS 6301 (type 3) at a crosshead speed of 500 mm/min. For the tear testing, the specimens were cut using die C conformance with ASTM D624 and the rate of grips separation was 500 mm/min. The reported values for each sample were averaged from five specimens.

2.4.9 Determination of abrasion resistance

Abrasion resistance of vulcanized rubbers was measured by using abrasion tester (Hung Ta, HT-86218) according to DIN 53516. The vulcanized rubbers were cut into cylindrical shaped with approximately 16 mm in diameter and 6 mm in thickness at 24°C. The reported values for each sample were averages derived from at least three specimens. The abrasion resistance was evaluated by

$$S = \Delta m_0 \qquad (3)$$

and

$$A = (\Delta m \cdot S_o)/(\rho \cdot S) \qquad (4)$$

Where A is the abrasion resistance (mm^3), Δm_0 is the lose in mass of standard (mg), Δm is the lose in mass of sample (mg), ρ is the density of sample (g/cm^3), S_o is the nominal abrasive grade (200 mg) and S is the abrasive grade (mg).

CHAPTER III

RESULTS AND DISCUSSION

3.1 Preparation of nanosilica slurry

In order to explore the grinding conditions, the particle size and particle size distribution of silica slurry were measured every 15 min after adding all original silica into storage tank, employing static light scattering technique. The particle mean size (X_{50}) of silica slurry was evaluated as 69 nm or 0.069 μm, ±2.202 μm in range of 0.050-5.122 μm, with grinding time 30 min while the highest particle size (X_{99}) was found in micron size (about 5 micron). After grinding time was taken for 90 min, the highest particle size was deduced to lower than 300 nm with similar particle mean size. The comparison of particle size distribution between original silica and nanosilica without treating agent is demonstrated in Figure 3.1. The original silica, WL180, indicated the particle mean size about 72 microns and the highest particle size about 210 micron, Figure 3.1a. The particle size distribution of untreated nanosilica after grinding 90 min is exhibited in Figure 3.1b with the particle mean size about 68 nm, ±0.150 μm in range of 0.050-0.260 μm.

The particle size of original silica and untreated nanosilica were also explored by SEM and TEM, respectively, to confirm the particle size of silica. The SEM of original silica is shown in Figure 3.2. It was demonstrated that the particle size of original silica is approximately 12.5 micron (±4.4 micron, $N = 50$). In addition, the TEM images of silica slurry are exhibited in Figure 3.3 revealing the particle size of nanosilica being about 19.3 nm (±3.4 nm, $N = 60$).

The SMA treated nanosilica slurries were prepared after nanosilica slurry was obtained. The sample codes and the properties are demonstrated in Table A1 of Appendix A. The sample codes of SMA treated nanosilica slurry are relevant to the functional group on SMA molecules. SM is referred to **s**tyrene **m**aleic anhydride copolymer (SMA 1000F), SI is alluded to **s**tyrene male**i**mide resin (SMA 1000I), AA is related to styrene maleic anhydride **a**mic **a**cid (SMA 1000MA), EA is abbreviated from styrene maleic anhydride **e**ster **a**cid (SMA 1440F) and SC is pointed to **s**tyrene

maleimide methyl **c**hloride quat (SMA 7052P). In addition, the untreated nanosilica slurry was also exhibited and symbolized as NS0. The amount, by weight of silica, of SMA was revealed as the digit after sample codes. The particle size distributions of all samples were referred to particle size distribution before adding SMA to nanosilica slurry. The particle size distributions after adding SMA were not measured.
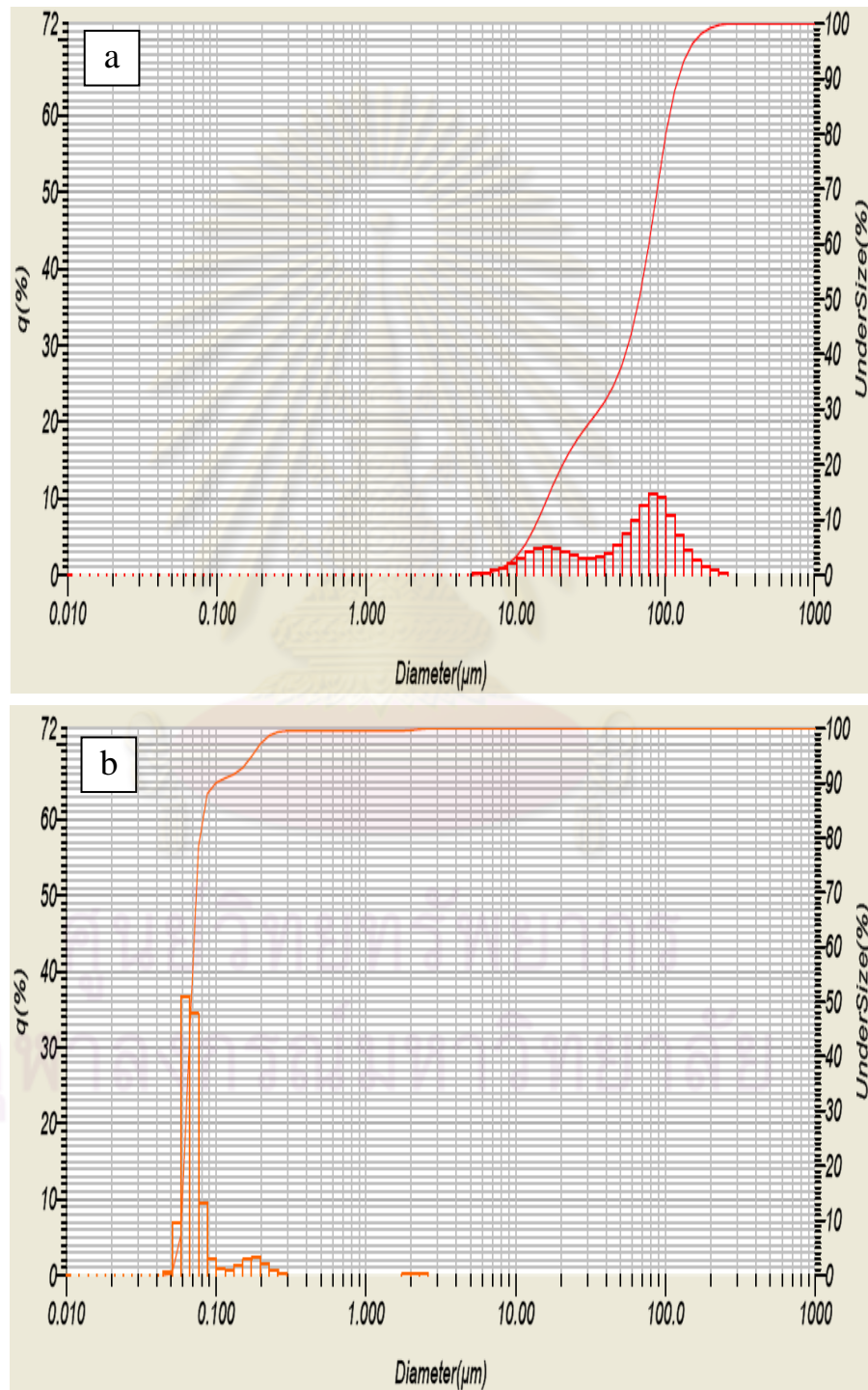
Figure 3.1 Particle size distributions of a) original silica and b) untreated nanosilica.
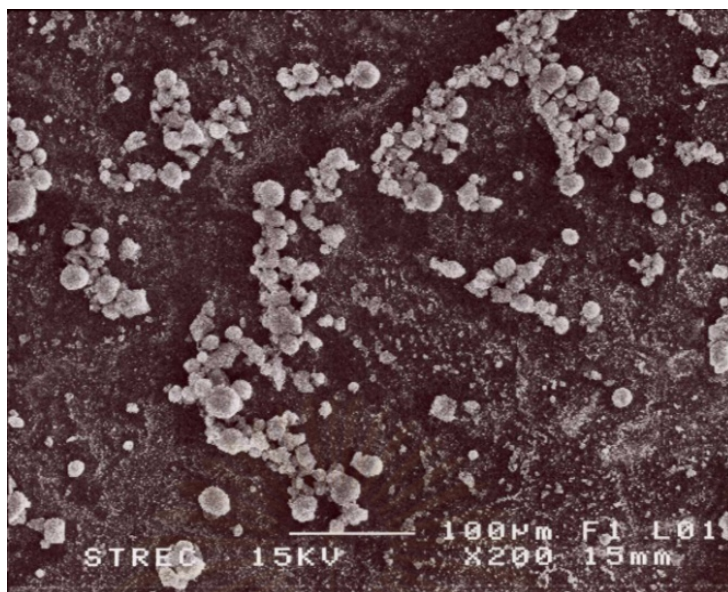
Figure 3.2 SEM picture of original silica.
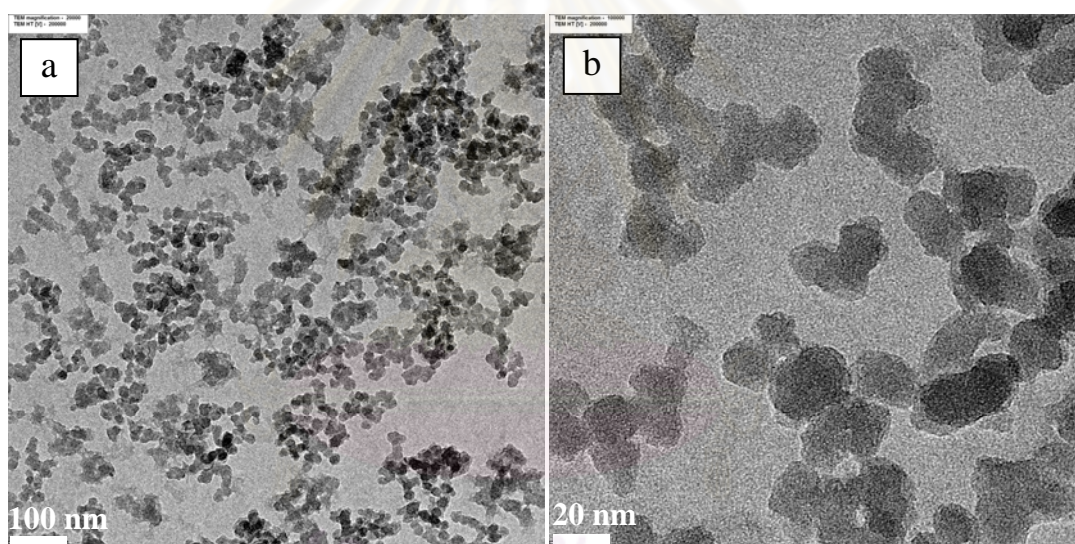
Figure 3.3 TEM images of nanosilica without Si-69 a) at 20,000 x magnifications and
b) at 100,000 x magnifications.

The sample codes and properties of silane coupling agents, PEG derivatives and PPG derivative treated nanosilica slurries were presented in Tables A4 and A5 of Appendix A. The sample codes of silane coupling agents treated nanosilica slurries are related to functional group on silane coupling agent molecular structures. TS is referred to tetrasulfide group on Si-69 structure, ME is corresponded to methacrylate group on MEMO strucuture, MT is related to thiol group in MTMO structure, GL is referred from glycidyl or epoxide group on Glyeo structure and AM is noticed as amino group on AMEO structure. In addition, the sample codes of PPG and PPG

derivatives treated nanosilica slurries are abbreviated from the nomenclature of PEG and PPG derivatives. MP is abbreviated from **m**ethoxy**p**olyethylene glycol (350) monomethacrylate (SR-550). EE is shortened of 2-(2-**e**thoxy**e**thoxy)ethyl acrylate (SR-256). PE is reduced from **p**oly**e**thylene glycol (400) dimethacrylate (SR-603). And PP is abbreviated from **p**oly**p**ropylene glycol (400) dimethacrylate (SR-604). The grinding results showed that the particle distribution of nanosilica slurries before adding treating agents similar to that of nanosilica slurries after adding treating agents. That means that the treating agents were not affected to the particle distribution of nanosilica slurries. The particle size distribution of AM10, after adding AMEO, was not exhibited because it transformed to cake form during treating process. In addition, ME10 and MT10 also transformed to cake form after cooling down. However, these samples were employed to prepare NR/silica nanocomposites.

The nanosilica slurries and cakes were adjusted to 15% by weight by adding DI water before mixing with NRL.

3.2 Preparation of NR/silica nanocomposites

NR/silica nanocomposites were prepared by mixing diluted NRL with nanosilica slurry (section 3.1), after that acid coagulation was performed. The properties of NR/silica nanocomosites including silica content, weight of nanocomposites, weight loss of rubber, weight loss of nanosilica and total weight loss were displayed in Tables B1-B6 of Appendix B. The sample name was symbolized as NCXX and followed by the sample code of nanosilica slurry that was used to prepare NR/silica nanocomposite. NC stands for NR/silica nanocomposite while XX represents the amount of silica content in NR/silica nanocomposite. For example, NC13-NS0 referrs to the NR/silica nanocomposite containing nanosilica 13 phr and untreated nanosilica slurry.

For the investigation of the effect of couple treating agent on the properties of NR/silica nanocomposite, the SMA 7052P was used as secondary treating agent at constant amount, 1% by weight of silica. In addition, P character was present at the sample code and referred to SMA 7052P. For example, NC31-TS1P represents the NR/silica nanocomposite containing nanosilica 31 phr and Si-69 treated nanosilica

slurry, 1% by weight of silica, was used and SMA 7052P, 1% by weight of silica, was used as secondary treating agent.

3.3 The effect of SMA and its derivatives on the properties of NR/silica nanocomposite

The effect of SMA and its derivatives on the properties of vulcanized NR/silica nanocomposites was investigated on silica loading, SMA loading and SMA type. Firstly, three types of silica were selected to investigate at variable silica loadings consisting of original silica (WL180 and powder form), untreated nanosilica slurry and treated nanosilica slurry with SMA 7052P at constant loading at 1% by weight of silica. Secondly, the variable amounts of SMA 7052P including 0.1, 1, 2 and 3% by weight of silica were investigated with control silica content at 30 phr. Lastly, five types of SMA derivatives were employed at constant silica content at 30 phr.

The vulcanized NR/silica nanocomposites were prepared by mixing NR/silica nanocomposite (Section 3.2) with vulcanizing agent as listed in Table 2.1. Dry NR was added, if necessary, to compound for adjusting the desired silica content.

3.3.1 The silica loading and silica type

The standard silica-filled NR vulcanizates were prepared by mixing dry NR with original silica at silica loading 10, 20, 30, 35 and 40 phr, Table C1 of Appendix C. The properties of vulcanized NR/silica nanocomposites are displayed in Table C2 of Appendix C. The sample name was represented as VXX and follow by the sample code of nanosilica slurry that was used to prepare NR/silica nanocomposites. V character was cited for vulcanized silica-filled NR whereas XX was represented to the amount of silica content in vulcanized silica-filled NR. WL, NS0 and SC1 were represented to original silica, untreated nanosilica and treated nanosilica with SMA 7052P at 1% by weight of silica, respectively. The hardness and curing behavior consisting of scorch time, optimum cure time, cure rate index, minimum torque and maximum torque are also presented in Tables C1 and C2.
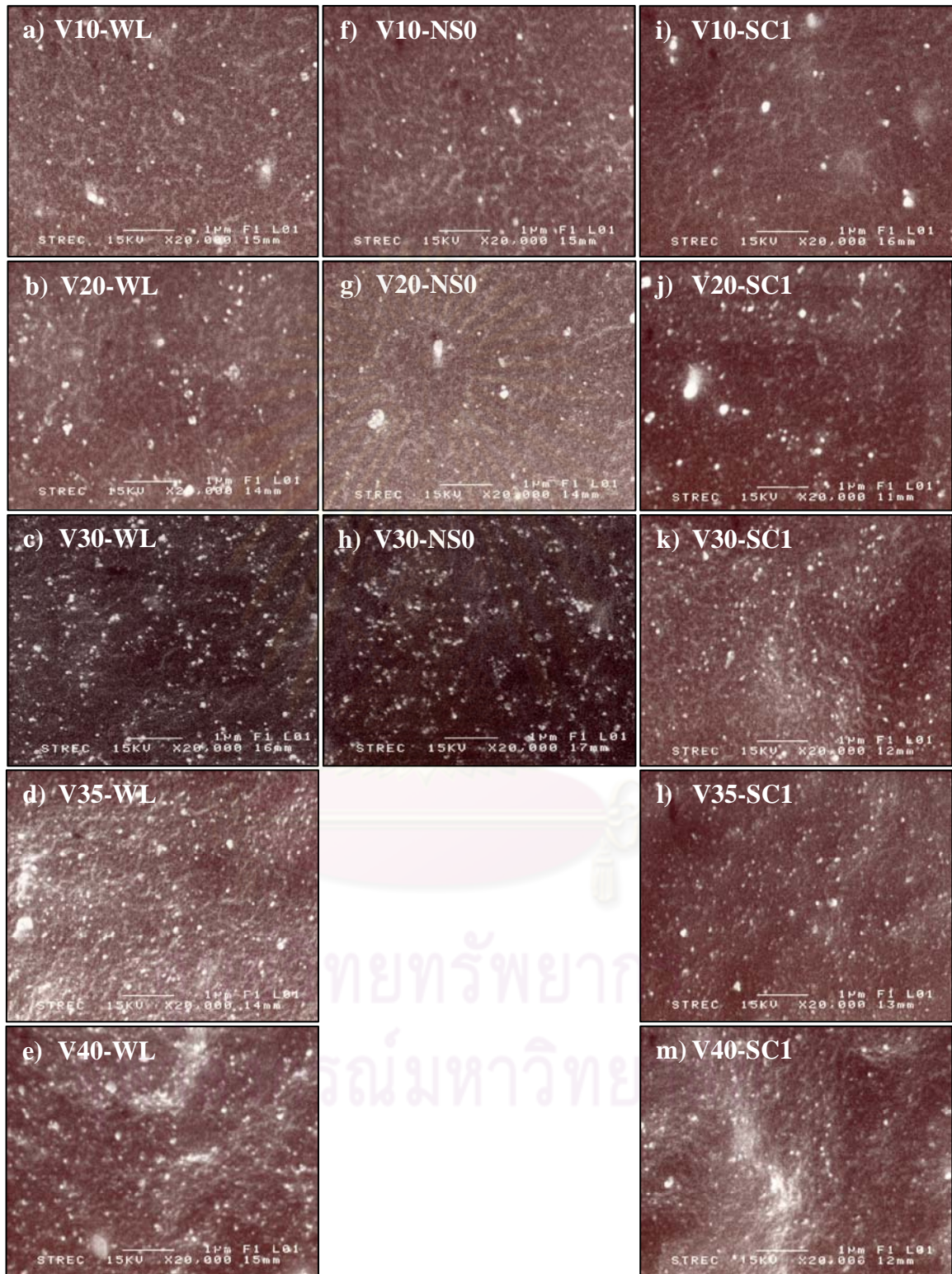
Figure 3.4 SEM micrographs of the fractured surfaces of the vulcanized NR at variable silica content.

SEM analysis for the fractured surface of the vulcanized silica-filled NR having variable silica contents and silica type are exhibited in Figure 3.4. In the SEM micrographs, the silica particles are displayed as white spots while the darkness area belongs to the rubber matrix. When the silica loading was increased, many white spots appeared. In addition, comparing to original silica-filled NR, the presence of SC1 affected the increasing of silica dispersion, especially at silica contents 35 and 40 phr whereas the presence of NS0 unaffected to improve silica dispersion. Furthermore, a little amount of aggregation form is also presented. The presence of aggregation form might be due to the acid induce re-aggregation process during the preparation of NR/silica nanocomposites; however, the aggregation form was disappeared when the silica loading was raised up to 30 phr in both NS0 and SC1 filled NR vulcanizates.

The mechanical properties of vulcanized silica-filled NR are investigated. Figure 3.5 represents the tensile strength of vulcanized silica-filled NR with variable silica loading and silica type. The tensile strength was increased with increasing silica loading up to 30 phr and further silica content, more than 30 phr, the tensile strength was decreased. This observation might be due to the increasing of silica aggregation at high silica loading and the maximum silica loading of NR. In addition, the SC1 filled NR vulcanizates exhibited the tensile strength over WL and NS0 filled NR vulcanizates, respectively. This might be because of SC1 filled NR vulcanizates had stronger filler-rubber interaction over WL and NS0 filled NR vulcanizates. The stronger filler-rubber interaction was received from more compatibleness of low surface energy of silica that covers by SMA7052P and rubber. SMA 7052P had two difference segment on its molecule. The first one, polar segment, maleimide methyl chloride segment that could form hydrogen bond with silanol group on silica surface and another one, non polar segment, styrene segment could interact with rubber by forming Van der Waals forces. Moreover, the entanglement points between SMA 7052P and rubber could slightly increase filler-rubber interaction.

Figure 3.6 displays the modulus at 300% elongation (M300) of vulcanized silica-filled NR with variable silica loading and silica type. The M300 was raised up when silica loading was increased. The M300 of SC1 was higher than that of original silica and NS0, due to the stronger filler-rubber interaction and slightly better silica

dispersion in NR/silica nanocomposites, except in V30-NS0. This might be because of V30-NS0 exhibited the high filler network chain to provide the better filler-filler interaction while the SC1 contained SMA 7052P on the silica surface results in decreasing the filler-filler interaction.

The elongation at break of vulcanized silica-filled NR is displayed in Figure 3.7. Regarding to the tensile strength, the elongation at break was increased with increasing silica loading up to 30 phr, the further silica content, more than 30 phr, the elongations at break was decreased. The attained results might be because the aggregated form was present at high silica loading, 35 and 40 phr. According to strong filler-filler interaction of V30-NS0, as can be seen in high M300 result, the filler-filler interaction was destroyed at high elongation, resulting in elongation at break was intensively decreased.
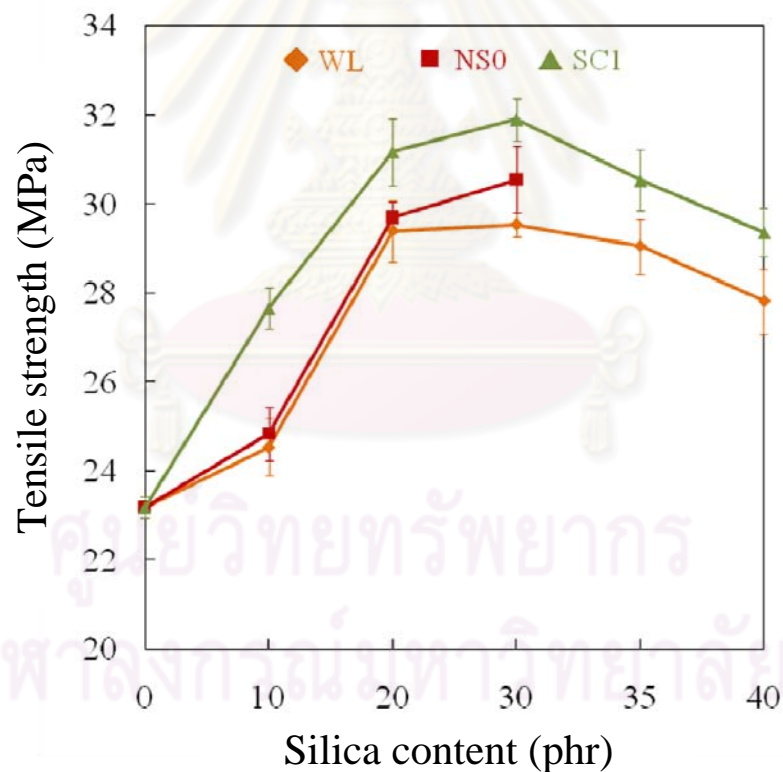
Figure 3.5 The tensile strength of vulcanized silica-filled NR with variable silica loading and silica type.
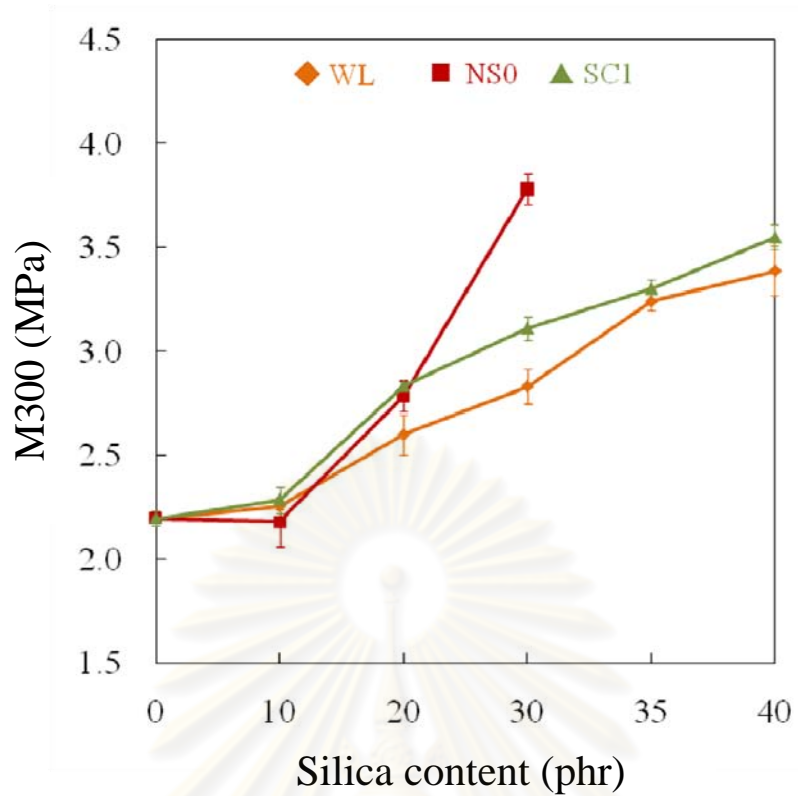
Figure 3.6 The M300 of vulcanized silica-filled NR with variable silica loading and silica type.
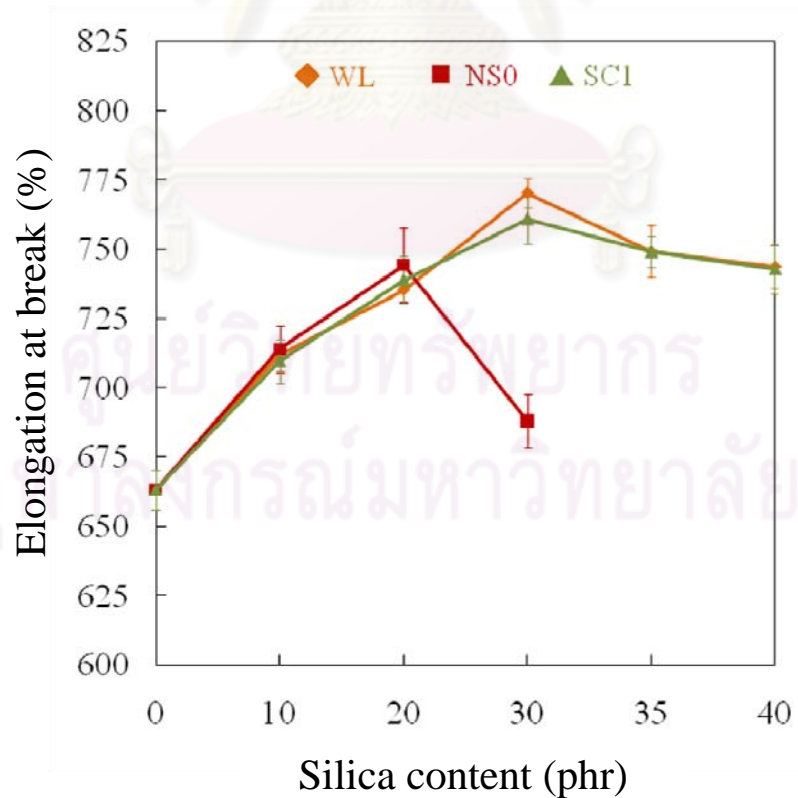
Figure 3.7 The elongation at break of vulcanized silica-filled NR with variable silica loading and silica type.

The tear strengths of vulcanized silica-filled NR are displayed in Figure 3.8. The resulting showed that when the silica content was raised up, the tear strength was improved. The tear strengths of NS0 and SC1 were abased than that of WL at silica content lower than 30 phr. This might be due to a little presence of aggregated form in both NS0 and SC1 at low silica loading, whereas at high silica loading, over 30 phr, SC1 presented higher tear strength than WL because of the stronger filler-rubber interaction of SC1 over WL.

The abrasion resistance of the silica-filled NR vulcanizates, revealed as abrasion loss, is shown in Figure 3.9. The results showed that the tendency of abrasion resistance was improved when silica content was increased close to 20 phr, especially, in NS0. The abrasion loss was demeaned at high silica loading. The resulting might be due to the presence of aggregated form at high silica loading. Whereas the presence of NS0 and SC1 as reinforcing filler in vulcanized NR was not improved the abrasion resistance comparing with original silica-filled NR vulcanizates.
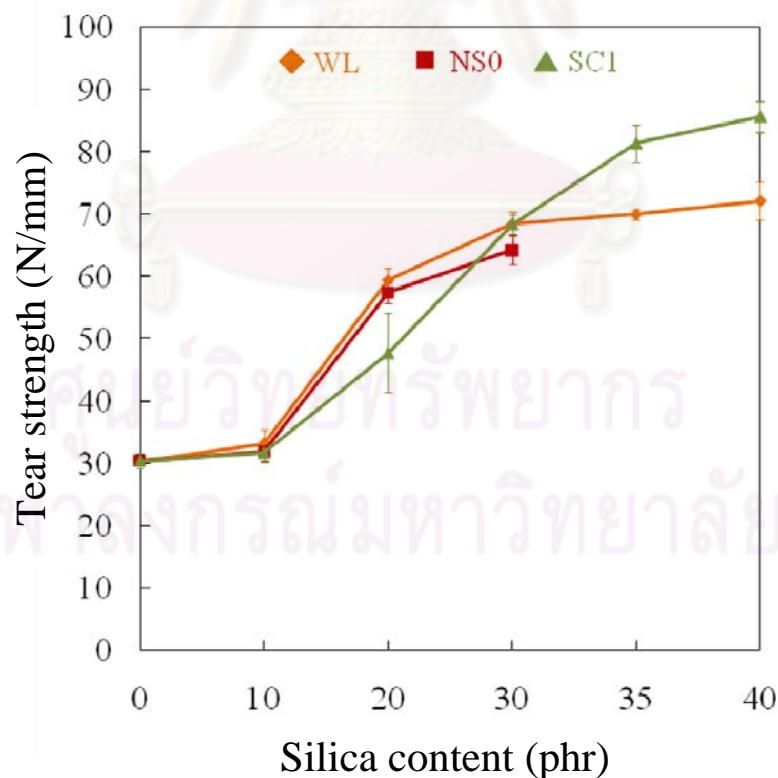
Figure 3.8 The tear strength of vulcanized silica-filled NR with variable silica loading and silica type.
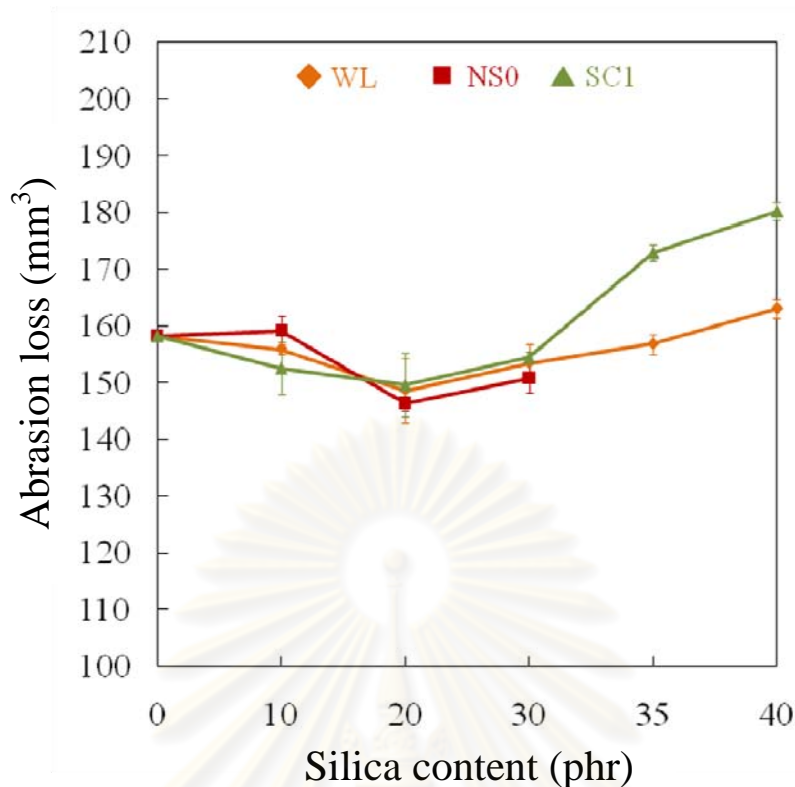
Figure 3.9 The abrasion loss of vulcanized silica-filled NR with variable silica loading and silica type.

Summary, the comparative study of three types of silica consisting of original silica (WL), untreated nanosilica (NS0) and treated nanosilica with SMA 7052P at constant loading at 1% by weight of silica (SC1) was investigated on mechanical properties on vulcanized NR at variable silica loadings. The obtained results showed that SMA 7052P treated nanosilica-filled NR vulcanizates provided the highest tensile strength by dominating filler-rubber interaction. The M300 was slightly increased in the presence of SMA 7052P while NS0 provided the highest M300 at silica loading 30 phr by dominating filler-filler interaction. The elongation at break, tear strength and abrasion resistance were not affected by presenting SMA 7052P.

3.3.2 The effect of SMA 7052P loading

The vulcanized nanosilica-filled NR with constant silica loading at 30 phr was prepared with variable SMA 7052P loading including 0, 0.1, 1, 2 and 3% by weight of silica. The sample names comprising of V30-NS0, V30-SC0.1, V30-SC1, V30-SC2 and V30-SC3 were represented to SMA 7052P loading including 0, 0.1, 1, 2 and 3% by weight of silica, respectively. The hardness and curing behavior consist of scorch

time, optimum cure time, cure rate index, minimum torque and maximum torque are also presented in Table C3 of Appendix C. It was noticed that the addition of SMA 7052P was affected to reduce both scorch time (t_s2) and optimum cure time (t_c90). Normally in a sulfur vulcanizing system, amine accelerators and Zn complex act as a cure activator. After that, the cure activator is further reacted with sulfur and rubber. In the presence of silica, a portion of cure activator could be trapped by the reactive silanol groups. Therefore, the vulcanization is rather retarded. In the presence of SMA 7052P, the partial silanol groups were caught by cationic functional group on SMA 7052P. The cations on SMA 7052P were balanced with oxide ions generated from silica silanol groups by releasing hydrogen atom (acidic proton). Furthermore, acidic proton was removed as HCl by watching NR/silica coagulated with DI water resulting in the decreasing of the amount of trapped cure activator which gave rise to faster cure rate. Therefore, both scorch time and optimum cure time were reduced with increasing the amount of SMA 7052P.
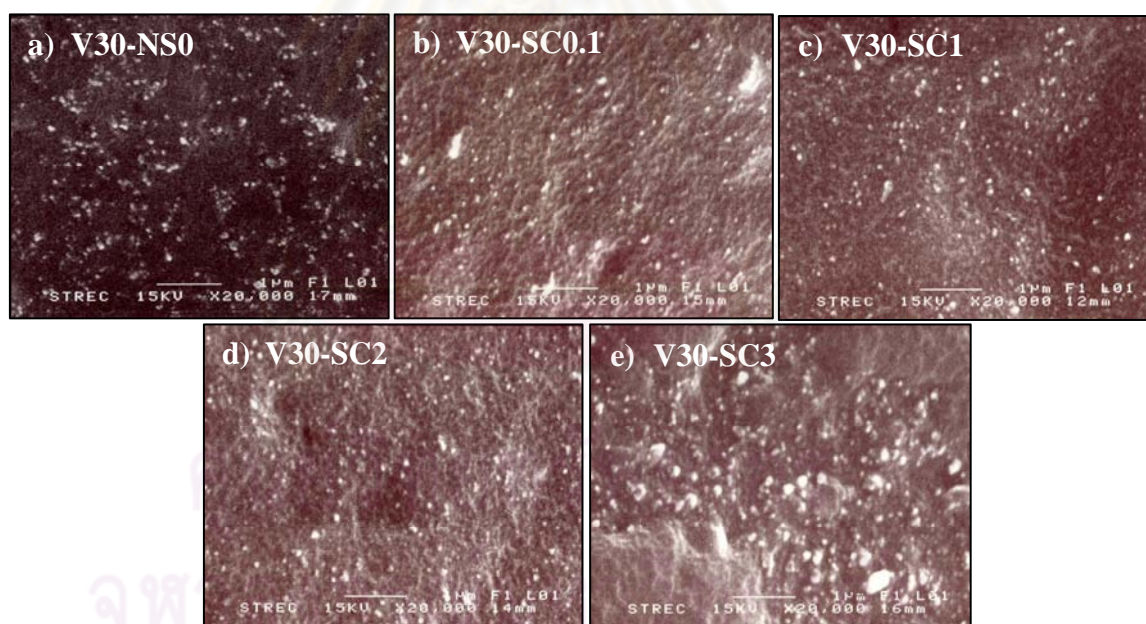
Figure 3.10 SEM micrographs of the fractured surfaces of the vulcanized NR at variable silica content.

The SEM micrographs of the fractured surfaces of vulcanized nanosilica-filled NR with variable SMA 7052P loading are shown in Figure 3.10. The results displayed that the silica dispersion was improved by increasing SMA 7052P loading up to 2% by weight of silica. The aggregated silica was appeared when further SMA 7052P was

added. This might be due to the large amount of SMA 7052P induced the aggregation process. Moreover, the mixture of SC3 and NRL was coagulated without adding formic acid. In other words, the self-coagulation of SC3 and NRL could occur under mechanical stirrer. The self-coagulation could be occurred *via* electrostatic interaction at silica surface, Figure 3.11 [44, 45]. The partial negative charge at silica surface was covered by cationic charge on SMA 7052P to produce a positive charge on silica surface. When excessive SMA 7052P was added, the negative charge NRL was attracted with high density of positive charge at silica surface. Then, self-coagulation was performed.
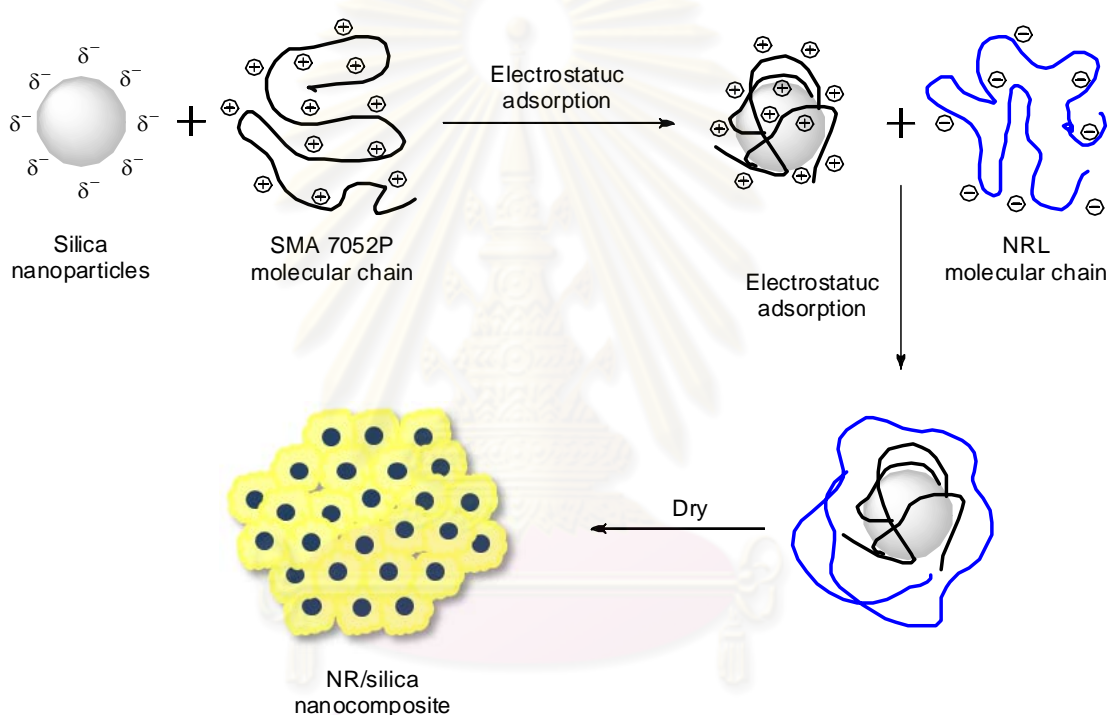
Figure 3.11 The schematic of the self-assembly process.

The mechanical properties are demonstrated in Figures 3.12-3.16. Tensile strength was slightly increased when SMA 7052P was present. It might be due to the improvement of filler-rubber interaction. On the other hand, filler-filler interaction was reduced which presenting SMA 7052P, resulting in the M300 being diminished by presenting SMA 7052P. In addition, M300 was continuously decreased which increasing SMA 7052P loading. Nevertheless, the tensile strength was not affected by increasing SMA 7052P loading, whereas the elongation at break, tear strength and abrasion loss were not affected by increasing SMA 7052P.
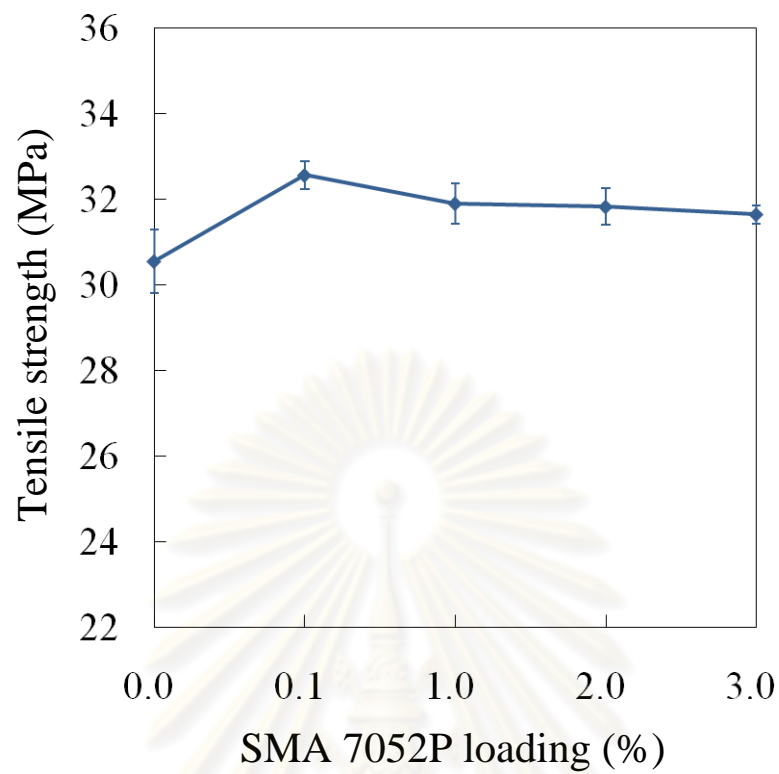
Figure 3.12 The tensile strength of vulcanized silica-filled NR with variable SMA 7052P loading.
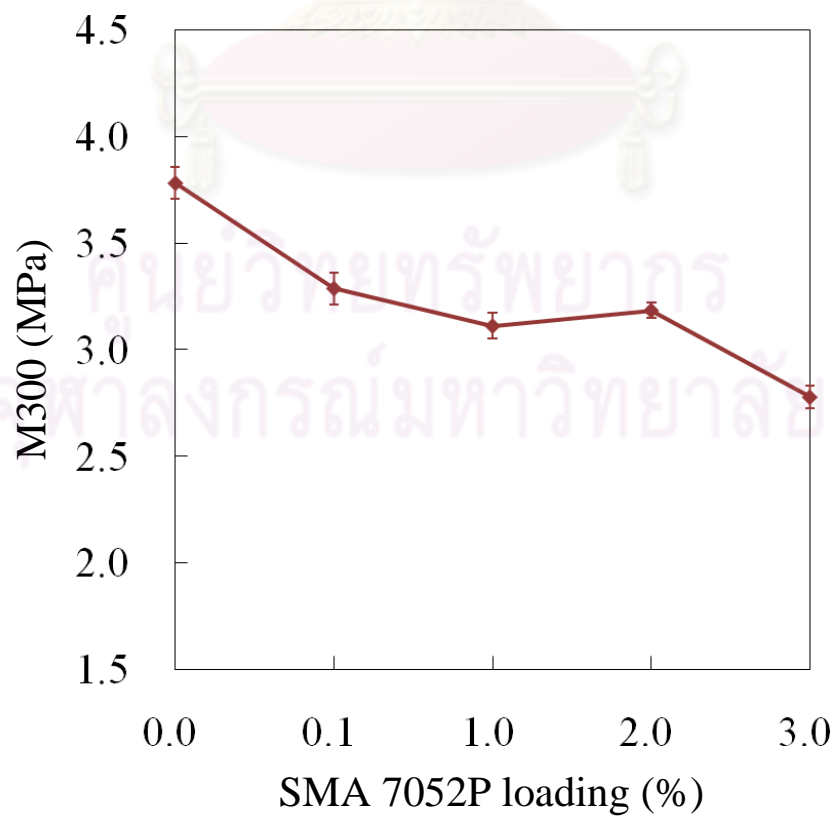
Figure 3.13 M300 of vulcanized silica-filled NR with variable SMA 7052P loading.
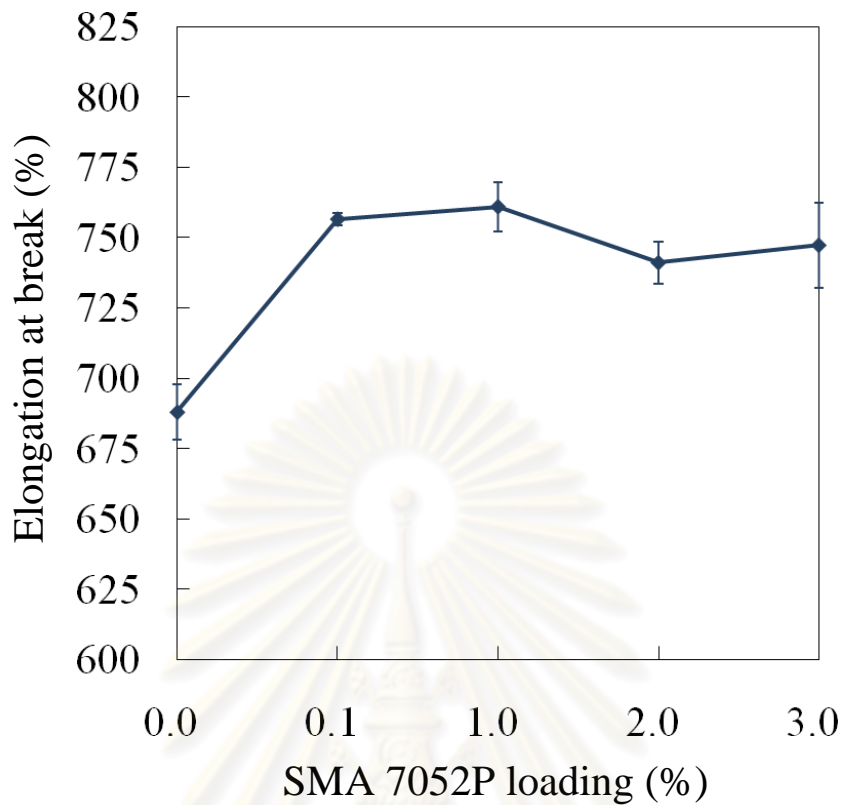
Figure 3.14 The elongation at break of vulcanized silica-filled NR with variable SMA 7052P loading.
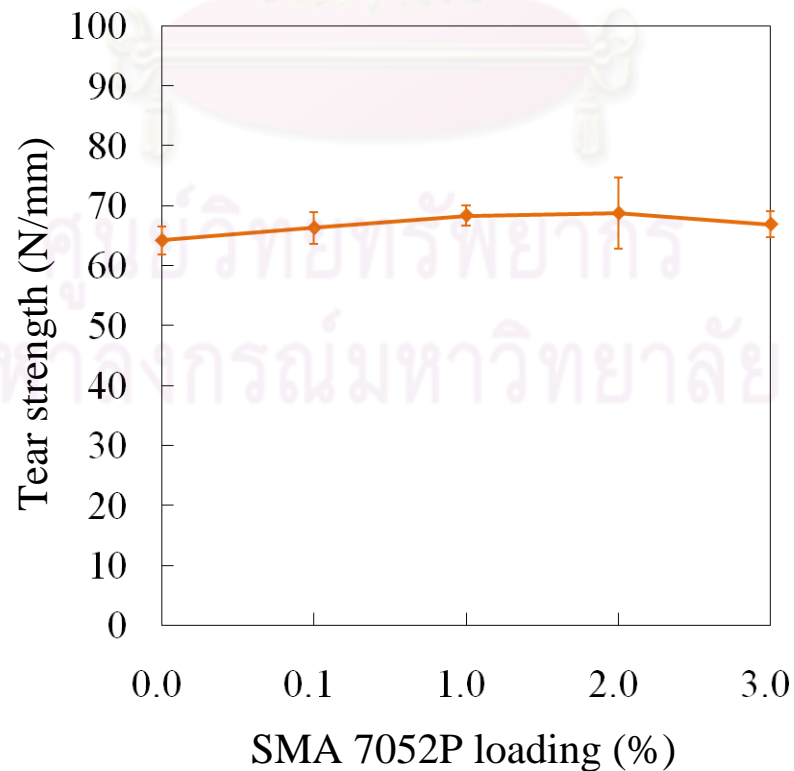
Figure 3.15 The tear strength of vulcanized silica-filled NR with variable SMA
7052P loading.
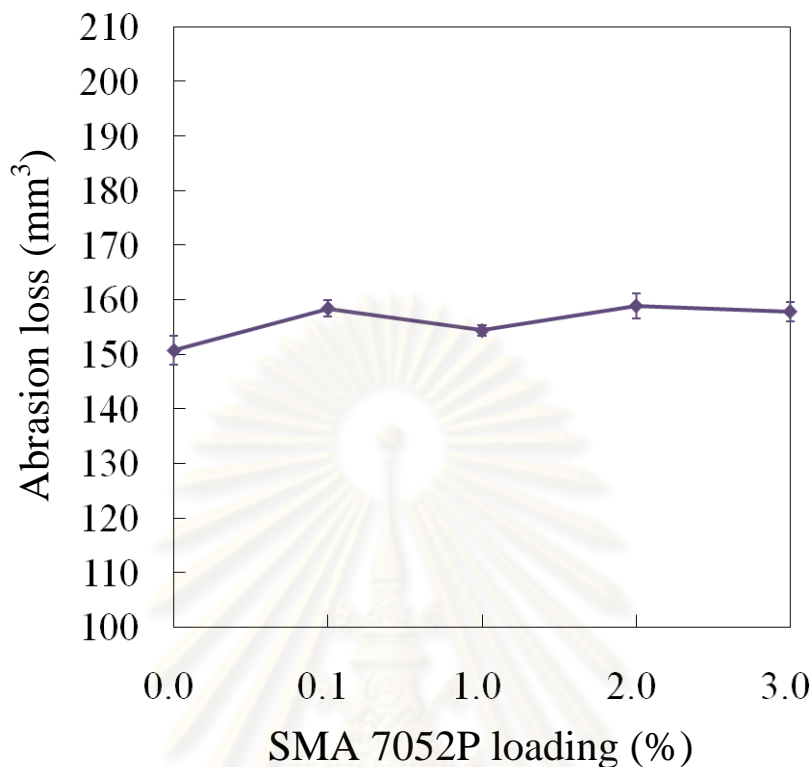
Figure 3.16 The abrasion loss of vulcanized silica-filled NR with variable SMA
7052P loading.

Finally, the increasing of SMA 7052P loading did not improve mechanical
properties of vulcanized NR/silica nanocomposites. In other words, the mechanical
properties especially M300, elongation at break and abrasion resistance had trend to
degrade when SMA 7052P loading was increased. Moreover, the mixture of
nanosilica slurry and NRL was coagulated without adding formic acid when SMA
7052P was raised up to 3%wt of silica.

3.3.3 The Effect of SMA types

The effect of variable types of SMA was investigated on the properties of
vulcanized nanosilica-filled NR. The sample names were represented to SMA types
such as SMA 7052P, SMA 1000F, SMA 1000I, SMA 1000MA and SMA 1440F. The
hardness and curing behavior consist of scorch time, cure time, cure rate index,
minimum torque and maximum torque are also presented in Table C4 of Appendix C.
The resulting showed that V30-SC1 revealed the shortest scorch time and optimum

cure time than V30-SM1, V30-SI1, V30-AA1 and V30-EA1. Similar to section 3.3.2, the presence of SMA 7052P, the partial silanol groups were caught by cationic functional group on SMA 7052P. The cations on SMA 7052P were balanced with oxide ions that generated from silica silanol groups by releasing hydrogen atom (acidic proton). Furthermore, an acidic proton was removed as HCl by watching NR/silica coagulated with DI water. Whereas SMA 1000F, SMA 1000I, SMA 1000MA and SMA 1440F only formed hydrogen bonding with silanol group on silica surface but not removed acidic proton, especially SMA 1000MA and SMA 1440F contained carboxylic group on their molecules. Therefore, higher acidic protons affected to longer scorch time and optimum cure time. In other words, higher acidic proton had a major effect to retard vulcanization reaction.
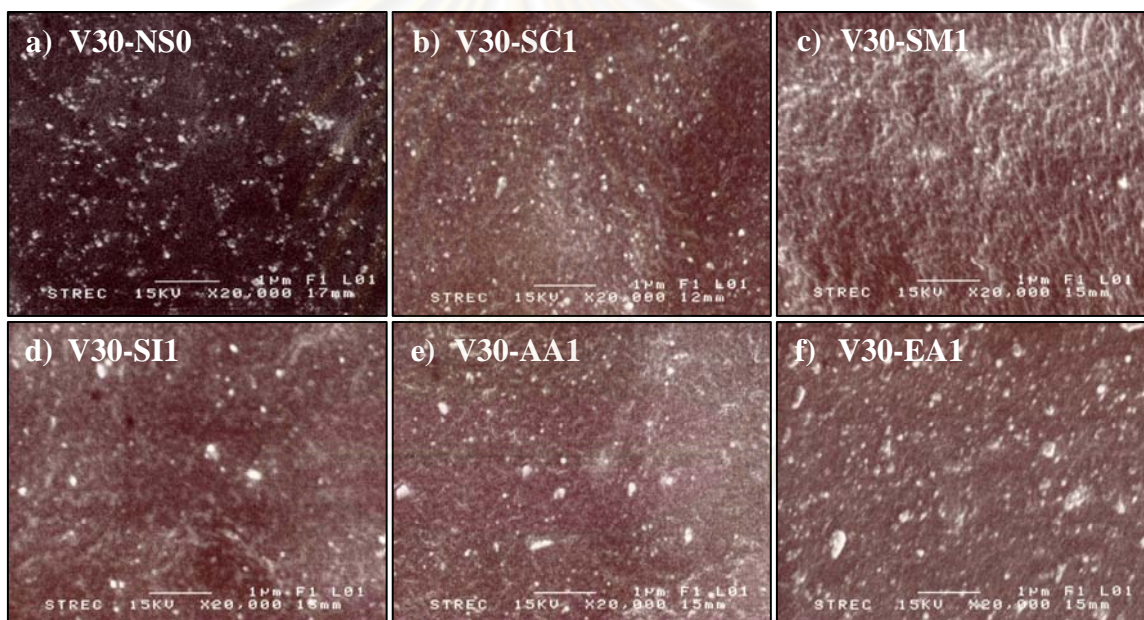
Figure 3.17 SEM micrographs of the fractured surfaces of the vulcanized NR with variable SMA type.

SEM micrographs of the fractured surfaces of vulcanized nanosilica-filled NR with variable SMA treating agent types are shown in Figure 3.17. The results showed that the SMA 1000F provided the best silica dispersion, while the aggregated form was appeared when SMA 1000I, SMA 1000MA and especially, SMA 1440F were present. The results might be due to the high polar functional groups on SMA 1000I, SMA 1000MA and SMA 1440F over maleic anhydride functional group on SMA

1000F molecule. The high polar molecules had more attractive silica particles. Therefore, high polar molecules had more possibility to prevent silica aggregation.

Tensile strength results displayed in Figure 3.18 showed that tensile strength was not affected by changing SMA type. It might be because all SMAs improved filler-rubber interaction in vulcanized NR/silica nanocomposites *via* physical bonding consisting of hydrogen bonding, electrostatic attraction and *Van der Waals* forces, not chemical bonding. Therefore, tensile strength was significantly affected by changing SMA types.
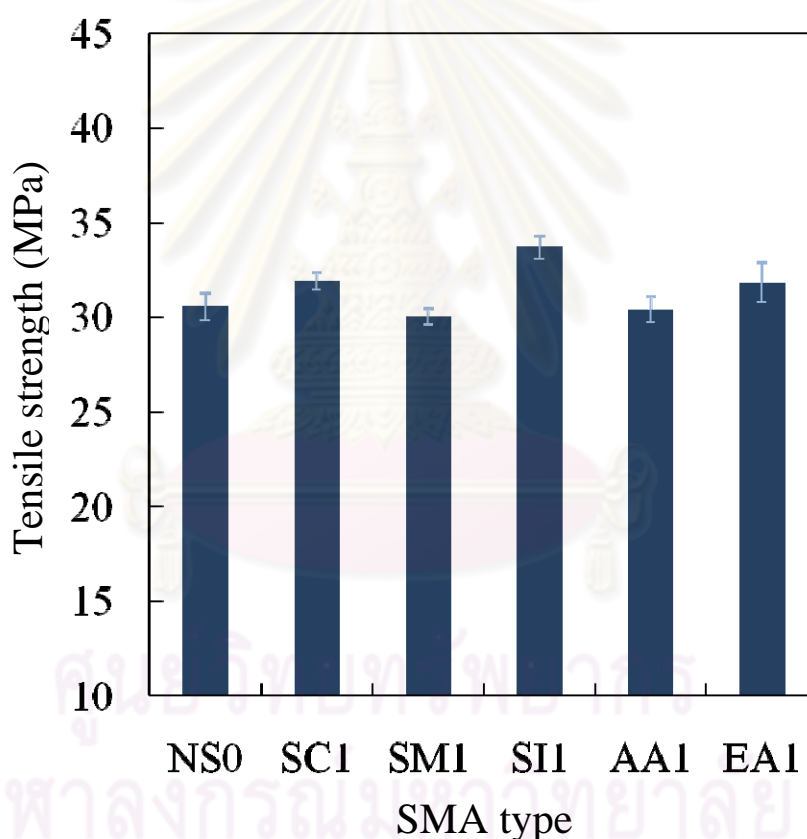
Figure 3.18 The effect of SMA type on tensile strength.

The M300 was also not affected by changing SMA type, Figure 3.19. Nevertheless, M300 of vulcanized NR/silica nanocomposites with presenting SMA treating agents was lower than that of vulcanized NR/silica nanocomposites without SMA, V30-NS0. The presence of SMA treating agents reduced silica surface energy, resulting in decrease filler-filler interaction.
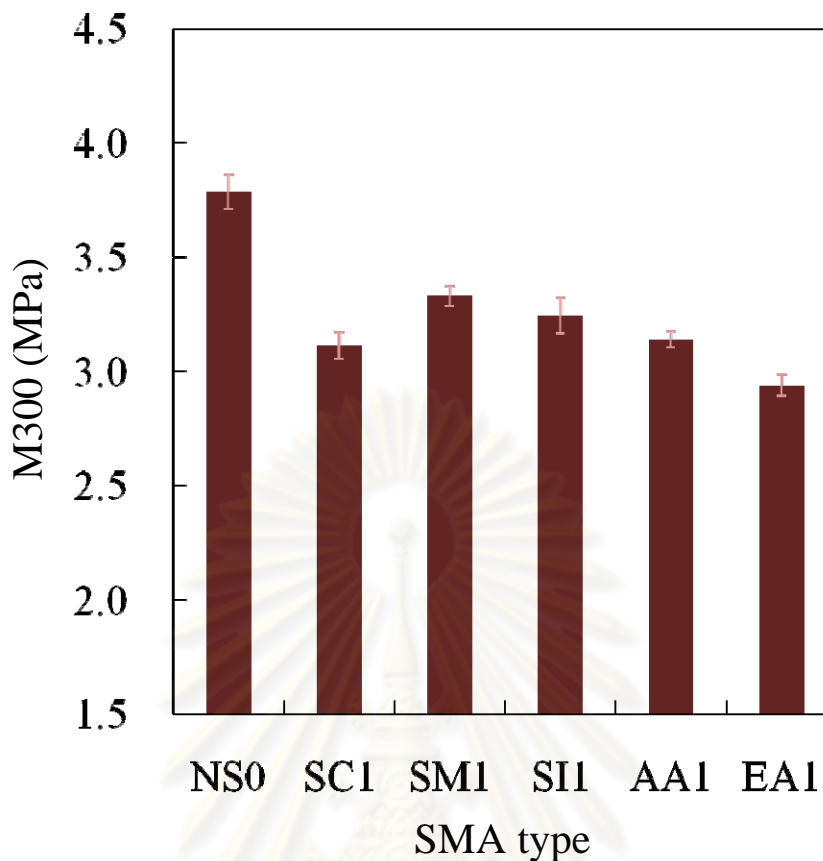
Figure 3.19 The effect of SMA type on M300.

The elongation at break, Figure 3.20, was higher extended when SMA 1000I and SMA 1440F were present. The results might be due to the bulky structure, SMA 1000I bearing normal alkylamine group while SMA 1440F containing three functional groups (maleic anhydride, alkyl ester and carboxylic acid). The bulky structure provided flexible molecule and higher stretching. However, the presence of SMA 7052P, the SMA 1000I derivative, furnished shorter elongation at break than presenting of SMA 1000I and SMA 1440F. It might be because SMA 7052P provided stronger electrostatic attraction with silica particles over hydrogen bonding of SMA 1000I and silica particles. The stronger interaction between SMA and silica demonstrated rigid SMA and shorter elongation at break.

Figure 3.21 exhibits tear strength. It was found that the presence of SMA 1000F provided the highest tear strength because V30-SM1 showed the best silica dispersion over other samples. However, V30-SM5 exhibited the poor abrasion resistance the same as V30-SM7, the presence of SMA 1000MA, Figure 3.22.
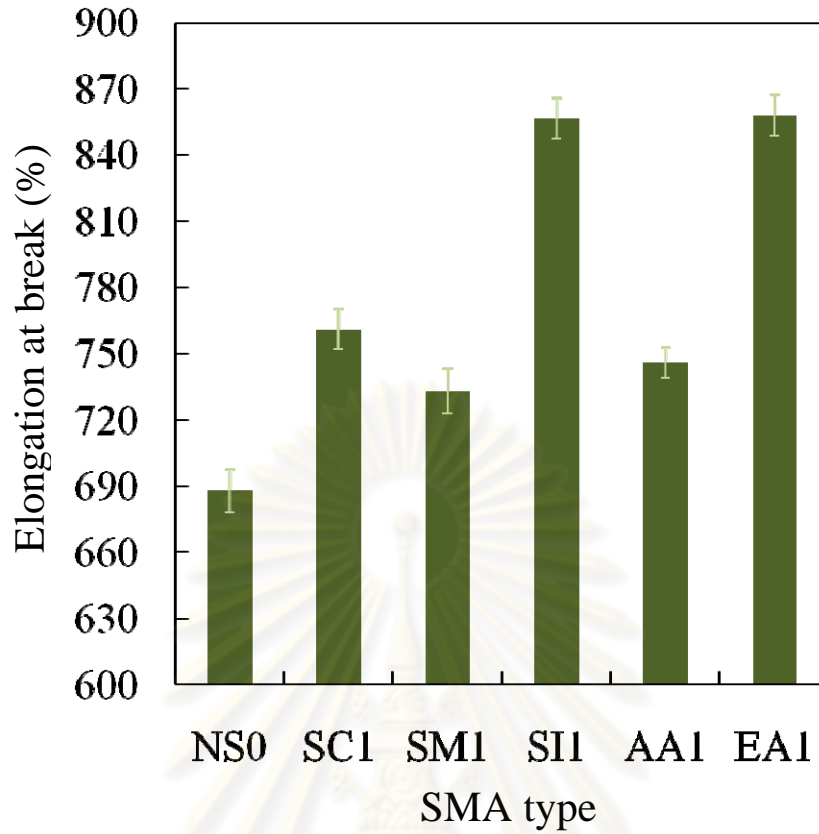
Figure 3.20 The effect of SMA type on elongation at break.
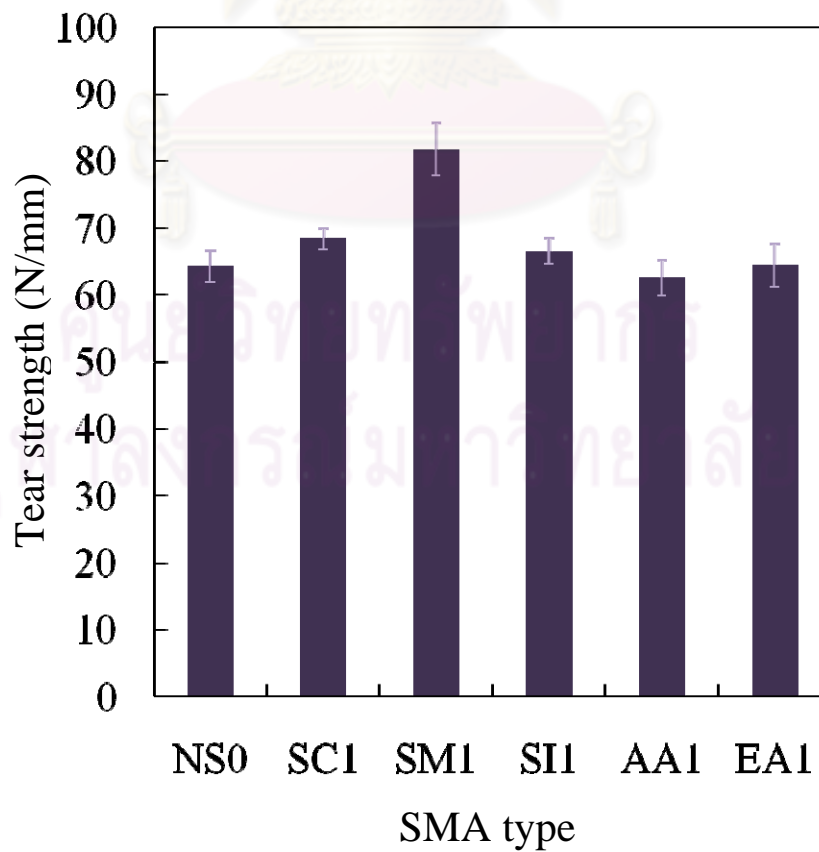
Figure 3.21 The effect of SMA type on tear strength.
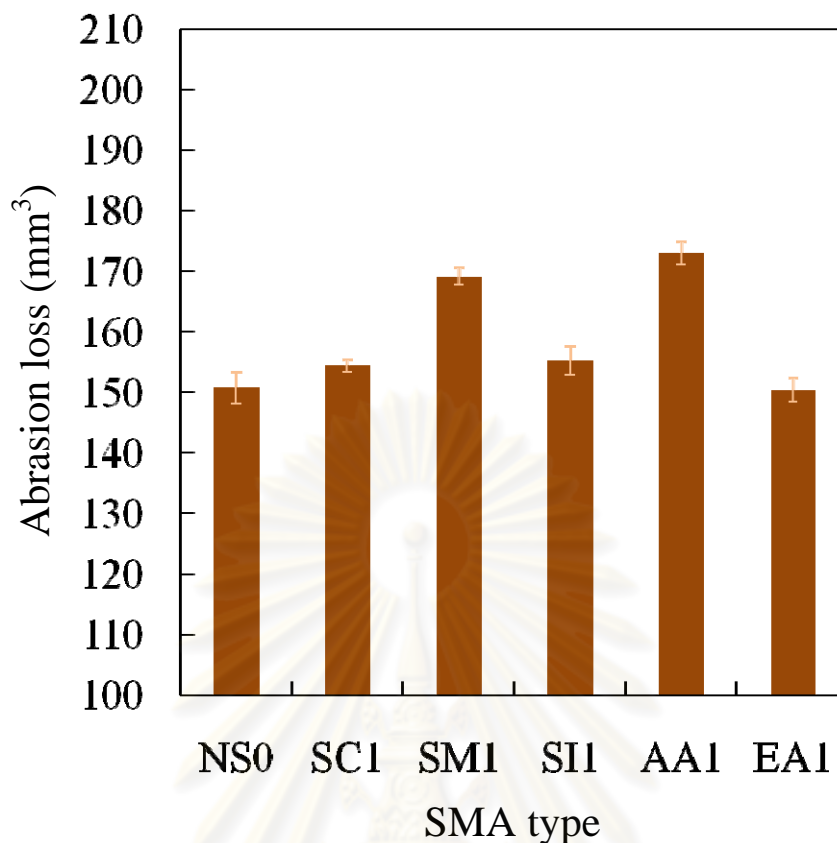
Figure 3.22 The effect of SMA type on abrasion resistance.

In summary, it could be concluded that tensile strength, M300 and abrasion resistance were not improved by changing SMA types. Elongation at break was stretched in the presence of bulky molecular structure of SMA 1000I and SMA 1440F. Tear strength was increased in the presence of SMA 1000F with providing best silica dispersion.

3.4 The effect of silane coupling agents on the properties of nanosilica-filled NR

The effect of silane coupling agents on the properties of vulcanized NR/silica nanocomposites was investigated on silica loading, silane loading and types, couple treating agent between silane and SMA 7052P. Firstly, three types of silica were selected to investigate at variable silica loading consist of original silica (WL180 and powder form), untreated nanosilica slurry and treated nanosilica slurry with Si-69 at constant loading at 10% by weight of silica. Secondly, the variable amount of Si-69 including 1, 3, 5, 10 and 15% by weight of silica was investigated with control silica content at 30 phr. Thirdly, five types of silane coupling agents were selected to study at constant silica content at 30 phr.

The silica surface was modified with silane coupling agents to reduce the polarity as same as polyethylene glycol, PEG 4000, was added to silica reinforced rubber compound. The effect of Si-69 and PEG 4000 ratio on the properties of vulcanized NR/silica nanocomposites was also investigated to explore the relationship of Si-69 and PEG 400.

3.4.1 Effect of treating time and temperature on the of treating efficiency

At first, the treating efficiency was investigated on treating time and temperature. The Si-69 with constant at 10% by weight of silica, treating time 30 min and treating temperature 60ºC were employed as standard treating condition. The treating time, 15-60 min, was counted after adding Si-69. The treating temperature, 60-90ºC, was adjusted by changing cooling water temperature after Si-69 was added. In this experiment, the interaction between silica surface and silane coupling agent could not directly be confirmed by IR and NMR experiments. Therefore, in this research, the treating efficiency was assured by examining in the properties of vulcanized NR/silica nanocomposites.

The effect of treating time and temperature on the properties of nanosilica slurry are demonstrated in Tables A2 and A3 of Appendix A. The results showed that the particle mean size and particle size distribution of nanosilica slurry were not affected by the treating time and temperature. The preparation and properties of NR/silica nanocomposites at variable treating time and temperature are shown in Table B2 of Appendix B.

3.4.1.1 Effect of treating time

The effect of treating time on scorch time, optimum cure time, cure rate index, minimum torque, maximum torque, hardness, mechanical properties and abrasion loss of vulcanized NR/silica nanocomposites are shown in Table 3.1. It could be concluded that the treating time was not affected on curing behavior and mechanical properties of vulcanized NR/silica nanocomposites.

Table 3.1 Treating time as a function of cure behavior, hardness, mechanical properties and abrasion loss of vulcanized NR/silica nanocomposites

Properties	Treating time (min)			
	15	30	45	60
t_s2 (min:sec)	2:33	2:25	2:31	2:28
t_c90 (min:sec)	3:03	2:54	3:01	2:59
CRI[a] (sec^{-1})	3.33	3.45	3.33	3.23
Torque (dN/m)				
ML	3.59	3.59	4.14	3.85
MH	15.70	16.46	16.81	16.73
Hardness (Shore A)	55	58	58	57
TS (MPa)	32.4±1.3	32.3±0.7	32.3±0.9	32.1±0.8
Eb (%)	715.1±18.6	689.2±10.7	722.8±5.2	686.6±4.1
M300 (MPa)	5.49±0.09	5.90±0.07	5.76±0.06	6.36±0.06
Tear (N/mm)	81.0±5.7	84.2±1.0	80.3±2.7	80.3±2.7
Abrasion loss (mm^3)	132.7±2.4	128.8±1.8	123.8±0.6	130.8±3.5

[a] Cure rate index.

3.4.1.2 Effect of treating temperature

The treating temperature as function of scorch time, cure time, cure rate index, minimum torque, maximum torque, hardness, mechanical properties and abrasion loss of vulcanized NR/silica nanocomposites are shown in Table 3.2. The resulting showed that the treating temperature was not affected on curing behavior mechanical properties of vulcanized NR/silica nanocomposites.

Table 3.2 Treating temperature as a function of cure behavior, hardness, mechanical
properties and abrasion loss of vulcanized NR/silica nanocomposites

Properties	Treating temperature (°C)			
	60	**70**	**80**	**90**
t_s2 (min:sec)	2:25	2:21	2:21	2:22
t_c90 (min:sec)	2:54	2:50	2:51	2:37
CRI[a] (sec^{-1})	3.45	3.45	3.33	4.00
Toque (dN/m)				
ML	3.59	2.15	2.54	2.28
MH	16.46	16.07	15.80	15.68
Hardness (Shore A)	58	58	58	56
TS (MPa)	32.3±0.7	32.3±0.2	32.2±0.6	33.0±0.4
Eb (%)	689.2±10.7	659.7±5.2	655.9±8.8	678.2±5.3
M300 (MPa)	5.90±0.07	7.07±0.12	6.93±0.22	6.30±0.18
Tear (N/mm)	84.2±1.0	75.5±1.5	78.6±3.2	77.2±2.9
Abrasion loss (mm^3)	128.8±1.8	131.3±2.3	135.3±3.5	130.4±2.0

[a] Cure rate index.

As mentioned in sections 3.4.1.1 and 3.4.1.2, the effects of treating time and
temperature did not affect on the properties of NR/silica nanocomposites. Therefore,
treating time and temperature at 30 min and 60°C, respectively were selected as the
standard treating condition.

**3.4.2 The comparative study of original silica, untreated nanosilica and Si-69
treated nanosilica on the properties of NR**

The effect of Si-69 treated silica surface on the properties of NR/silica
nanocomposites was investigated and compared with original silica and untreated
nanosilica filled NR. The comparative study was examined in variable silica loading
and surveyed in both uncured and sulfur cured NR/silica nanocomposites.

3.4.2.1 The properties of uncured NR/silica nanocomposites

The preparation and silica content of uncured of untreated and Si-69 treated
nanosilica-filled NR are shown in Table B3 of Appendix B including NC13-NS0,

NC21-NS0, NC34-NS0, NC13-TS10, NC21-TS10 and NC33-TS10. The properties of uncured NR/silica nanocomposites were studied including rheology behavior, stress-stretching ratio relationship, SIC and DMA.

- Filler-filler interaction of uncured NR/silica nanocomposites

The dynamic mechanical property at small strain was attractive to explore Payne effect of filled rubber due to it can be referred to the rolling resistance, that is, the one importance property in tire tread. The mechanism of Payne effect could be explained by Dannenberg's molecular slippage model and progressive destruction of the "filler network" under shear strain [46]. The first one is referred to desorption and resorption model of rubber molecule adsorption onto filler surface [47-52]. The filler with higher surface energy demonstrated the greater rubber molecular adsorption onto the filler surface over the lower one, *i.e.*, increasing bound rubber and decreasing rubber chain mobility. The second one is discussed in terms of the filler network chain density or filler network junction model that assume to filler-filler interaction [53-56]. The higher filler network chain density exhibited the larger Payne property. The filler network chain is annihilated by the appropriate effective strain amplitude.

Figure 3.23 reveals the Dannenberg's molecular slippage model. The rubber molecules were adsorbed onto the filler surface at the equilibrium, no strain, stage (i) in Figure 3.23a. The rubber molecules were progressive extension when strain was applied. As a result, rubber molecules acted as the bridges between filler particles, phase A in Figure 3.23a. At very low strain, the rubber molecules hoarded the macroscopic deformation energy as elastic energy and this energy can be completely recovered after strain decreasing, resorption process.

At higher extension, desorption and resorption were broken down. At the first higher extension, stored elastic energy overpasses adsorption energy and rubber molecules gradually desorbed from the filler surface, stage (iii) and the stars are desorption sites, Figure 3.23b. The rubber molecular bridge segments were lengthened by this desorption. Resulting in, first, storage modulus, G′, was gradually decreased depending on the length of rubber molecular bridges and second, a part of the stored elastic energy in deformed rubber molecules was converted into molecular mobility and mechanically damage.
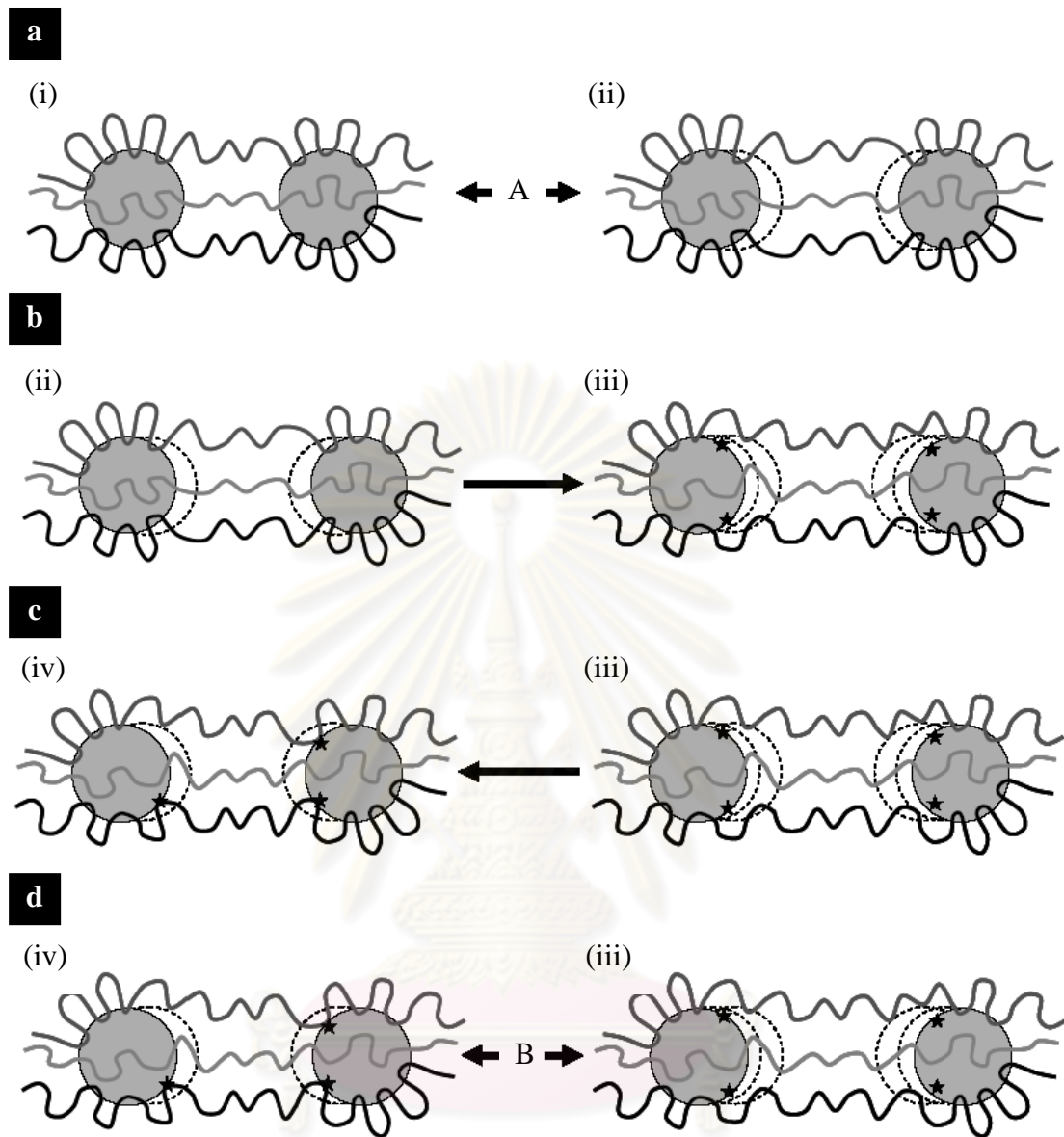
Figure 3.23 The mechanism of Dannenberg's molecular slippage model [46].

The remove of applied strain that instantaneously follows the extension at the higher rate does not accurately lead to initial stage, state (i). Indeed, in the short time of the dynamic deformation cycle, the resorption could not reach the equilibrium state and remains imperfect, as demonstrated by state (iv) in Figure 3.23c. Thus during phase B, the desorption-resorption of the rubber molecular bridges were undergone between pseudo equilibrium states (iii) and (iv), Figure 3.23d. Certainly, rubber molecules desorption were progressively taken place because of the very enlarge interfiller distance distribution that induces an also broad distribution of rubber molecular bridge segments. This explains the smooth decreased of G′, Figure 3.24. A

homogenization of rubber molecular bridge segment lengths was induced by progressively desorption.
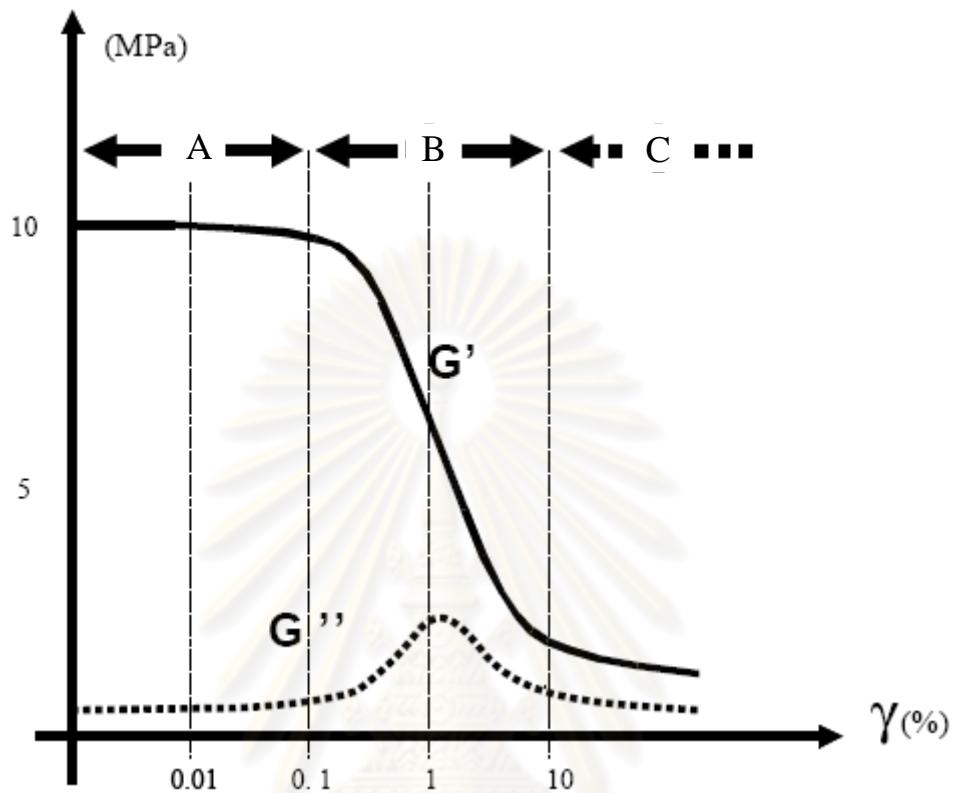
Figure 3.24 Schematic illustration storage modulus (G′) and loss modulus (G′′) dependent on the strain displacement (γ) [46].

The rheology measurement was employed to study the Payne effect of uncured NR/silica nanocomposites. Figure 3.25 displayed the strain displacement as a function of storage modulus (G′) of uncured NR/silica nanocomposites with variable silica content.
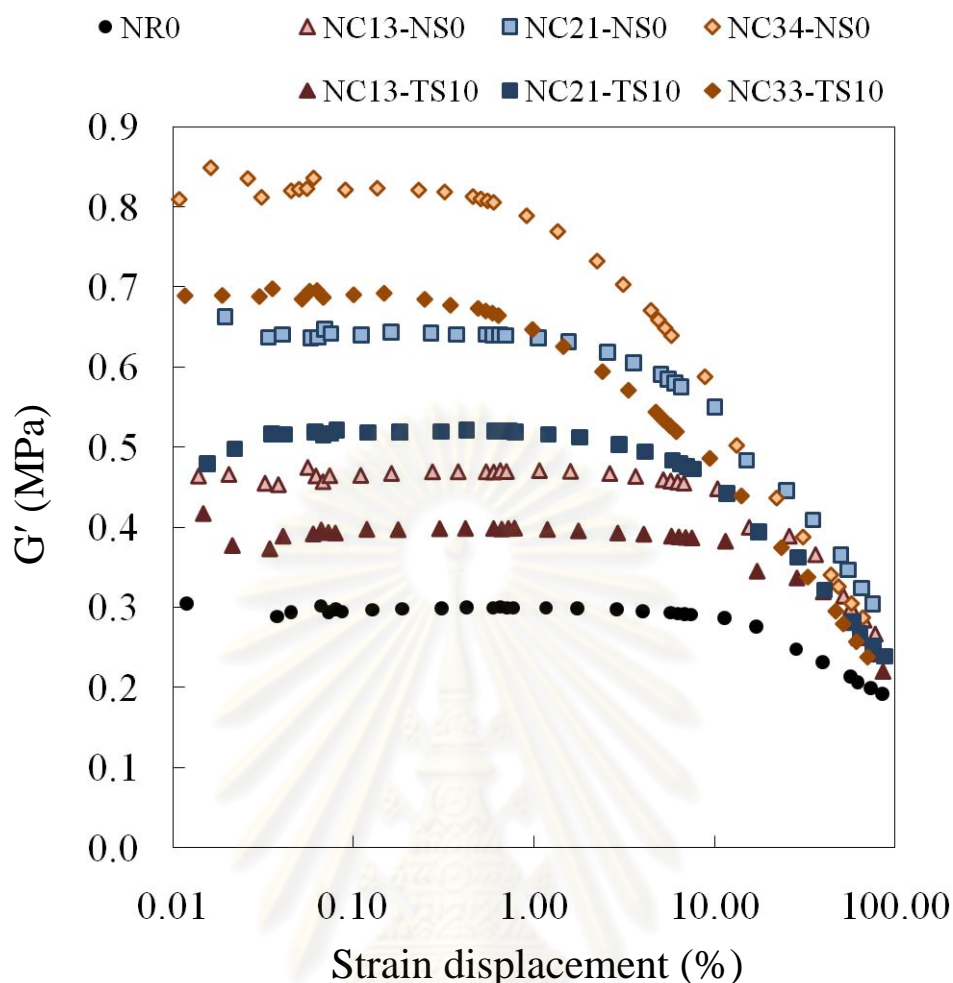
Figure 3.25 The storage modulus (G′) as a function of dynamic strain displacement of uncured NR/silica nanocomposites with variable silica content.

The results clearly showed that, at the low strain (less than 1%), untreated nanosilica-filled NR "NC13-NS0, NC21-NS0 and NC34-NS0" exhibited the higher G′ than Si-69 treated nanosilica-filled NR "NC13-TS10, NC21-TS10 and NC33-TS10". The resulting might be due to the filler-filler interaction of untreated nanosilica-filled NR was stronger than that of Si-69 treated nanosilica-filled NR because of untreated nanosilica had stronger silica surface energy to form stronger filler-filler interaction. In contrast, Si-69 treated nanosilica contains silane coupling agent on the silica surface, resulting in, decreasing the surface and reducing filler-filler interaction. Nevertheless, the filler-filler interaction was demolished which apply the higher strain amplitude, more than 1%, resulting in the G′ was rapidly decreased. Finally, the G′ of all samples were reacted at a same value when the homogeneously silica dispersion was achieved at effectively strain displacement.

Furthermore, the G′ was increased when silica loading was increased in both untrated and Si-69 treated nanosilica-filled NR. Resulting in, the filler network chain and adsorption site were increased regarding to the increasing of silica loading because of, the former, the filler-filler interaction and, the latter, the filler-rubber interaction were enlarged. In other word, the storage modulus was raised up which increasing silica loading. The filler-filler interaction was destroyed by apply the higher strain amplitude.

- Filler-rubber interaction of uncured NR/silica nanocomposites

The stress-stretching ratio relationship, strain induced crystallization (SIC) and dynamic mechanical analysis were corroborated the filler-rubber interaction of uncured NR/silica nanocomposites. The stress-stretching ratio relationship is reveled in Figure 3.26. It was shown that, the untreated nanosilica-filled NR exhibited higher stress than Si-69 treated nanosilica-filled NR at all silica loadings. In addition, the stress was increased according to increasing silica loading because of the increasing of filler-filler interaction.
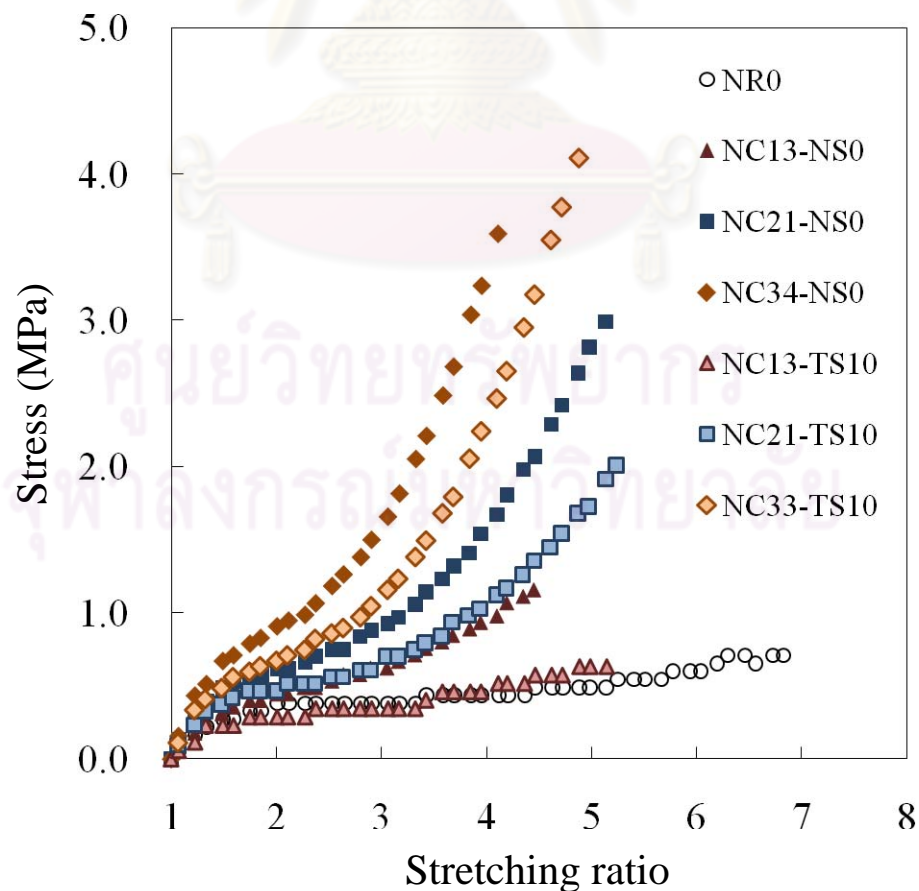
Figure 3.26 The stress-stretching ratio relationship of uncured samples.

According to the untreated nanosilica-filled NR exhibiting higher stress than Si-69 treated nanosilica-filled NR, the SIC was investigated to explain that phenomena. Generally, SIC was attended to study the crystallization of rubber and the molecular rubber chain orientation during deformation because it can be related to mechanical properties of rubber. The early research work has been reported by Katz in 1925, the existence of isotopic amorphous halo under strain of NR using conventional X-ray diffraction [57]. Mitchell, sixty years later, published the orientation of molecular chain in NR vulcanizate by utilizing conventional wide angle X-ray diffraction (WAXD) technique [58]. Nowadays, synchrotron WAXD measurement was intensively employed to study the SIC behavior because it showed a very impressive fraction of isotropic scattering halo under applying stretch, due to the high intensity of X-ray light [59-61]. Therefore, the synchrotron WAXD measurement was applied to study SIC behavior of NR/silica nanocomposites that prepared in this study.

In the previous work which investigated the SIC in both unfilled and filled rubber. It was found that, the onset strain induced crystallization (α^0) and crystallization rate index (CRI) were influenced by many parameters including filler type, specific surface area (SSA) and network chain density (ν). Chenal and coworkers [62, 63], for example, reported that the CRI was increased regarding to increasing SSA and decreasing network chain density in carbon black-filled NR. In silica-filled NR, CRI enlarged with improving network chain density, whereas, α^0 was not affected by filler type, SSA and network chain density in both carbon black and silica-filled NR system at same filler loading. In addition, Ikeda *et al.* investigated the SIC behavior in unfilled NR [64-66]. It was found that in peroxide curing system the increasing network chain density affected to increase CRI while reduce α^0 whereas in sulfur cross-linking system the improved network chain density also increase CRI but not affected on α^0.

In this work, NC34-NS0 and NC33-TS10 were selected to subject in the synchrotron WAXD instrument at BL-40XU beam line in SPring-8, Harima, Japan. The results were calculated from intensity of plane 200 of the WAXD pattern and displayed in Figure 3.27.
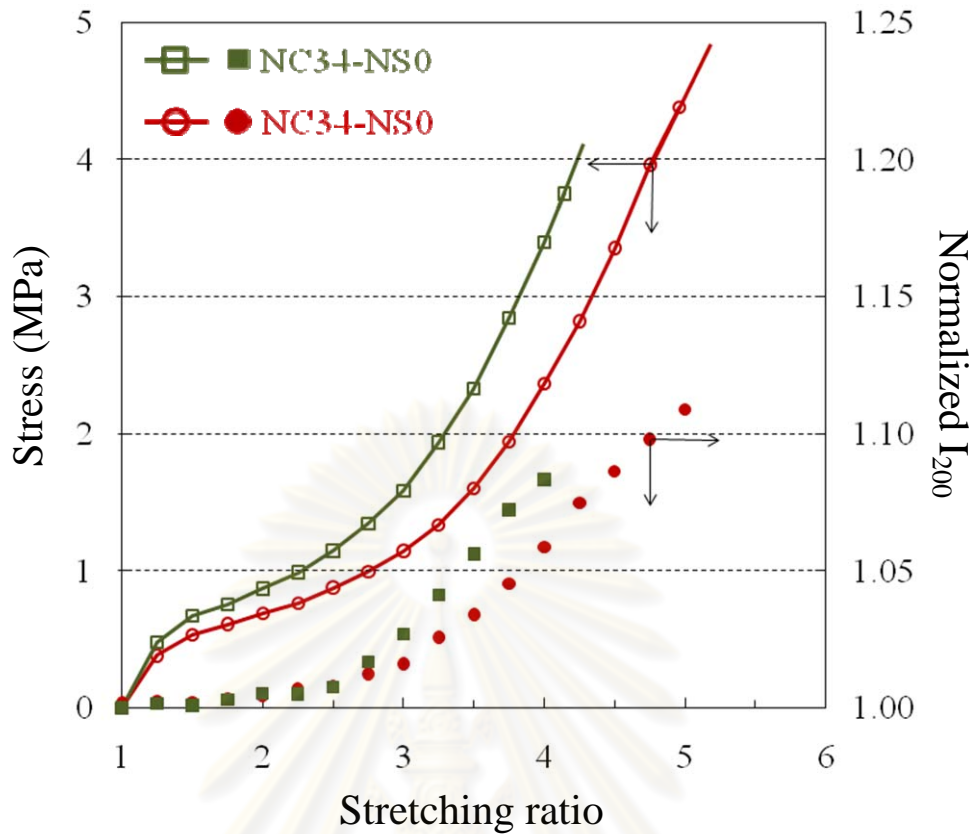
Figure 3.27 The stress as a function of stretching ratio and normalized *I200* showing SIC behaviors for NC34-NS0 and NC33-SL4.

The results clearly showed that the stress results were supported by SIC data. The α^0 of NC34-NS0 was reacted at 2.75 as same as the α^0 of NC33-TS10. Nevertheless, NC34-NS0 demonstrated the higher CRI than that NC33-TS10. It means that NC33-SL4 exhibited better fill-rubber interaction and lower the rubber chain mobility NC34-NS0. The strain-induced crystals were nucleated from the stretching of rubber chain mobility, the higher rubber chain mobility showed the comfortable crystal growth. According to SIC results, it could be concluded that the Si-69 treated nanosilica-filled NR provided better fill-rubber interaction than untreated nanosilica-filled NR. In addition, SIC results were fulfilled the stress-stretching ratio results.

Figure 3.28 displayed the DMA results. The temperature at tan δ_{max}, which is ascribable to T_g, was almost similar to among all samples, Figure 3.28a. The E′ at 25°C of NC34-NS0 exhibited stronger than that of NC33-TS10, referred to stronger filler-filler interaction, Figure 3.28b.
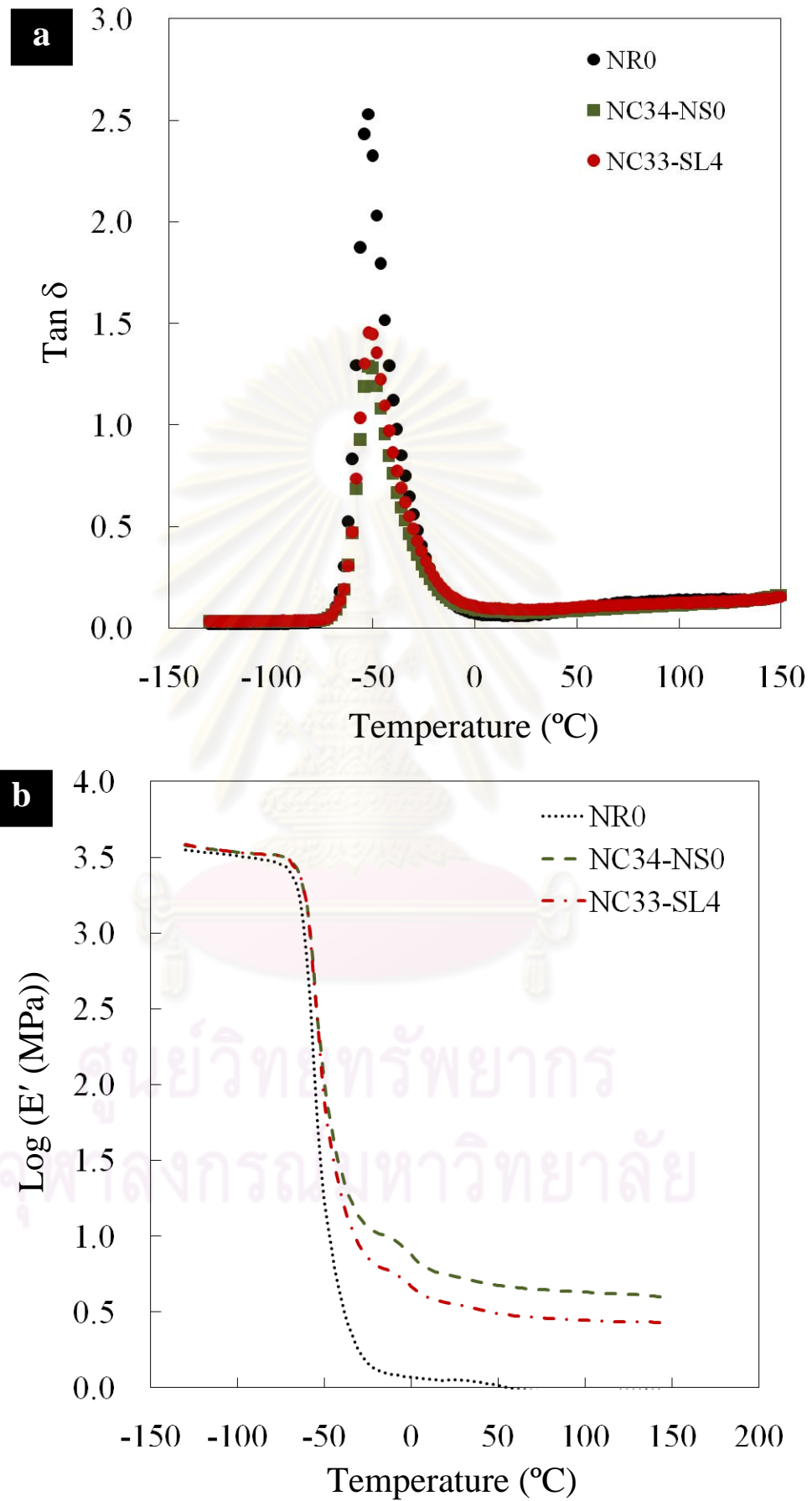
Figure 3.28 Temperature dependence of uncured NR on a) tan δ and b) log E′.

In summary, the untreated nanosilica-filled NR demonstrated the filler-filler interaction over the Si-69 treated nanosilica-filled NR. Whereas the Si-69 treated nanosilica-filled NR manifested filler-rubber interaction overpass the untreated nanosilica-filled NR.

3.4.2.2 The properties of vulcanized NR/silica nanocomposites

The properties of vulcanized NR/silica nanocomposites were investigated on Payne effect, mechanical properties and abrasion loss. The morphology of silica-filled NR was also investigated by SEM. This section, the original silica-filled NR was investigated as standard samples including V10-WL, V20-WL and V30-WL, Table C1 of Appendix C. The untreated and Si-69 treated nanosilica-filled NR vulcanizates were investigated in this study including V10-NS0, V20-NS0, V30-NS0, V10-TS10, V20-TS10 and V30-TS10 that prepared by using NC13-NS0, NC21-NS0, NC34-NS0, NC13-TS10, NC21-TS10 and NC33-TS10, respectively. The curing behavior and hardness of untreated and Si-69 treated nanosilica-filled NR vulcanizates are presented in Tables C2 and C5 of Appendix C, respectively.

SEM analysis for the fractured surface of the vulcanized silica-filled NR having variable silica contents and silica types are exhibited in Figure 3.29. The SEM pictures shown that, the silica particles are displayed as white spots while the darkness area belongs to the rubber matrix. It was found that, when the silica loading was increased, the many white spots were appeared. It was found that the presence of untreated and Si-69 treated nanosilica could not improve silica dispersion. Furthermore, a little amount of aggregation form is also presented. The presence of aggregation form might be due to the acid induce re-aggregation process during the preparation of NR/silica nanocomposites, however, the aggregation form was disappeared when the silica loading was raised up to 30 phr in both untreated and Si-69 treated nanosilica.

The Payne effect was also investigated in NR vulcanizates. Figure 3.30 exposed the G′ as a function of the dynamic strain displacement of unfilled NR vulcanizate (VNR) comparable with original silica-filled NR vulcanizates (WL), untreated nanosilica-filled NR vulcanizates (NS0) and Si-69 treated nanosilica-filled NR vulcanizates (TS10) at variable silica loading including 10 , 20 and 30 phr.
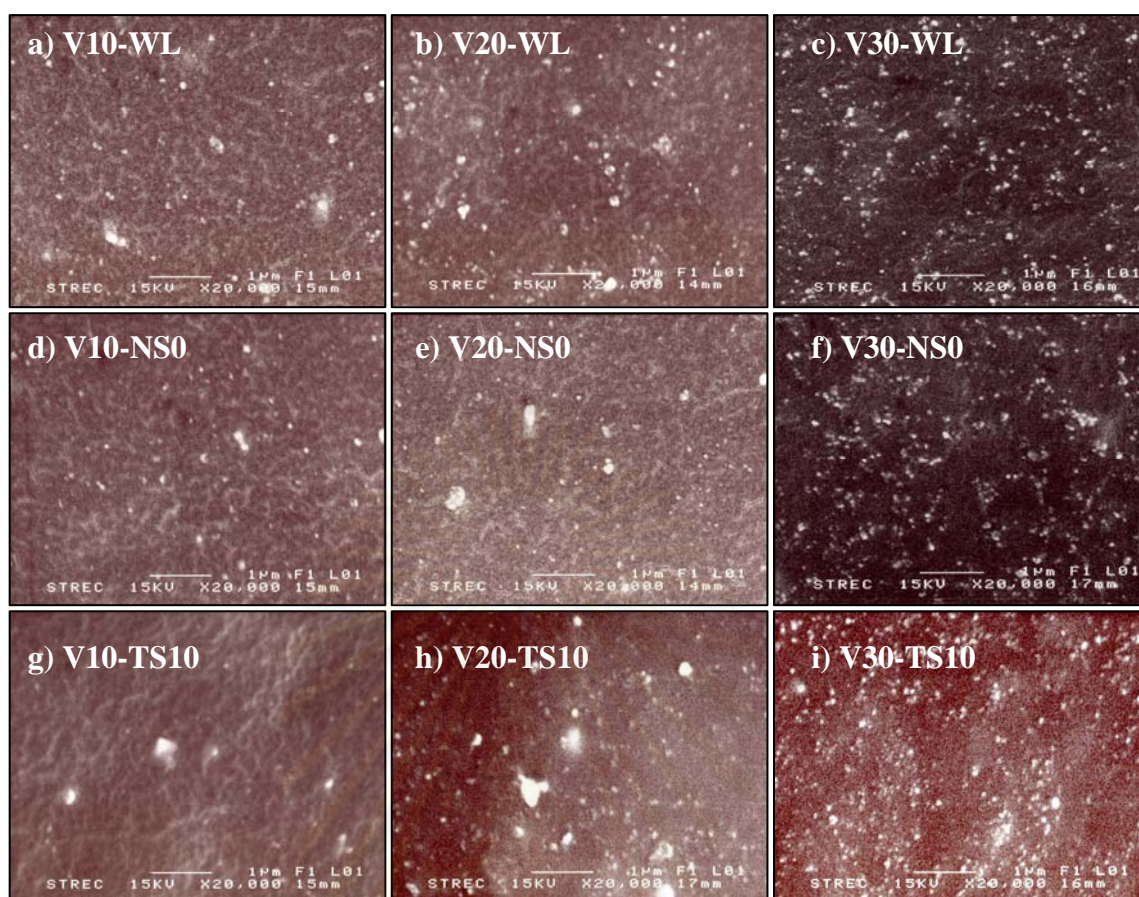
Figure 3.29 SEM pictures of the fractured surfaces of the vulcanized NR at variable silica content.

The results exhibited a different trend from the uncured one. At the low strain, < 1%, the Si-69 treated nanosilica-filled NR vulcanizates shown highest G′ at low silica loading, 10 and 20 phr, overpass the original silica-filled NR vulcanizates and untreated nanosilica-filled NR vulcanizates whereas the lowest G′ at high silica loading, 30 phr, was appeared, Figure 3.30. The results might be due to at low silica loading, the strong filler-rubber interaction in Si-69 treated nanosilica-filled NR vulcanizates was achieved from precipitating in vulcanizing reaction of the organo functional group on Si-69, in addition, the triethoxy silanes were reached with silanol groups on the silica surface, resulting in the higher G′. While, at the high silica loading, original silica-filled NR vulcanizate and untreated nanosilica-filled NR vulcanizate were consisted of higher filler network chain that provide by the shear stress during mixing process, affect on, higher filler-filler interaction and rise up G′. Nevertheless, at the high strain, > 1%, the G′ of original silica-filled NR vulcanizate and untreated nanosilica-filled NR vulcanizate was lower than that of Si-69 treated

nanosilica-filled NR vulcanizate due to the filler network chain, filler-filler interaction, was destroyed during the deformation process whereas Si-69 treated nanosilica-filled NR vulcanizate remained filler-rubber interaction, resulting in, the keeping the G′. It was noticed that, from the Payne results, the G′ of original silica-filled NR vucanizates was stronger than untreated nanosilica-filled NR vucanizates at all silica loading. The results might be due to original silica-filled NR vucanizate contained higher filler-filler interaction and lower silica dispersion than untreated nanosilica-filled NR vucanizate. Moreover, the rapidly decreasing G′ of original silica-filled NR vucanizate exhibited higher silica aggregation over untreated nanosilica-filled NR vucanizate. It could assume that, the NR/silica nanocomposites that prepared in this study provided better silica dispersion over the silica-filled NR that prepared by conventional mixing process.
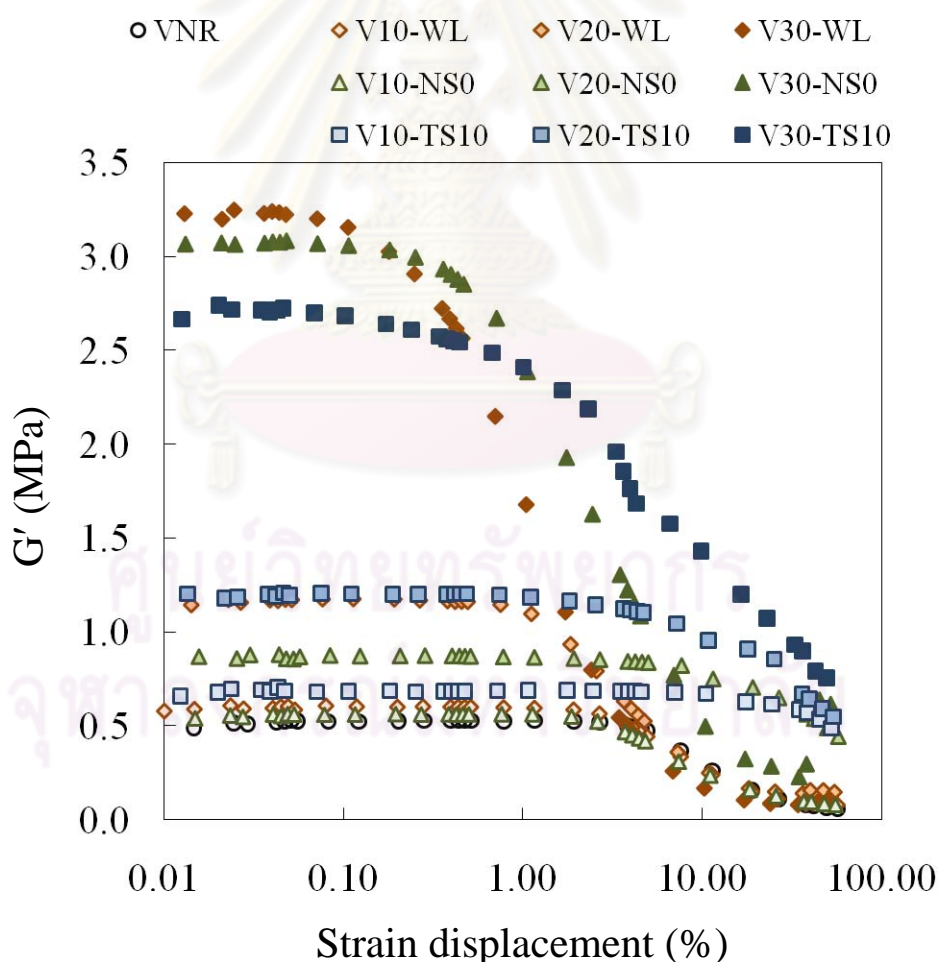
Figure 3.30 The comparative studies on the storage modulus (G′) as a function of the strain displacement of unfilled NR and silica-filled NR vulcanizates with variable silica type and silica loading.
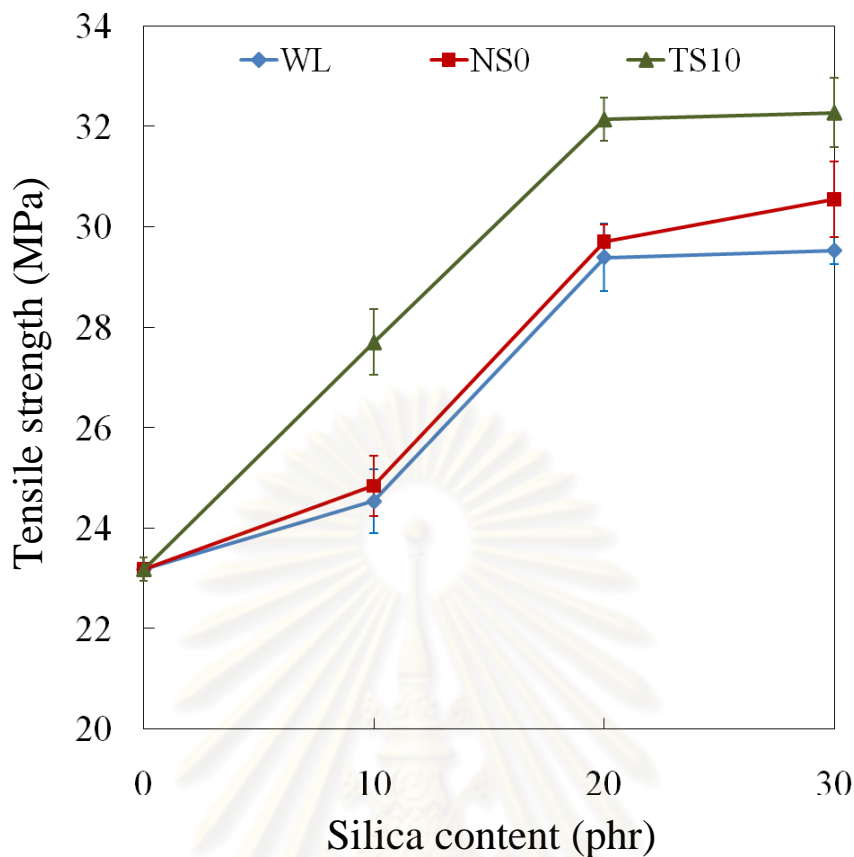
Figure 3.31 The influence of silica contents on tensile strength.

The effect of silica types and silica loadings on the mechanical properties of silica-filled NR vulcanizates were investigated on tensile strength, M300, elongation at break, tear strength and abrasion loss. Their properties of vulcanized NR were attracted by changing the silica loading and type of silica. Figure 3.31 displayed the effect of silica loading on tensile strength of variable silica types. The results shown that, tensile strength or strength at break increased with rising of silica but its tendency was rather remain constant over 30 phr at about 30.6 MPa for nanosilica-filled NR and 32.3 MPa for treated one. In addition, regarding to the tensile results in Section 3.3.1, the tensile strength weaken when the excess amount of silica was added perhaps because of silica aggregation. Moreover, the Payne study revealed that the stronger filler-rubber interaction and lower silica aggregation in Si-69 treated nanosilica-filled, resulting in, Si-69 treated nanosilica-filled NR vulcanizates exhibited stronger tensile strength than untreated nanosilica-filled NR vulcanizates and original silica-filled NR vulcanizates, respectively. In additonn, untreated nanosilica-filled NR vulcanizates had slightly stronger tensile strength than original silica-filled NR vulcanizates because it had lower silica aggregation.

The M300 of silica reinforced NR vulcanizates with variable silica loading are summarized in Figure 3.32. When the silica loading was raised, M300 was increased. Exclusively, in the presence of Si-69, M300 closely increased to threefold from 2.2 to 5.9 MPa when the silica content was increased from 0 to 30 phr. The greatest M300 of Si-69 treated nanosilica-filled NR vulcanizates was explained by dominating stronger filler-rubber interaction via covalent bond.
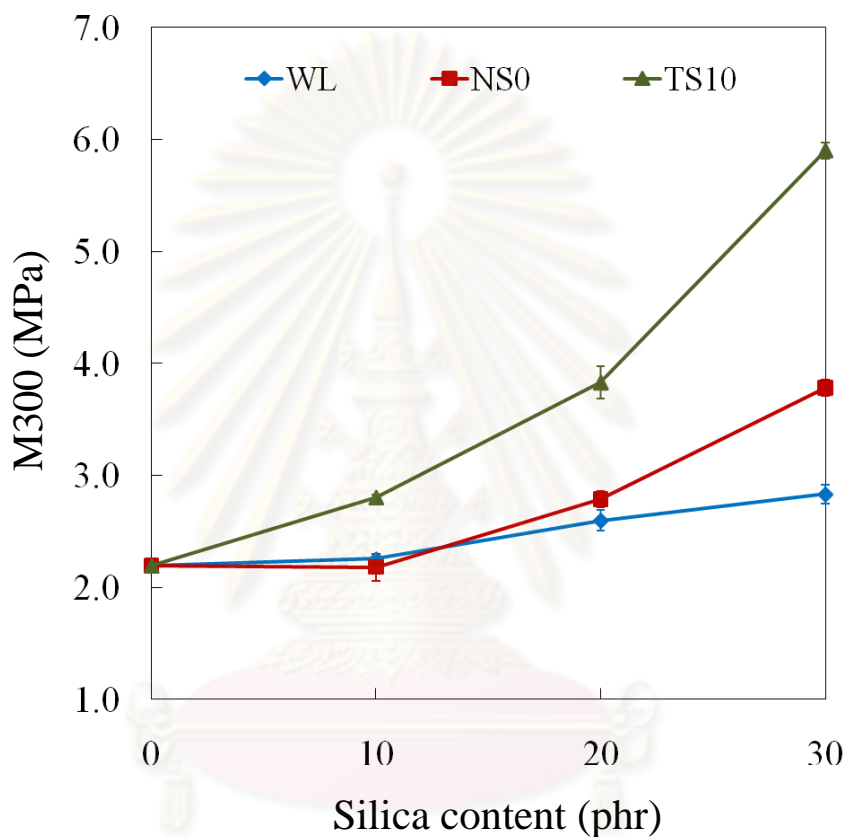
Figure 3.32 The influence of silica contents on M300.

Figure 3.33 displays the elongation at break of silica reinforced NR vulcanizates. The results showed that NS0 and TS10 exhibited elongation at break over WL except at silica loading 30 phr. It might be because, at silica loading 30 phr, V30-WL had higher silica aggregation and lower cross-linked density than V30-WL V30-NS0 and V30-TS10, respectively, resulting in lower filler-rubber interaction. The lower filler-rubber interaction related to higher rubber molecular chain mobility. As a result, it could be deform with longer elongation.
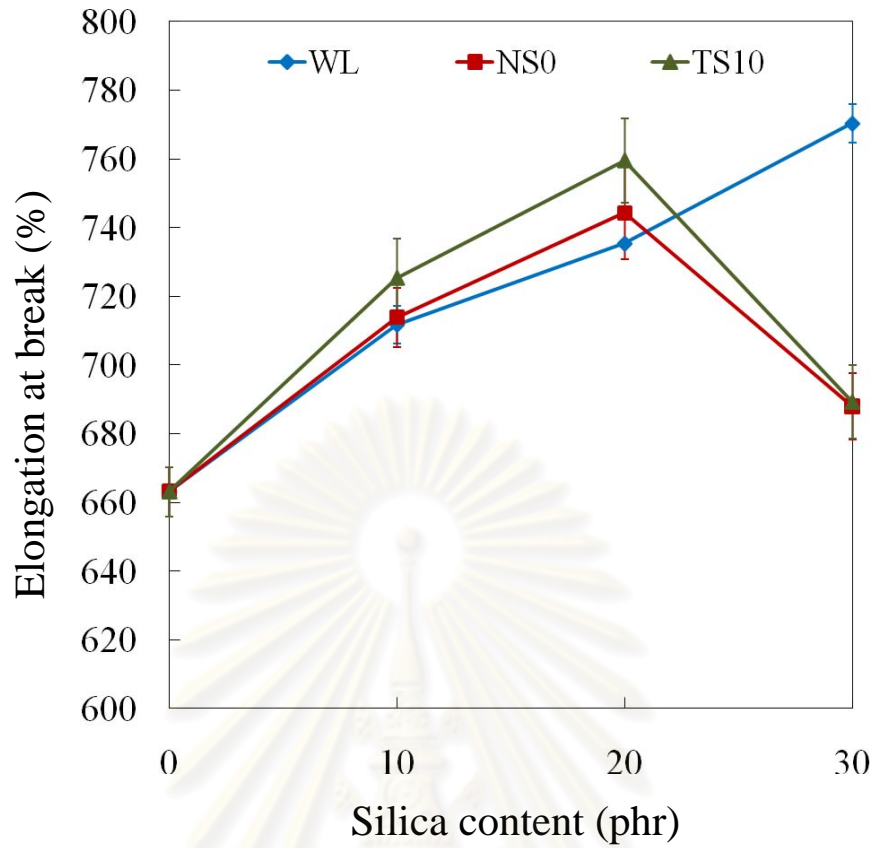
Figure 3.33 The influence of silica contents on elongation at break.
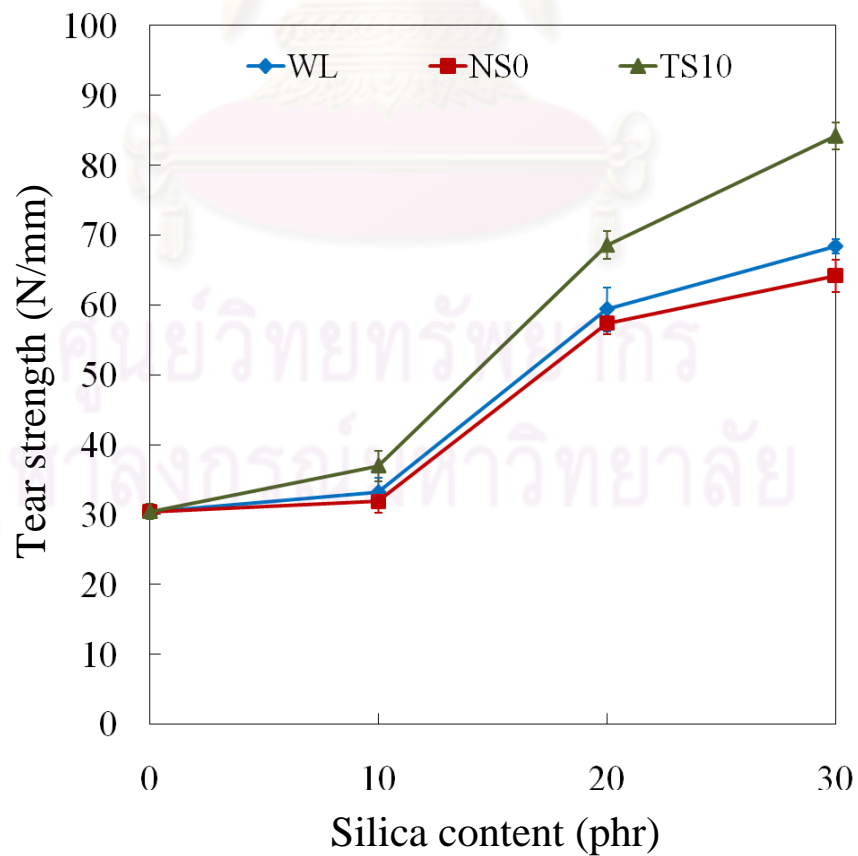
Figure 3.34 The influence of silica contents on tear strength.

Similar to tensile strength and M300, tear strength was improved by increasing silica loading and presenting of Si-69 with stronger filler-rubber interaction and lower silica aggregation, Figure 3.34. M300 of Si-69 treated nanosilica-filled NR vulcanizates was also increased nearly threefold from 30.4 to 84.2 N/mm when the silica content was raised up from 0 to 30 phr for the Si-69 treated nanosilica-filled NR vulcanizates.

The abrasion loss of the silica-filled NR vulcanizates is revealed in Figure 3.35. The results showed that the tendency of abrasion loss was improved when silica content increased, extremely in the appearance of Si-69. It might be due to Si-69 treated nanosilica-filled NR vulcanizates had stronger filler-rubber interaction and lower silica aggregation. In addition, Rattanasom *et al.* [67] has been reported that abrasion resistance is controlled by the modulus of the vulcanizate. Higher modulus grants the vulcanizates with better abrasion resistance. For the Si-69 treated nanosilica-filled NR vulcanizates, the results resemble to agree well with the moduli.
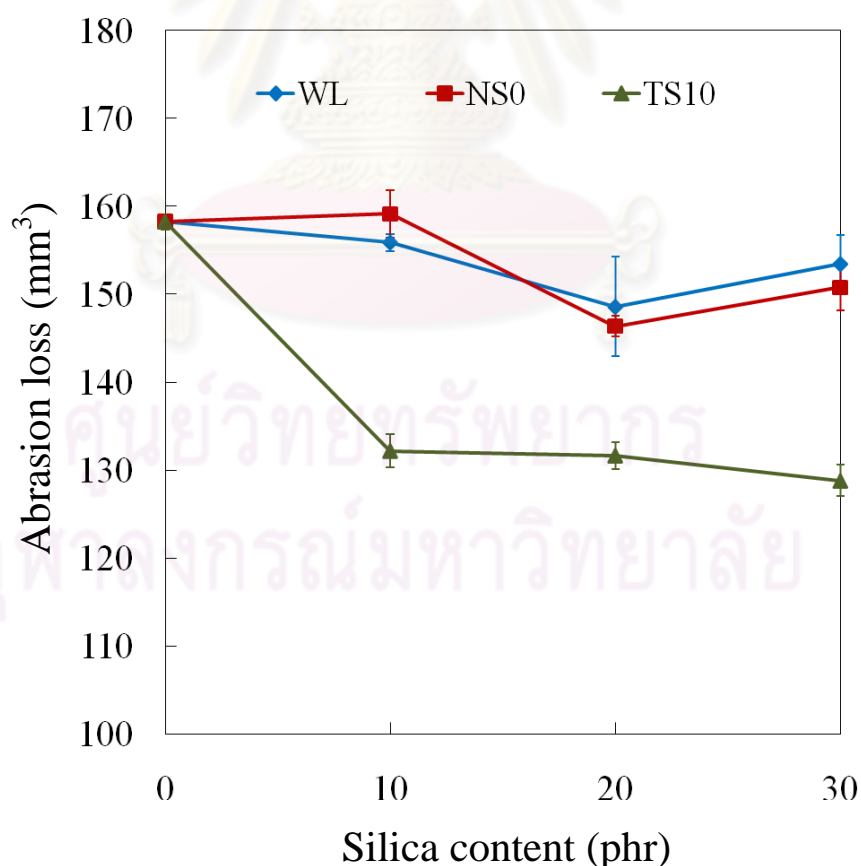
Figure 3.35 The influence of silica contents on abrasion resistance.

In summary, silica types and silica loadings on the properties of vulcanized NR/silica nanocomposites, the presence of Si-69 could improve the mechanical properties of vulcanized NR/silica nanocomposites. The Payne study showed that WL and NS0 exhibited strong filler-filler interaction over TS10 at silica content 30 phr.

3.4.3 The effect of Si-69 loading

The effects of Si-69 loading on the properties of nanosilica-filled NR were surveyed at 0, 1, 3, 5, 10 and 15% by weight of silica. In this section, the experimental study was investigated on the effect of Si-69 loading on the properties of unvulcanized and vulcanized nanosilica-filled NR.

3.4.3.1 The properties of unvulcanized NR/silica nanocomposites

The filler-filler and filler-rubber interactions of nanosilica-filled NR were investigated on the Payne effect and DMA to study the effect of Si-69 loading. The results are demonstrated in Figures 3.36 and 3.37, respectively.

The study of effect of Si-69 loading on the Payne effect exposed that, the Si-69 loading at 10% by weight granted the lowest G′, refer to, the lowest filler-filler interaction and silica aggregation. In addition, the presence of Si-69 below 10% by weight of silica exposed the higher silica aggregation and filler-filler interaction.

The DMA results revealed the similar tan δ_{max}, it mean, T_g of unvulcanized nanosilica-filled NR was not affected by Si-69 loading, Figure 3.36. In addition, the temperature dependence on log E′ shown that, The Si-69 loading at 10% by weight of silica exhibited the best silica dispersion while the SI-69 loading at 3% by weight of silica provided the cheapest silica dispersion.

In summary, it could be concluded that the lowest filler-filler interaction and highest filler-rubber interaction were achieved which presented Si-69 at 10% by weight of silica.
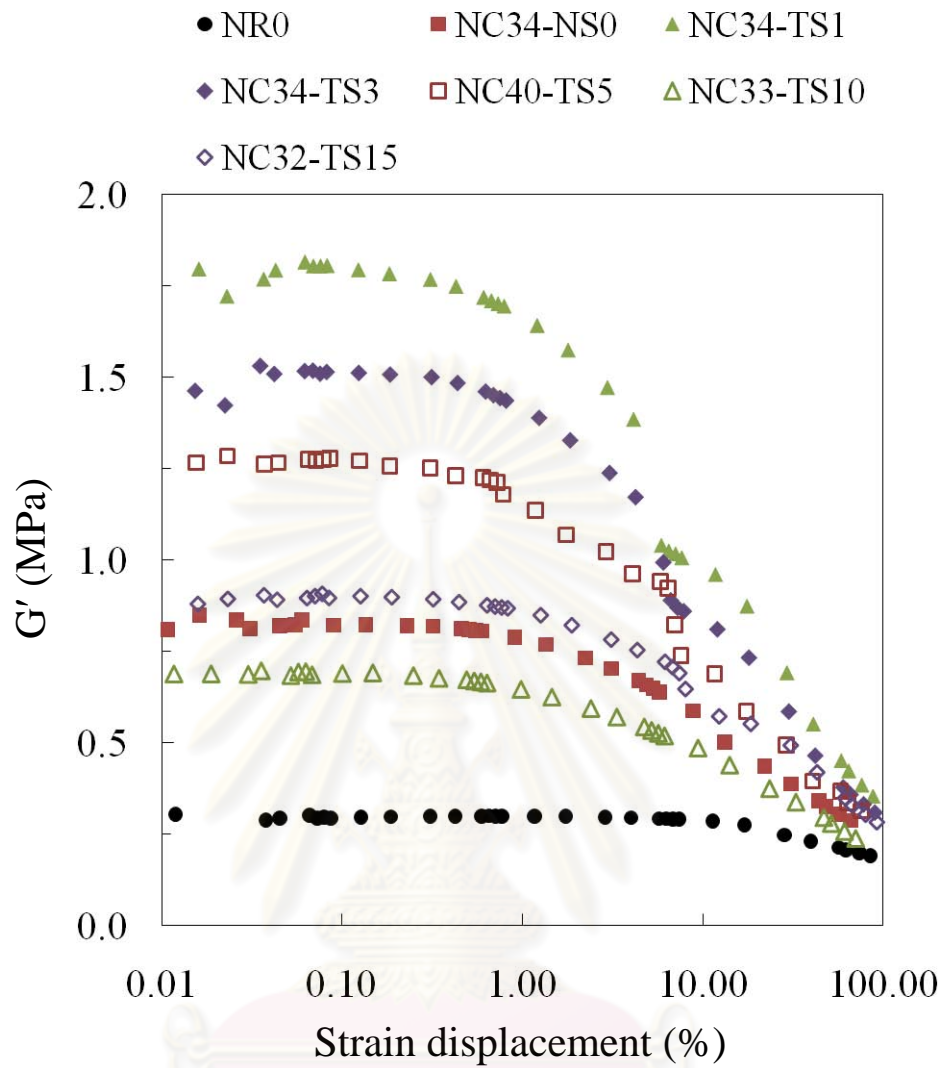
Figure 3.36 Comparative studies on the storage modulus (G′) as a function of the strain displacement (%) of uncured of unfilled NR and nanosilica-filled NR with variable Si-69 loading.
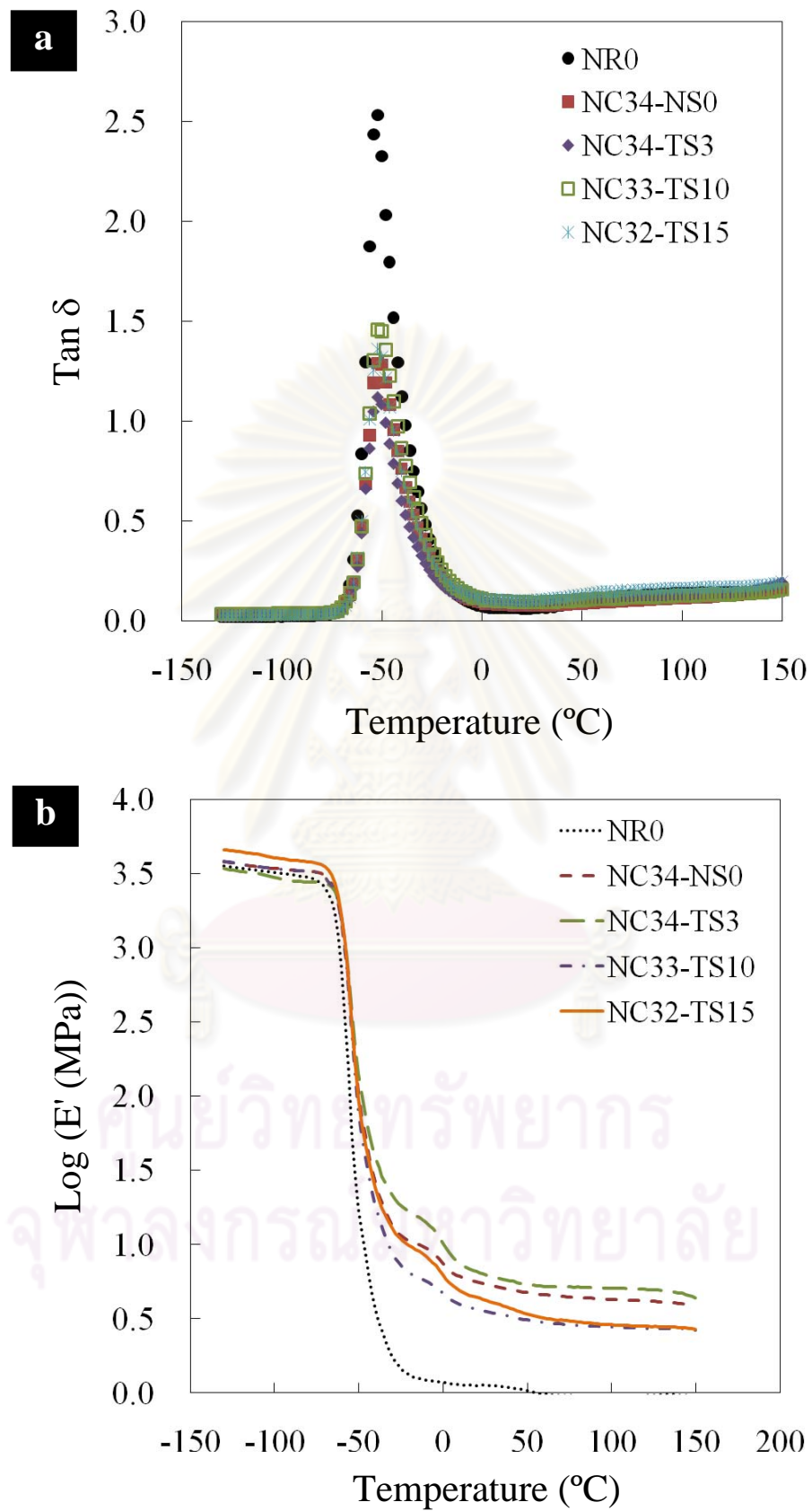
Figure 3.37 Temperature dependence of uncured NR on a) tan δ and b) log E' with variable Si-69 loading.

3.4.3.2 The properties of sulfur cross-linked NR/silica nanocomposites

The effect of Si-69 loading on the properties of vulcanized NR/silica nanocomposites were investigated on mechanical properties and abrasion loss. The untreated and Si-69 treated nanosilica-filled NR vulcanizates were investigated in this study including V30-NS0, VL30-TS1, V30-TS3, V30-TS5, V30-TS10 and V30-TS15 and referred to Si-69 loading at 0, 1, 3, 5, 10 and 15% by weight of silica, respectively. In addition, the effect of couple treating agent between Si-69 and SMA 7052P was also investigated. The amount of SMA 7052P loading was fixed at 1% by weight of silica. The curing behavior and hardness of VL30-TS1, V30-TS3, V30-TS5, V30-TS10 and V30-TS15 are presented in Table C5 of Appendix C whereas Table C6 of appendix C displayed the curing behavior and hardness of V30-SC1, VL30-SL1P, V30-SL2P, V30-SL3P, V30-SL4P and V30-SL5P.

The outcomes of Si-69 treated nanosilica on silica-filled NR vulcanizates were examined for silica dispersion by utilizing SEM. The fractured surfaces of the vulcanized silica-filled NR gotten ready with variable amounts of Si-69 are shown in Figure 3.38. The micrographs of vulcanized nanosilica-filled NR were revealed that the aggregation form was presented when Si-69 was added, comparing with untreated one. This might be due to Si-69 contain two active triethoxysilane groups. In the case of low Si-69 loading, the active sites of Si-69 vary small when compared with silanol group on silica surface. Resulting in, it could react with difference silica particles and induced silica aggregation. This incident will be decrease in higher Si-69 loading, the excess amount of Si-69 prevented, by steric hindrance effect, to react with difference silica particles. In other word, Si-69 reacted with first silica particle but could not react with other one because other Si-69 already reacted on that silica surface. It was found that, the micrographs showed the reducing of aggregated form, decreasing in white spot size, when Si-69 was increased.
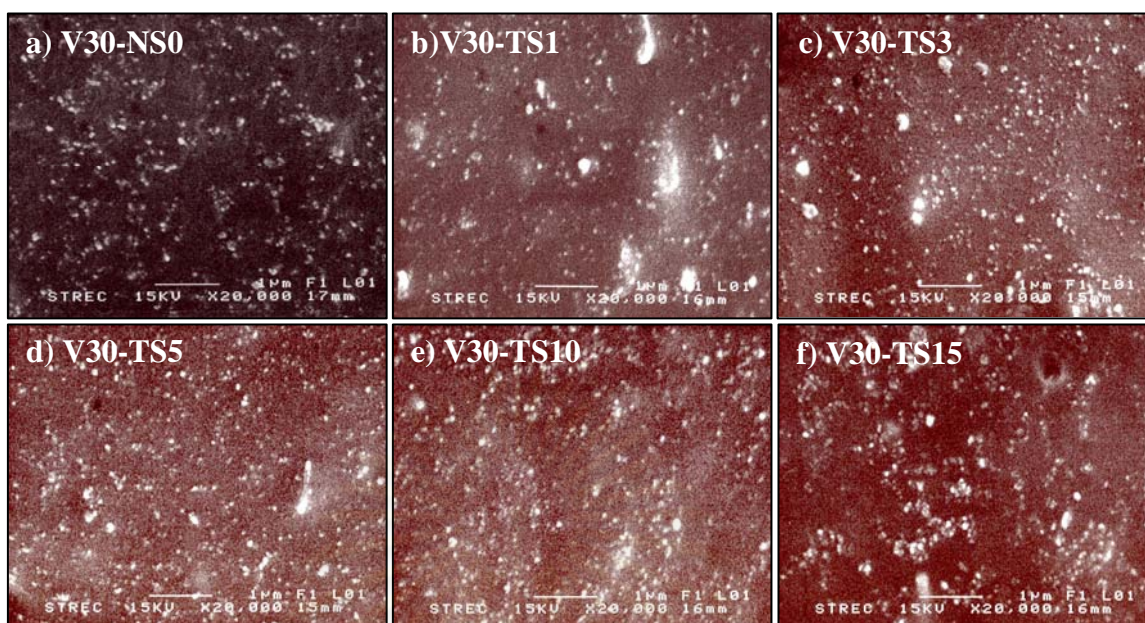
Figure 3.38 SEM micrographs of the vulcanized NR at 30 phr silica loading with variable Si-69 loading.
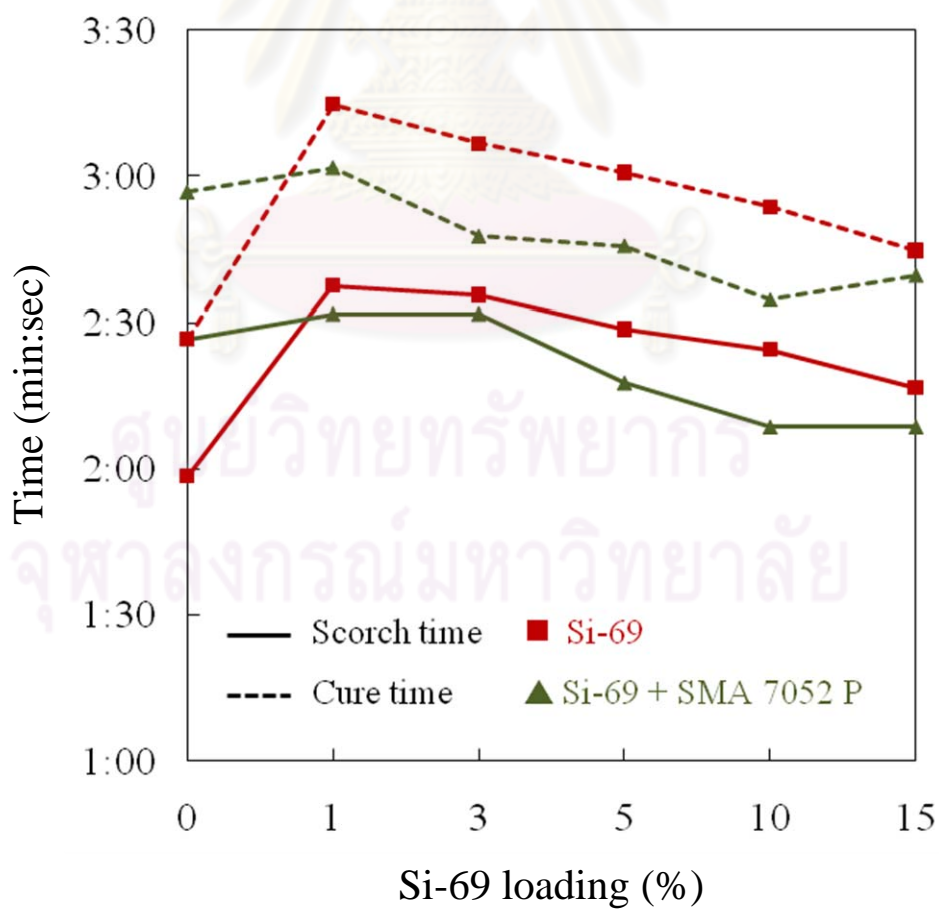
Figure 3.39 Curing characteristics of sulfur cross-linked nanosilica-filled NR.

Figure 3.39 represents the effect of Si-69 on curing characteristics of vulcanized nanosilica-filled NR. As the resulting, the addition of Si-69 reduces both scorch time (t_s2) and optimum cure time (t_c90). The curing behavior results were regarded to the results that achieve in the effect of SMA 7052P loading on curing behavior, Section 3.3.2. In the presence of silane coupling agent, the partial silanol groups was reacted with alkoxy siloxane. Resulted in, the amount of trapped cure activator is decreased. Resulting in, both scorch time and optimum cure time were reduced with increasing Si-69. Similar results were also observed by other workers [41, 42], Sae-oui P. et al. reported that the scorch time and optimum cure time are reduced with raising silane coupling agent in both conventional vulcanization (CV) and efficient vulcanization (EV) system. In addiotn, the presence of SMA 7052P also affected to the curing behavior, the scorch time and optimum cure time were diminished when the SMA 7052P was added at all Si-69 loading.

The effect of Si-69 on tensile strength of the nanosilica-filled NR vulcanizates is displayed in Figure 3.40. It was observed that the tensile strength gradually extended with increasing Si-69 content. The improvement of tensile strength with increasing silane loading is brought about by the combination of two factors, the improved filler-rubber interaction and filler dispersion (as mention in the Payne effect of uncured NR). In addition, the presence of SMA 7052P was not significantly affected on tensile strength of Si-69 treated nanosilica-filled NR vulcanizates. The tensile property was slightly decreased except at 10% Si-69 loading which presented SMA 7052P.

The result of M300 is shown in Figure 3.41, M300 continuously increased with raising Si-69 loading. Similarly to the result of tensile strength, M300 result was developed by improving the filler-rubber interaction. The presence of Si-69 induced the formation of strong bonding between Si-69 and rubber molecules to improve filler-rubber interaction and prevent the recombination of filler aggregates after mixing to achieve better silica dispersion, especially, in high Si-69 loading. Whereas the presence of SMA 7052P was also slightly affected on M300 of Si-69 treated nanosilica-filled NR vulcanizates.
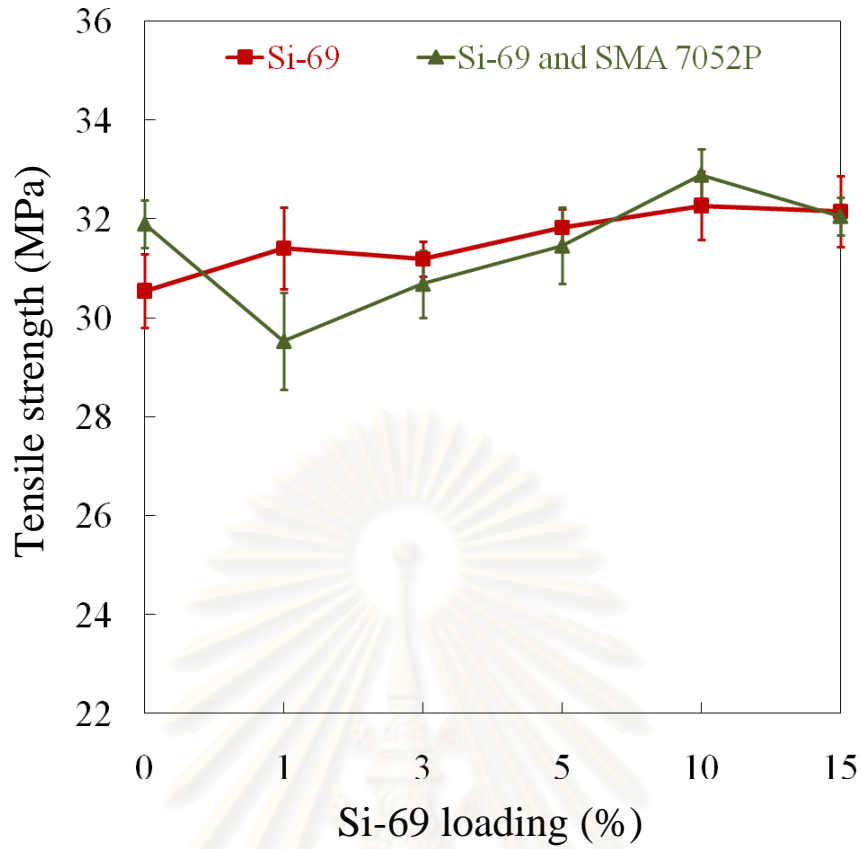
Figure 3.40 The effect of Si-69 loading on tensile strength.
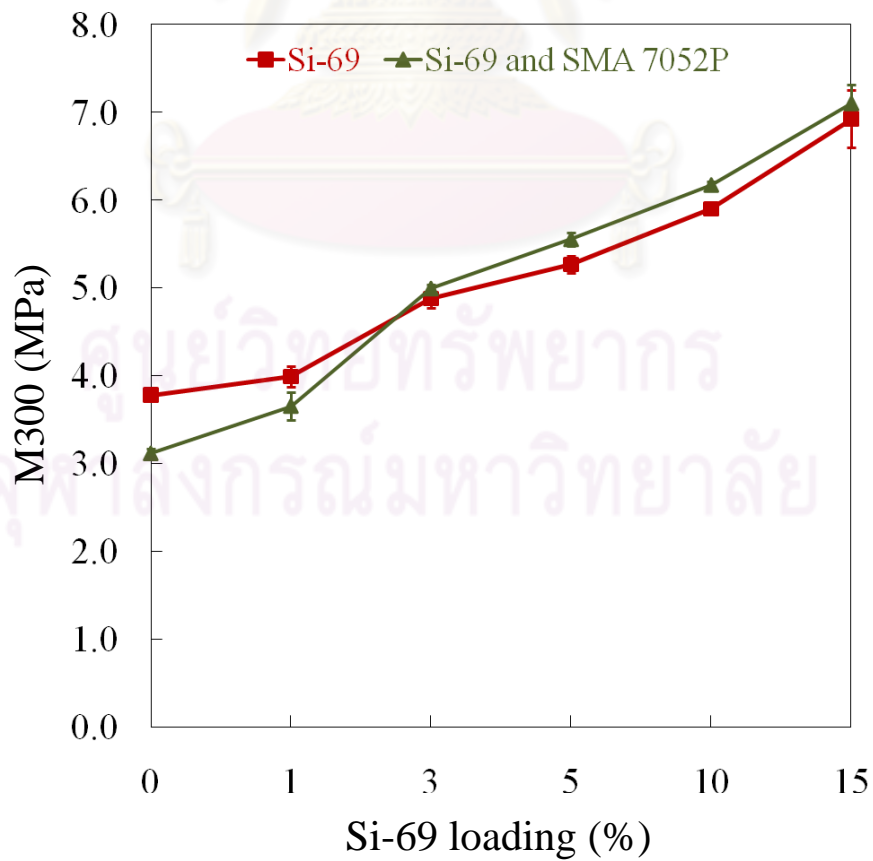
Figure 3.41 The effect of Si-69 loading on M300.

Elongation at break of nanosilica-filled NR vulcanizates is exhibited in Figure 3.42. As can be seen, the elongation at break tends to decrease with increasing silane coupling agent content. The results might be due to cross-linking density was increased with increasing Si-69. Similarly to the tensile strength and M300, elongation at break was insignificantly effect by SMA 7052P.
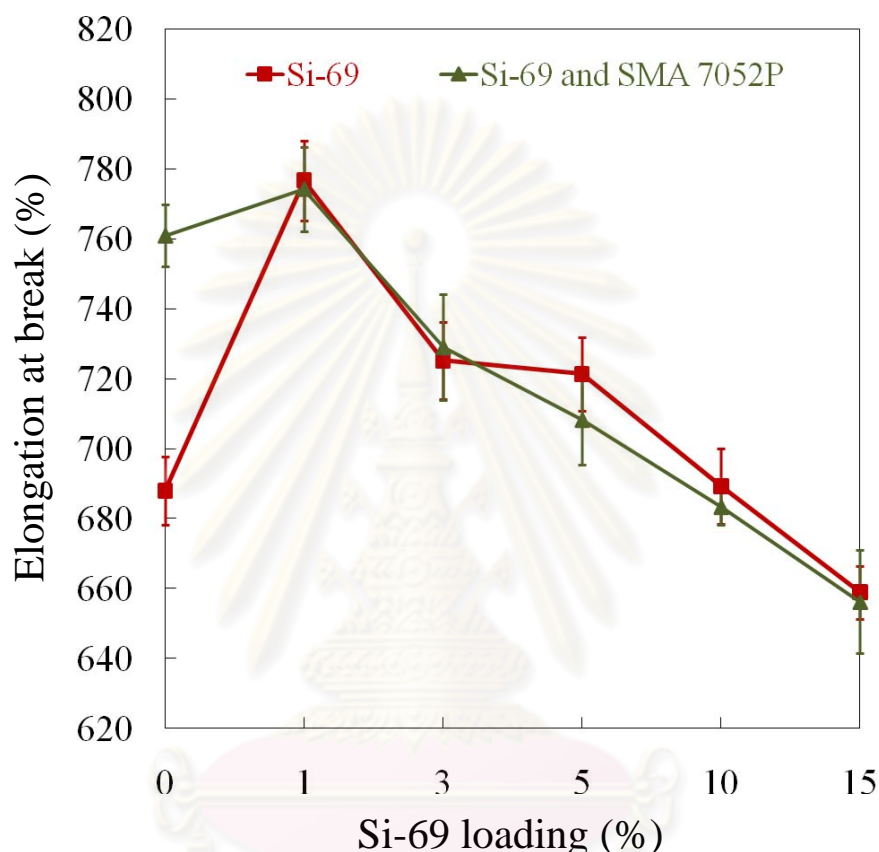
Figure 3.42 The effect of Si-69 loading on elongation at break.

Figure 3.43 represents the effect of silane coupling agent on tear strength of the rubber vulcanizates. The tear strength noticeably increases with raising Si-69 loading up to 1.5 phr or 5% by weight of silica. At higher Si-69 loadings, the tear strength slightly decreased. This result might be due to the excessive crosslink density with increasing Si-69 content. The abrasion resistance of the nanosilica-filled NR vulcanizates is presented in Figure 3.44. It can be seen that, the presence of Si-69 resulted in significantly improved the abrasion resistance of the rubber vulcanizates. In addition, the abrasion loss is found to decrease continuously with increasing silane loading. However, as can be seen in Figure 3.38, a little aggregated form was found at lower Si-69 loading, resulting in, the abrasion resistance was slightly increased at Si-69 content 0.3 phr or 1% by weight of silica.
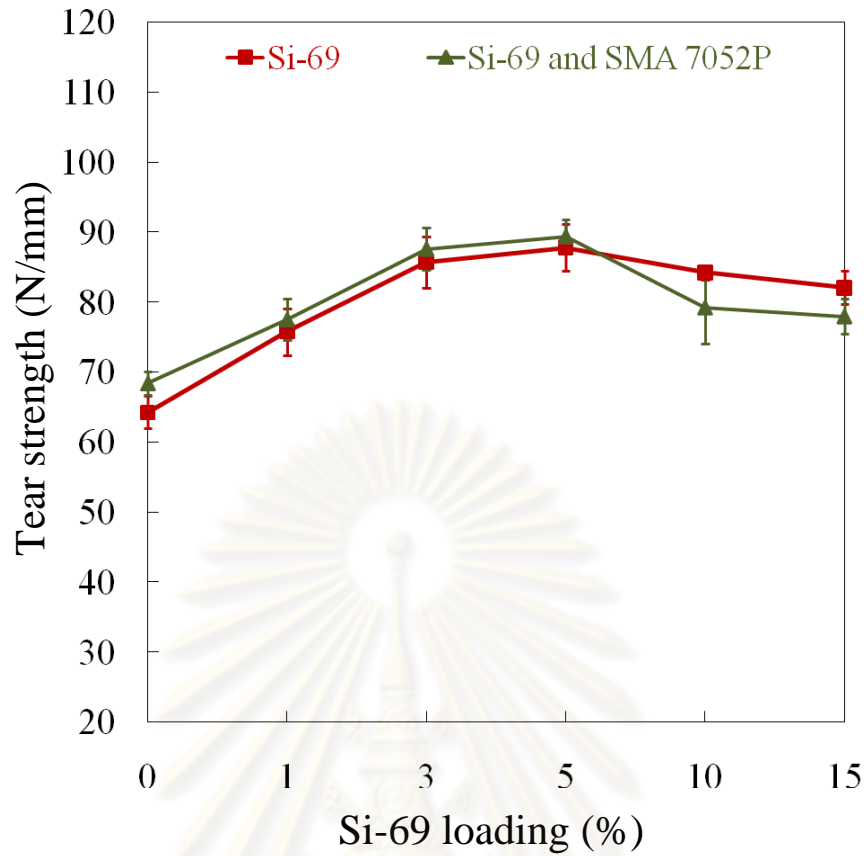
Figure 3.43 The effect of Si-69 loading on tear strength.
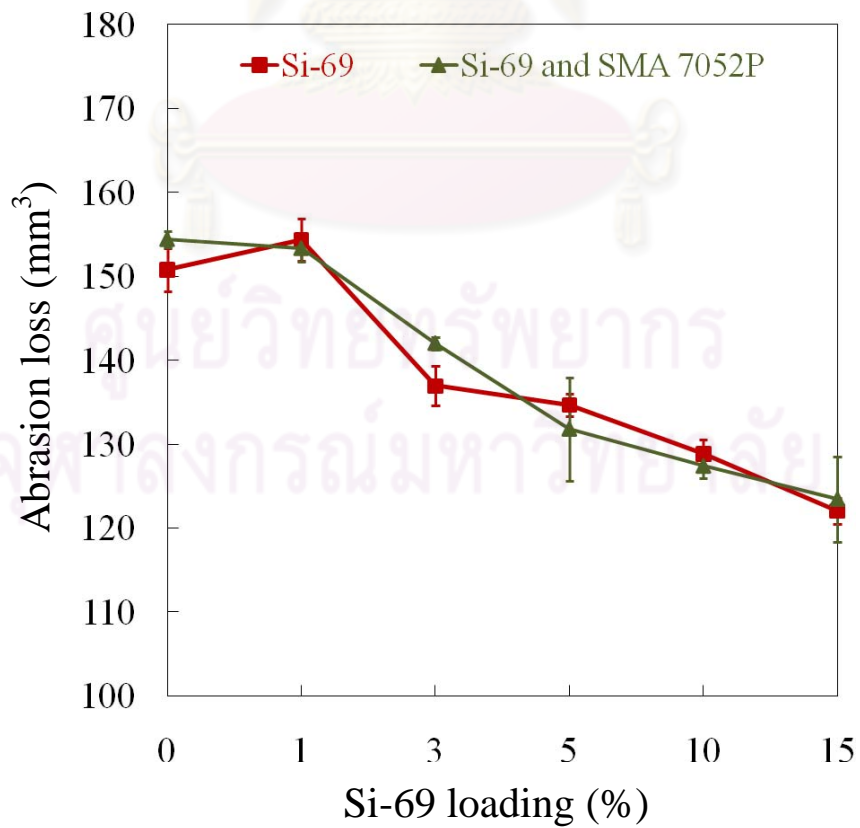
Figure 3.44 The effect of Si-69 loading on abrasion resistance.

Conclusions, the mechanical properties of silica-reinforced NR vulcanizates were enhanced by increasing Si-69 loading. In addition, the presence of SMA 7052P had insignificantly affected on the mechanical properties of Si-69 treated nanosilica-filled NR vulcanizates.

3.4.4 Effect of Si-69 and PEG 400 ratio

The silica surface was modified with silane coupling agents to reduce the polarity and surface activity as same as polyethylene glycol, PEG 4000, was added to silica reinforced rubber compound. The study of Si-69 and PEG 4000 ratio on the properties of vulcanized NR/silica nanocomposites was also investigated to study the relationship of Si-69 and PEG 4000. The Si-69 and PEG 4000 ratio was investigated at 10:0, 1:9, 3:7, 5:5 and 10:0. The numbers were corresponded to the amount of Si-69 and PEG 4000, % by weight of silica, in rubber compounds. The curing behavior and hardness are demonstrated in Table C7 of Appendix C. The mechanical properties, except elongation at break, were exhibited the finest Si-69 and PEG 4000 ratio at 5:5 by weight of silica or 1:1 weight ratio, Figures 3.45-3.49. It might be due to at that ratio presented the highest filler-rubber interaction and cross-linked density. In addition, when PEG 4000 was removed, all properties were alleviated, especially, tensile strength and abrasion loss.

It could be assumed that in this study the best Si-69 and PEG 4000 ratio was 1:1 weight ratio. In addition, PEG 4000 must be present in the recipe of silica reinforced rubber compound. However, the Si-69 and PEG 4000 ratios which presence Si-69 higher than PEG 4000 were not explored, therefore the greatest ratio could be appear in their ratios. The mechanical properties of vulcanized NR with Si-69 and PEG 4000 ratio at 5:5, 10:10 and 15:10 %wt of silica were compared. The vulcanized NR with Si-69 and PEG 4000 ratio at 10:10 and 15:10 %wt of silica were related to V30-TS10 and V30-TS15, respectively. The mechanical properties are summarized in Table 3.3. It was found that tensile strength, M300 and tear strength were not significantly changed. In addition, when Si-69 and PEG 4000 ratio was switched from 10:10 to 15:10 %wt of silica or 1:1 to 1.5:1 ratio by weight, the elongation at break was decreased and abrasion resistance was improved. The increasing of Si-69 affected to raise cross-linked density.
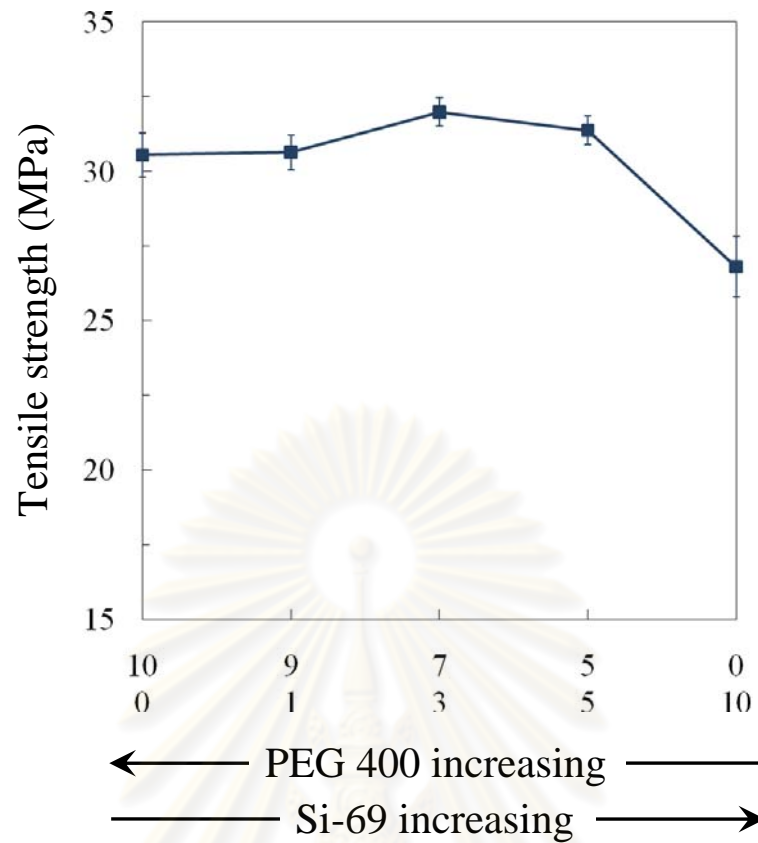
Figure 3.45 The effect of Si-69 and PEG 4000 ratio on tensile strength.
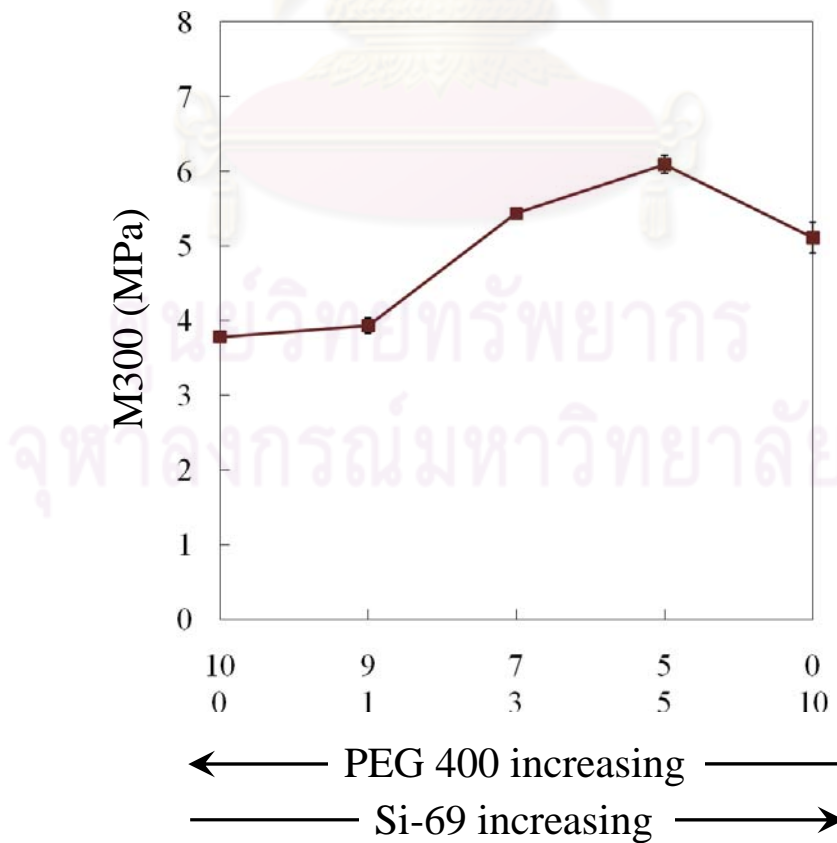
Figure 3.46 The effect of Si-69 and PEG 4000 ratio on M300.
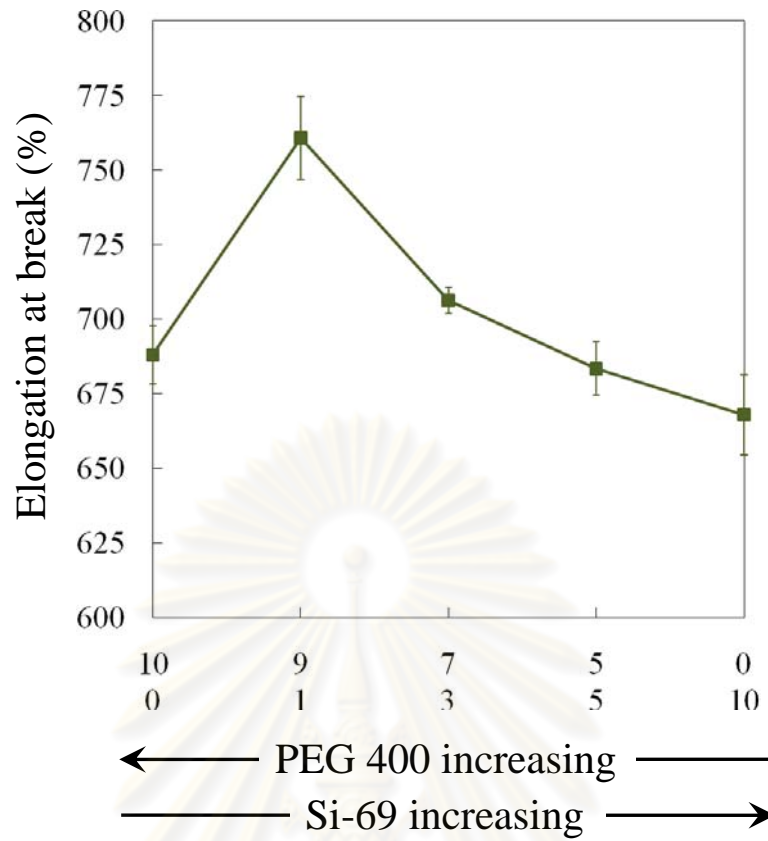
Figure 3.47 The effect of Si-69 and PEG 4000 ratio on elongation at break.
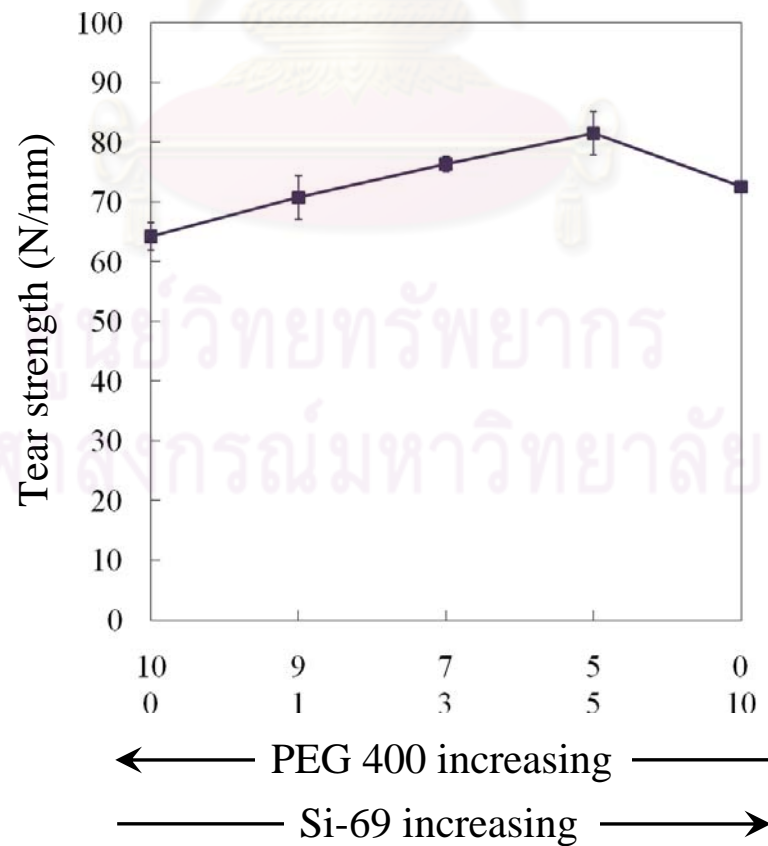
Figure 3.48 The effect of Si-69 and PEG 4000 ratio on tear strength.
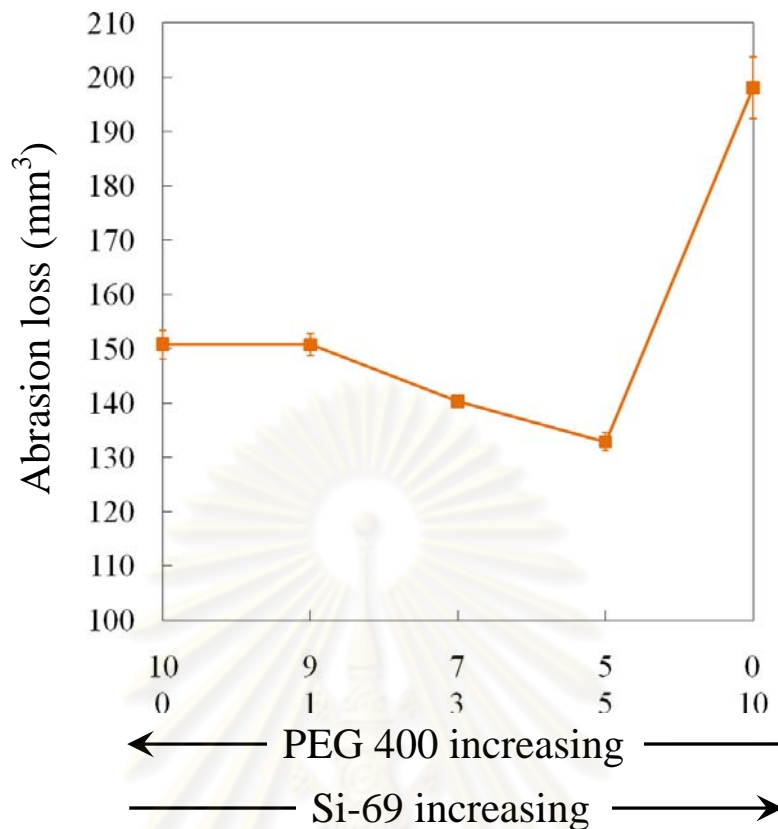
Figure 3.49 The effect of Si-69 and PEG 4000 ratio on and abrasion resistance.

Table 3.3 The comparative study of Si-69 and PEG 4000 ratio on mechanical properties of vulcanized NR with difference ratio and loading

Properties	Si-69 : PEG 4000 ratio (%wt of silica)		
	5:5 (1:1)[a]	10:10 (1:1)[a]	15:10 (1.5:1)[a]
Hardness (Shore A)	56	58	58
TS (MPa)	31.4±0.5	32.3±0.7	32.2±0.7
Eb (%)	683.5±8.9	689.2±10.7	658.9±7.6
M300 (MPa)	6.09±0.12	5.90±0.07	6.93±0.33
Tear (N/mm)	81.5±3.6	84.2±1.0	82.0±2.4
Abrasion loss (mm^3)	132.8±1.6	128.8±1.8	122.1±1.6

[a] Ratio by weight.

3.4.5 The effect of silane coupling agent types

The effect of silane coupling agent types including MEMO, MTMO, Glyeo and AMEO were also examined on the properties of nanosilica-filled NR vulcanizates and silica content was controlled at 20 phr. The treating condition was applied from the treating condition of Si-69 treated silica surface. The vulcanized NR/silica nanocomposites consisting of V20-TS10, VL20-ME10, V20-MT10, V20-GL10 and V20-AM10 were referred to treated nannosilica with Si-69, MEMO, MTMO, Glyeo and AMEO, respectively. Figure 3.50 revealed SEM micrographs of the fractured surfaces of the vulcanized silica-filled NR. It was shown that, the silica aggregation was presented in all samples. The presence of aggregation form might be due to the acid induce re-aggregation process during the preparation of NR/silica nanocomposites.
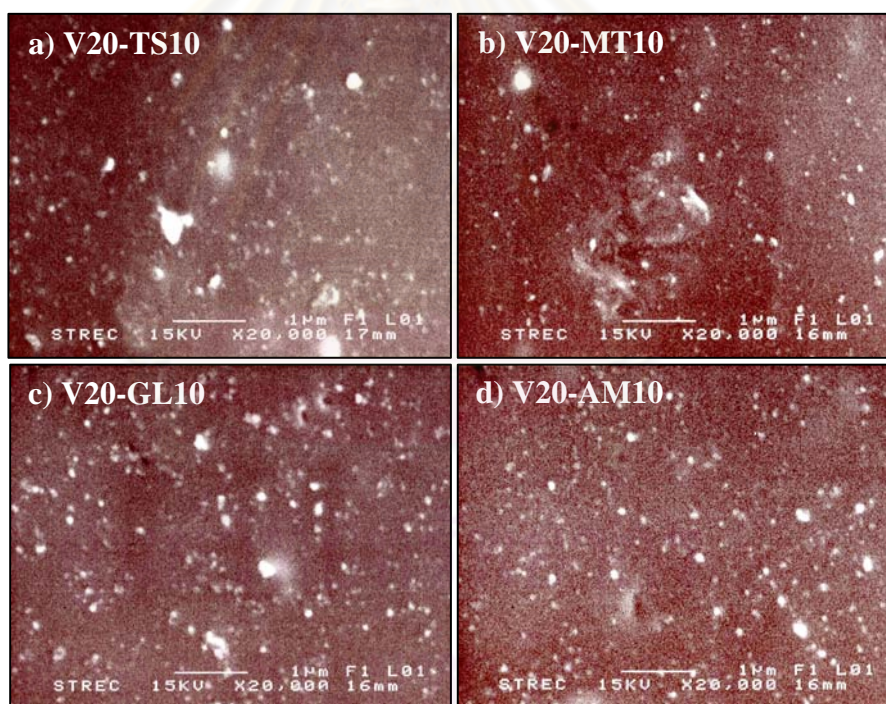
Figure 3.50 The SEM micrographs of the fractured surfaces of the silica-filled NR vulcanizates.

The effect of silane types and couple treating agents between silanes and SMA 7052P treated nanosilica on mechanical properties of vulcanized NR/silica nanocomposites were also explored. The vulcanized NR/silica nanocomposites comprise of V20-TS10P, VL20-ME10P, V20-MT10P, V20-GL10P and V20-AM10P

were corresponded to treated nannosilica with fixed amount of SMA 7052P, 1% by weight of silica and Si-69, MEMO, MTMO, Glyeo and AMEO, respectively. The properties of silane treated nanosilica-filled NR vulcanizates were displayed in Table C8 of Appendix C, whereas, the properties of silane and SMA 7052P treated nanosilica-filled NR vulcanizates were demonstrated in Table C9 of Appendix C. The properties of V20-ME10 were not shown because its nanocomposite could not prepare via acid coagulation. The results shown that, V20-MT10 and V20-MT10P were revealed the succinct scorch time and optimum cure time. The resulting might be due to silane coupling agent, MTMO, contained highest reactive thiol group on its molecule. The thiol group could be precipitate in vulcanization reaction but rapidly reactive over tetrasulfide group on the Si-69 molecule, because it locates at terminal molecule. The extremely reactive of thiol group was affected to greatly increase cross-linked density resulting in the minimum and maximum toque were enlarged.

Figures 3.51 demonstrated the tensile strength of silane treated nanosilica-filled NR vulcanizates. It could be seen that the presence of Glyeo revealed the greatest tensile strength. It might be due to the stronger C-O bonding energy of Glyeo over C-C, C-N and C-S bonding energy among MEMO, AMEO and Si-69, respectively. However, the greatest tensile strength with presence Glyeo was not too much when comparing with the presence of other silane coupling agents. In addition, the tensile strength was depressed with presence of MTMO because the excessive cross-linked density of V20-MT10 and V20-MT10P were exposed. The presence of SMA 7052P was insignificantly affected to tensile strength of silane treated nanosilica-filled NR vulcanizates.

Figure 3.52 displayed M300. The results showed that the presence of MTMO, Glyeo and AMEO manifested M300 overpass Si-69 and MEMO. Generally, M300 was achieved which increasing filler loading, filler structure, surface area and surface activity to perform filler-filler interaction. In addition, as mention in Section 3.4.3.2, M300 was increased with increasing Si-69 loading. In other hand, M300 was enhanced with increasing filler-rubber interaction. In this study, the type of silane was only varied. Therefore, the increasing of M300 with presence MTMO, Glyeo and AMEO might be become from stronger filler-rubber interaction in V20-MT10, V20-

GL10 and V20-AM10 over V20-TS10 and V20-ME10. In addition, the presence of SMA 7052P was not relate to M300 result.

The highest cross-linked density in V20-MT10 and V20-MT10P related to the diminish elongation at break, Figure 3.53. The higher cross-linked density affected to lower rubber molecular mobility or shorter rubber chain that able stretch under stress. Resulting in the elongation at break was decreased with increasing cross-linked density. Similar to tensile strength and M300, elongation at break was not influenced by presenting of SMA 7052P.

For the tear strength, Figure 3.54, the presence of Si-69 and Glyeo in V20-TS10 and V20-GL10, respectively, exhibited the best tear strength while the presence of MTMO and AMEO in V20-MT10 and V20-AM10, respectively, showed the diminish tear strength. It might be due to the higher silica aggregation in V20-MT10 and V20-AM10. According to the preparation of MTMO and AMEO treated nanosilica slurry, the treated nanosilica slurries were became to cake form. Resulting in silica aggregation was achieved and follows by diminishing tear strength. The tear strength was not affected by the presence of SMA 7052P except in MTMO treated nanosilica-filled NR vulcanizate. The result might be due to the presence of SMA 7052P was affected to reduce silica aggregation in V20-MT10P.

Figure 3.55 exhibited the abrasion loss. It was shown that the best abrasion loss was obtained which presented of MTMO and AMEO. Regarding to the mention in Section 3.4.2.2, higher modulus grants the vulcanizates with better abrasion resistance, the abrasion resistance results resemble to agree well with the moduli with the presence of Si-69, MEMO, MTMO and AMEO. In addition, abrasion reseistance of silane treated nanosilica-filled NR vulcanizates was not influenced by the presence of SMA 7052P.
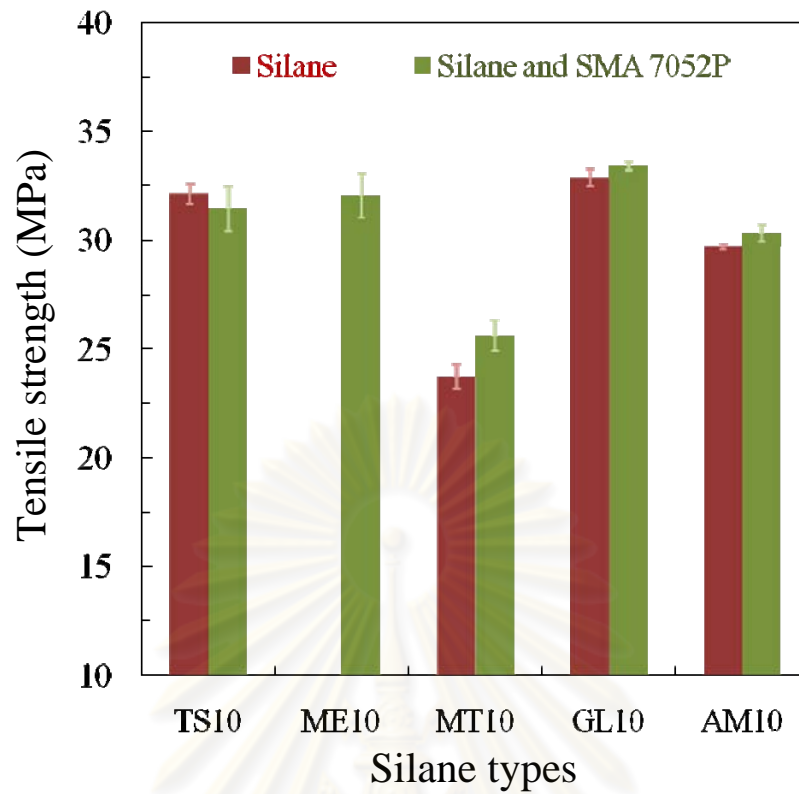
Figure 3.51 The effect of silane types on tensile strength.
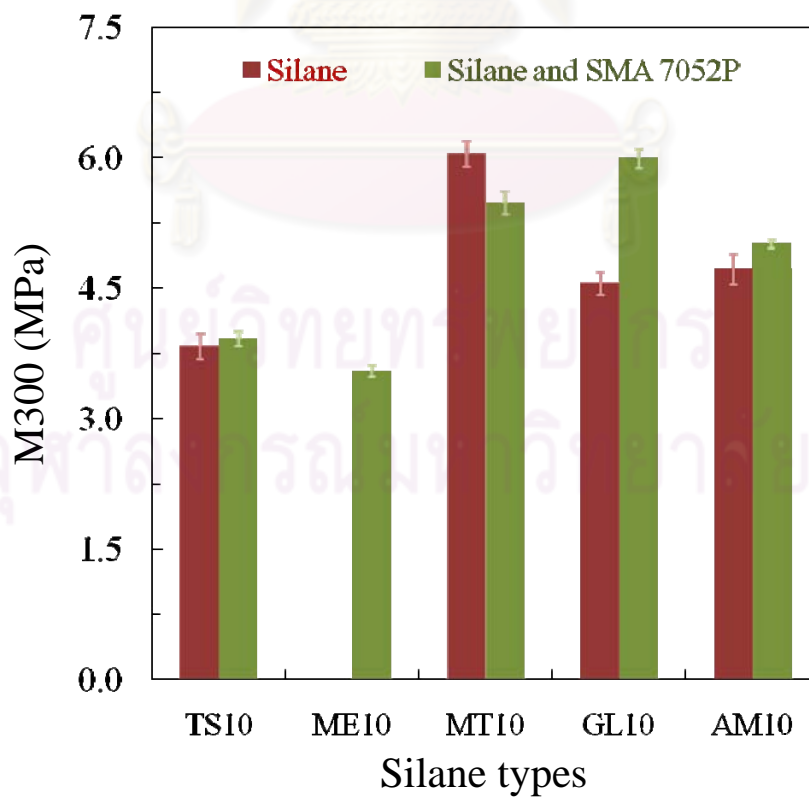
Figure 3.52 The effect of silane types on M300.
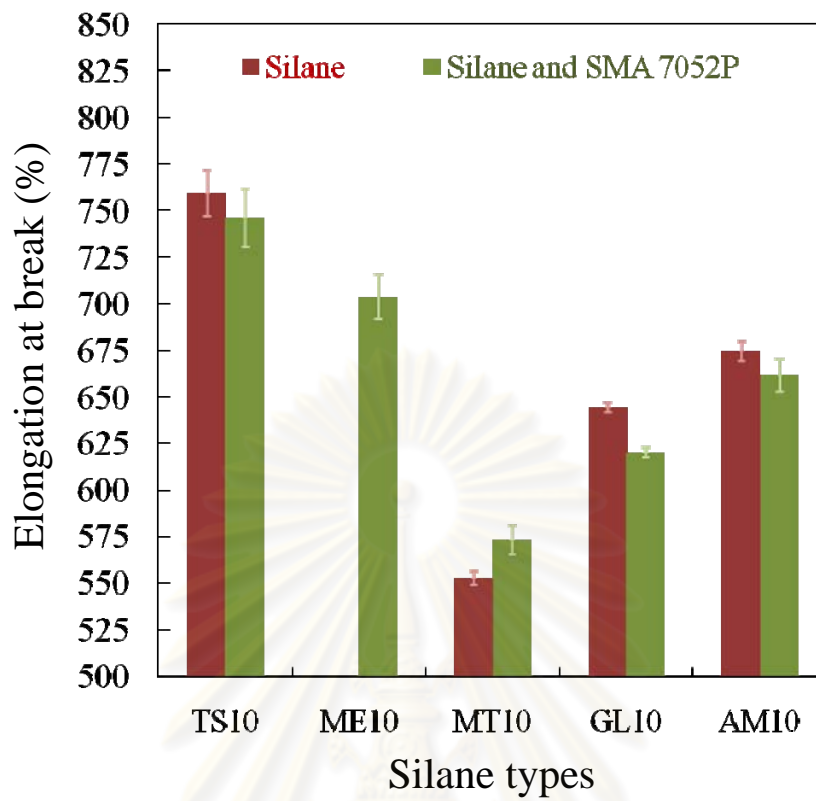
Figure 3.53 The effect of silane types on elongation at break.
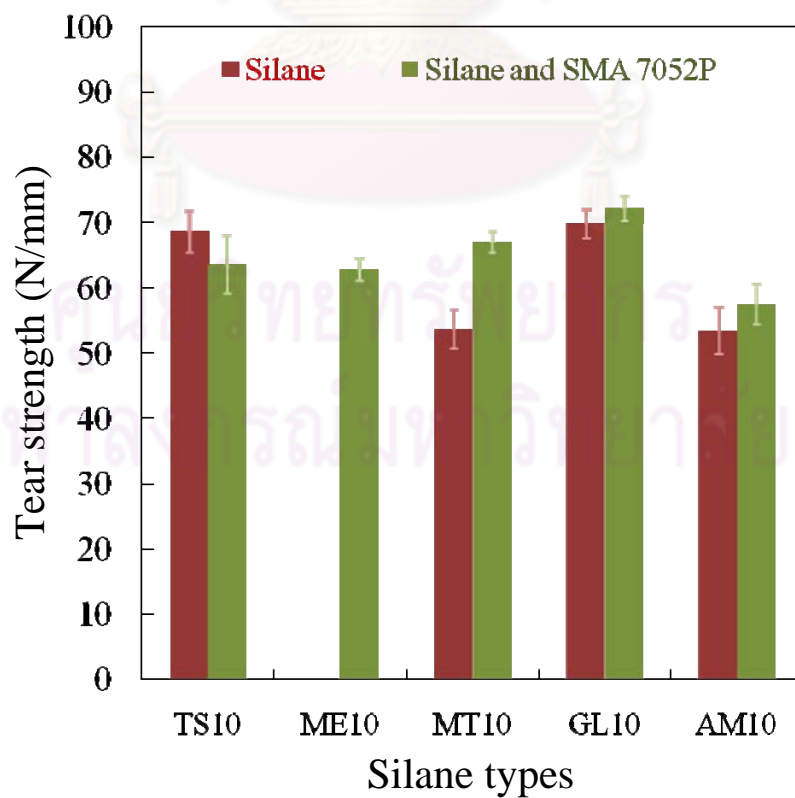
Figure 3.54 The effect of silane types on tear strength.
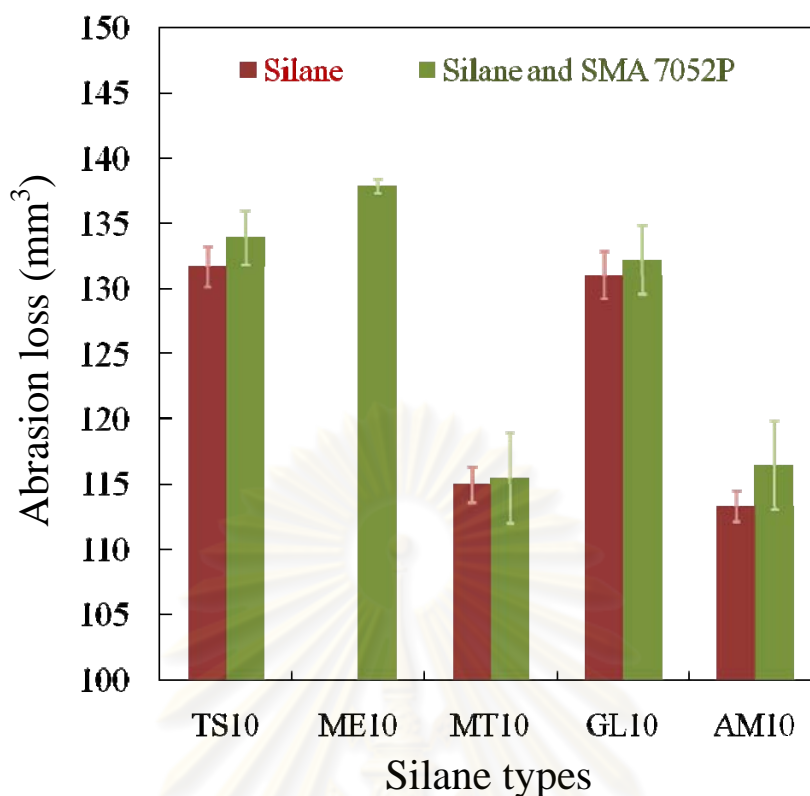
Figure 3.55 The effect of silane types on abrasion resistance.

In summary, the thiol group on terminated of MTMO could be precipitated in vulcanization reaction and reactive over other functional groups on other silane molecule, especially tetrasulfide group on Si-69. As a result of the high cross-linked density in vulcanized NR/silica nanocomposites, V20-MT10 and V20-MT10P, the lower tensile strength, higher M300, lower elongation at break, lower tear strength and better abrasion resistance were achieved. Similar to MTMO, AMEO had reactive amino group on terminated molecule. Resulting in good tensile strength and abrasion resistance were obtained. However, the presence of high polarity amino group on terminated of AMEO molecule affected to nanosilica slurry transform to cake form during treating process. Resulting in silica aggregation was established and low tear strength was appeared. In addition, the presence of silica aggregation could be enhancing the M300. The similar mechanical properties consisting of tensile strength, tear strength and abrasion resistance were achieved with presence of lower reactive functional groups including tetrasulfide, acrylate and glycidyl on Si-69, MEMO and Glyeo molecules, respectively. In addition, the presence of SMA 7052P had no affected on mechanical properties of silane treated nanosilica-filled NR vulcanizates.

Therefore, it could be assume that the mechanical properties of V20-ME10 closely related to the mechanical properties of V20-ME10P.

3.5 Polyethylene glycol (PEG) derivatives and polypropylene glycol (PPG) derivative

In this section, the effect of PEG and PPG on the properties of vulcanized NR/silica nanocomposites was examined including silica loading, treating agent loading and types, couple treating agent between PEG, PPG and SMA 7052P. The first one, three type of silica were chosen to investigate at variable silica loading consist of original silica, untreated nanosilica slurry and treated nanosilica slurry with S550 with control loading at 10% by weight of silica. The second one, the variable amount of SR550 such as 1, 3, 5, 10 and 15% by weight of silica were investigated with control silica content at 30 phr. The fourth one, four types of treating agents including SR256, SR550, SR603 and SR604 were selected to study at constant silica content at 30 phr. In addition, the effects of couple treating agents were examined. First, the effect of SMA 7052P, 1% by weight of silica, and variable SR550 loading was contemplated and compared with the results of the study on SR550 loading. And last, the effect of SMA 7052P, 1% by weight of silica, and variable treating agent types was inspected and compared with the results of the study on the effect of treating agent types. The study of SR550 and PEG 4000 ratio on the properties of vulcanized NR/silica nanocomposites was also investigated to study the relationship of SR550 and PEG 400

3.5.1 The comparative study of original silica, untreated nanosilica and SR550 treated nanosilica on the properties of vulcanized NR

The effect of SR550 treated silica surface on the properties of NR/silica nanocomposites was surveyed and compared with original silica and untreated nanosilica filled NR. The comparative study was examined in variable silica loading such as 10, 20 and 30 phr. The morphology of silica-filled NR was proved by SEM and displayed in Figure 3.56. The SEM micrographs revealed that, the abundant silica aggregation was presented, especially, at silica loading 20 phr. The result exposed that, SR550 was not appropriated to use as treating agent because it could not improve silica dispersion. On the contrary, the silica aggregation was increased which

presented SR550. Nevertheless, the curing behavior, mechanical properties and abrasion loss were still examined. The curing behavior is listed in Table C10 of Appendix C. The results attested that, SR550 was affected to extend the scorch time and optimum cure time. Actually, the scorch time and optimum cure time should be shortening because the silica surface was covered by SR550 molecules. The results might be due to SR550 had acrylate group on its molecule. The acrylate group could be precipitate in vulcanization reaction, therefore, the increasing of double bond affected to reduce vulcanization reaction rate.
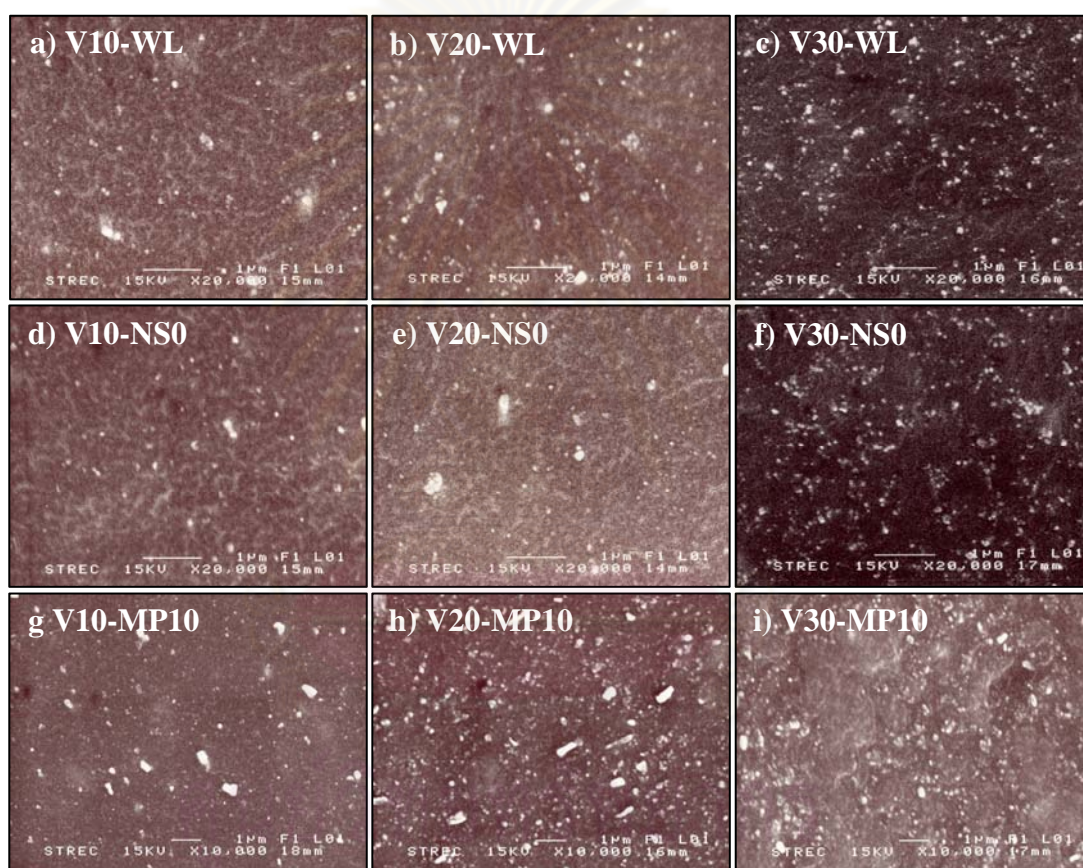
Figure 3.56 The SEM micrographs of the fractured surfaces of the vulcanized silica-filled NR at variable silica loading.

Figure 3.57 revealed the tensile strength at variable silica loading and presented SR550 comparable with original silica-filled NR vulcanizates and untreated nanosilica-filled NR vulcanizates. The result shown that, the tensile strength was gradually increased when SR550 was added. Actually, SR550 contained the acrylate group on the molecule which enable precipitated in vulcanization reaction and act as bridge-linkage between silica particle and rubber molecules to improve filler-rubber

interaction. The results might be due to the appearance of silica aggregation eclipsed the efficiency of SR550.
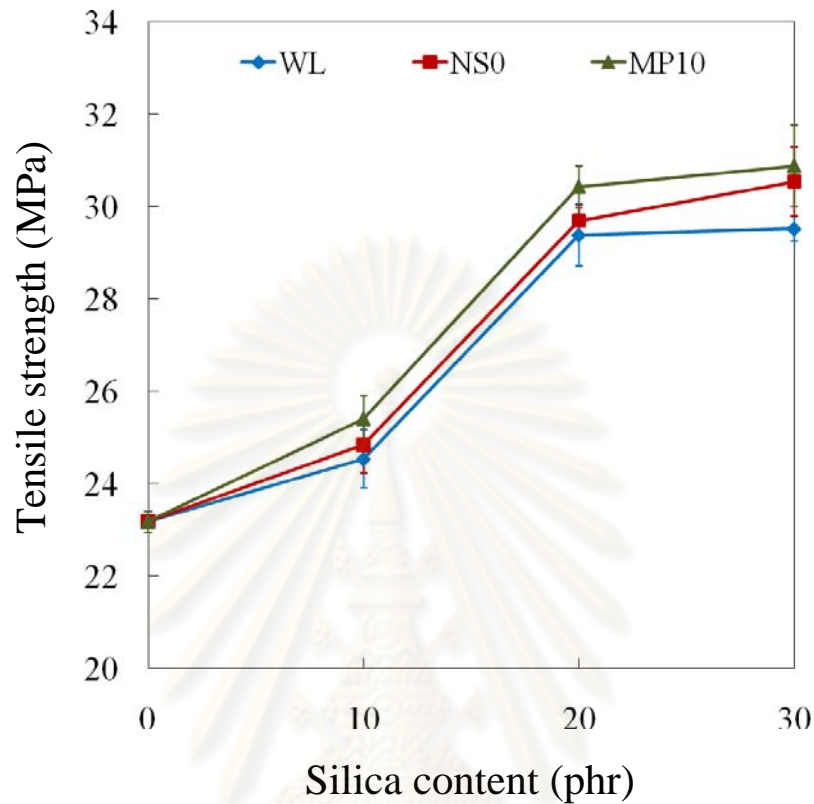
Figure 3.57 The comparative study on tensile strength with variable silica loading.

M300 results are demonstrated in Figure 3.58. The results showed that the presence of SR550 affected to increase M300 over original and untreated nanosilica at silica contents 10 and 20 phr. It might be due to silica aggregation was appeared which presenting SR550. In addition, at silica content 30 phr, M300 was decreased which presenting SR550. The result might be because silica aggregation was reduced when silica loading was raised up to 30 phr. Moreover, silica surface activity was reduced by presenting SR550, resulting in decreasing the filler-filler interaction.

Figure 3.59 displayed the elongation at break. The result exhibited that the elongation at break was abated when SR550 was added. The results could be explained by SEM results. SEM micrographs clearly showed that silica aggregation was presented when SR550 was added. The presence of silica aggregation affected to reduce the elongation at break.
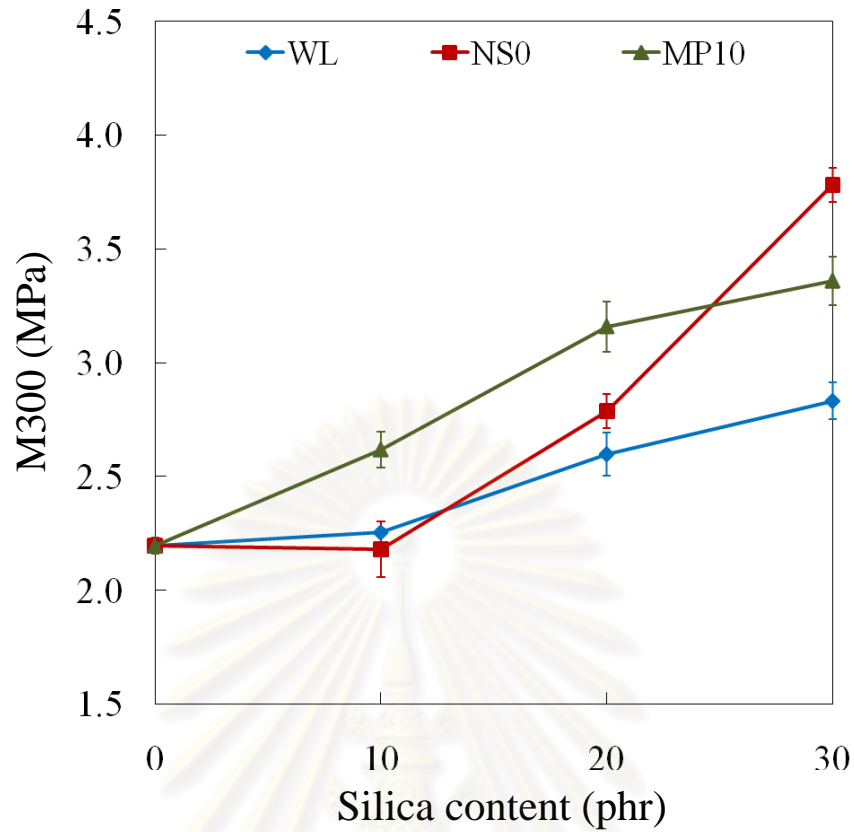
Figure 3.58 The comparative study on M300 with variable silica loading.
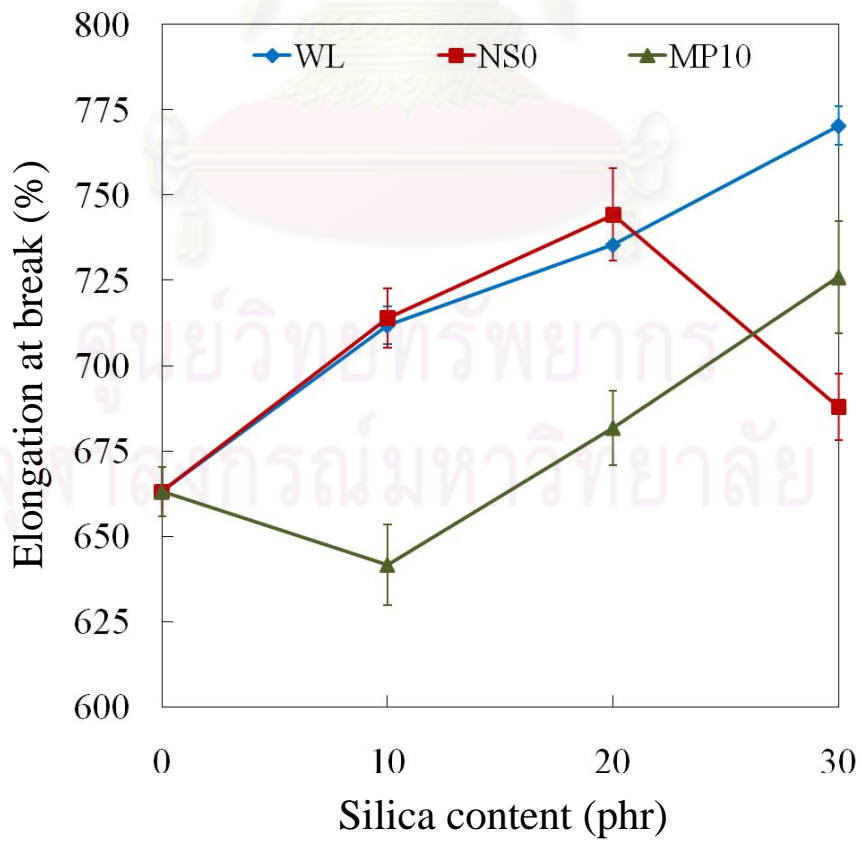
Figure 3.59 The comparative study on elongation at break with variable silica loading.

Figure 3.60 exhibited tear strength. Tear strength was not significantly increased when SR550 was presented. Similar to the reason for tensile strength, M300 and elongation at break results, It might be due to the appearance of silica aggregation eclipsed the efficiency of SR550.

The unacceptable results were demonstrated in abrasion resistance, Figure 3.61. The presence of SR550 was not developed the abrasion loss. On the other hand, the abrasion loss was subsided when SR500 was employed as surface treating agent. The presence of silica aggregation also affected to deteriorate the abrasion resistance of vulcanized NR.

In summary, the presence of SR550 was not influenced to improve the mechanical properties at all silica content, especially the reducing abrasion loss was found. In addition, the silica aggregation was presented which added SR550. Moreover, the extension of scorch time and optimum cured time were achieved when SR550 was present.
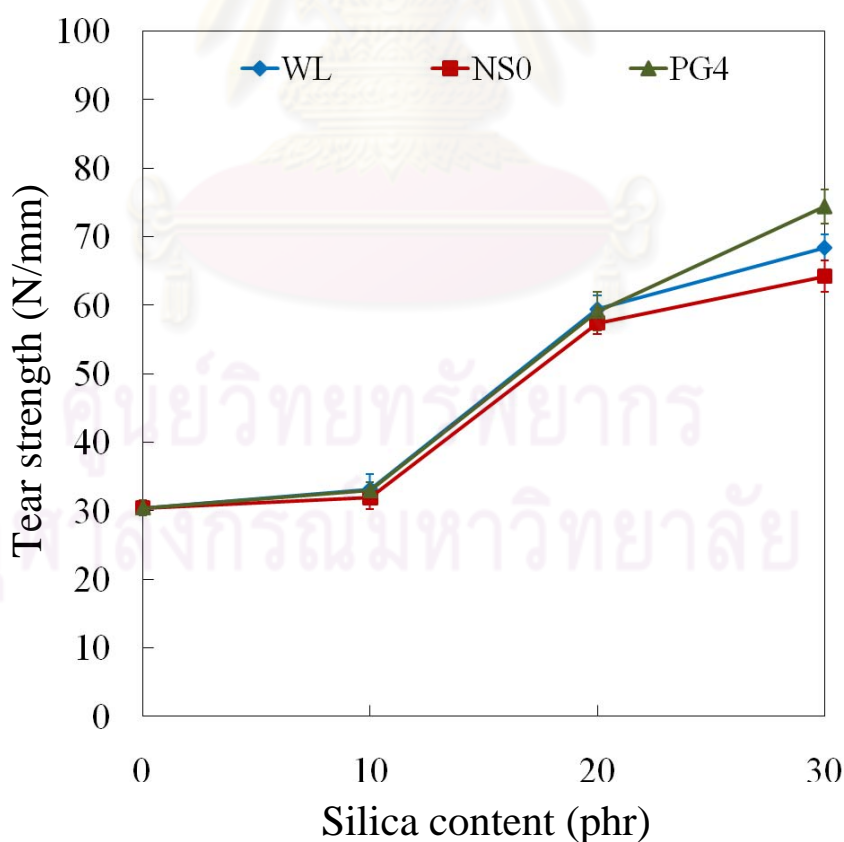
Figure 3.60 The comparative study on tear strength with variable silica loading.
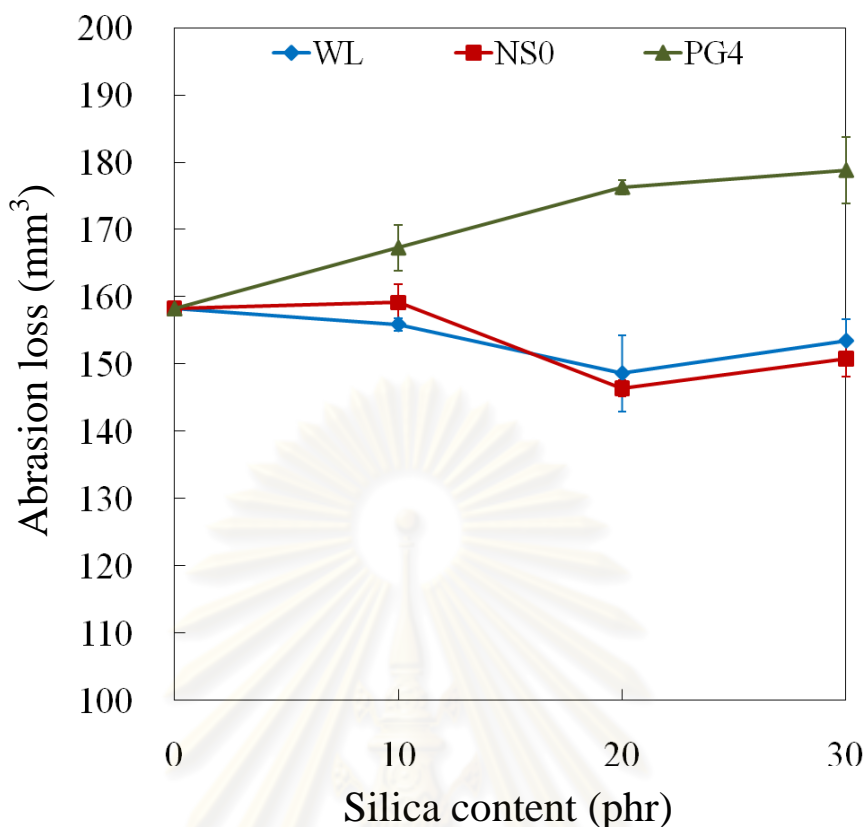
Figure 3.61 The comparative study on abrasion resistance with variable silica loading.

3.5.2 The effect of SR550 loading on the properties of vulcanized NR

The variations of SR550 loading including 1, 3, 5, 10 and 15% by weight of silica were investigated on curing behavior, mechanical properties and abrasion loss of nanosilica-filled NR vulcanizates. Figure 3.62 displayed the SEM micrographs of SR550 treated nanosilica-filled NR vulcanizates. The micrographs demonstrated that, the phase separation was observed when SR550 was presented, especially, at SR550 loading below 10% by weight of silica. Moreover, the large size of silica aggregation was appeared at SR550 loading under 10% by weight of silica.

In addition, the effect of couple treating agent between SR550 and SMA 7052P on the properties of NR vulcanizates was also examined. The amount of SMA 7052P was fixed at 1% by weight of silica while the amount of SR550 was varied such as 0, 1, 3, 5, 10 and 15% by weight of silica. The curing behavior and hardness of vulcanized NR that contain the variable SR550 loading are shown in Table C10 of Appendix C. Whereas the curing behavior, hardness and elongation at break of

vulcanized NR containing couple treating agents are shown in Table C11 of Appendix C.
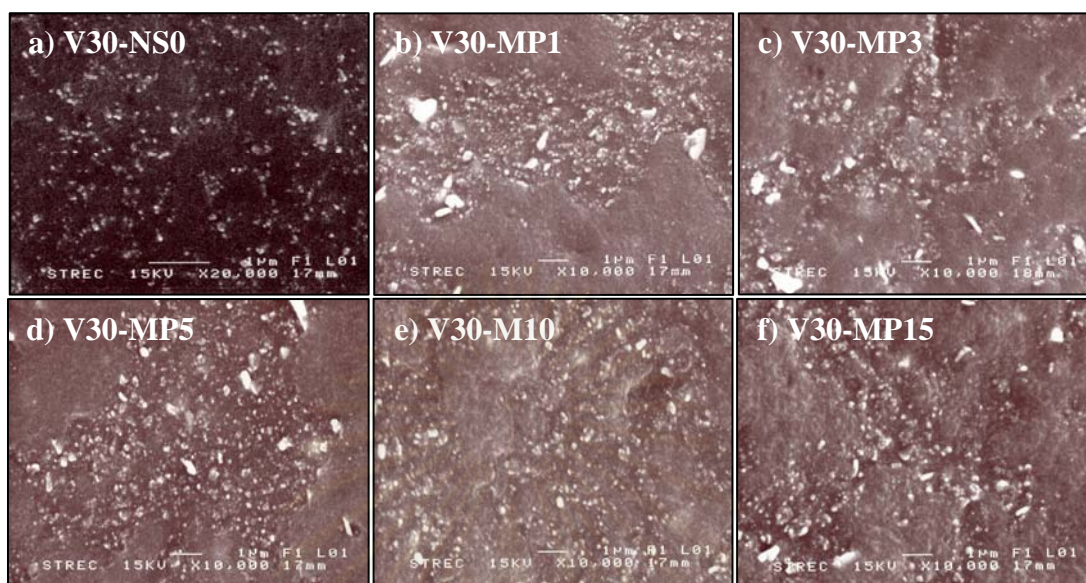
Figure 3.62 The SEM micrographs of the fractured surfaces of the vulcanized silica-filled NR at variable SR550 loading.

The effects of SR550 loading and the couple treating agents on curing behavior are displayed in Figure 3.63. The results revealed that the presence of SR550 extended the scorch time and optimum cure time, whereas the increasing of SR550 was not affected on curing behavior. In addition, similar to the results in Section 3.4.3.2, the scorch time and optimum cure time were shorten in the presence of SMA 7052P.

The tensile strength and M300 were insignificantly affected by SR550 loading, Figures 3.64 and 3.65, respectively. The SR550 loading at 5% by weight of silica exposed the highest values in both tensile strength and M300. Both tensile strength and M300 were slightly influenced by adding SMA 7052P. They were gradually increased below SR550 loading 5% by weight of silica and slightly decreased when SR550 loading was more than 5% by weight of silica. However, it could be assumed that tensile strength and M300 were not significantly influenced by increasing of SR550 loading and presenting of SMA 7052P.
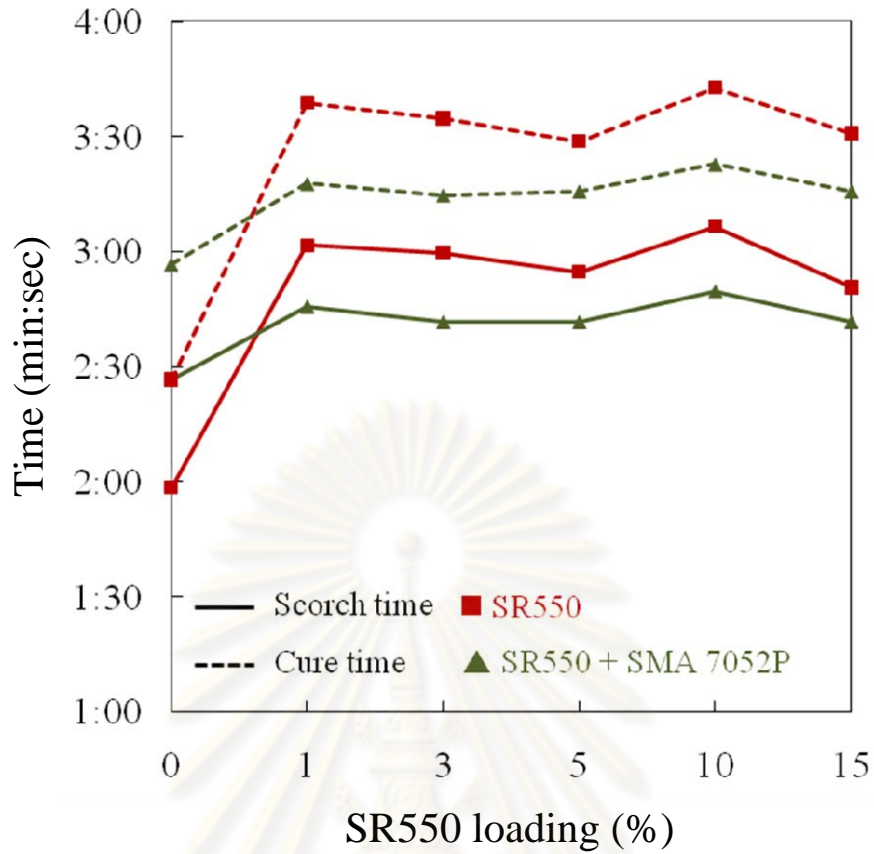
Figure 3.63 The effect of SR550 loading on curing behavior.
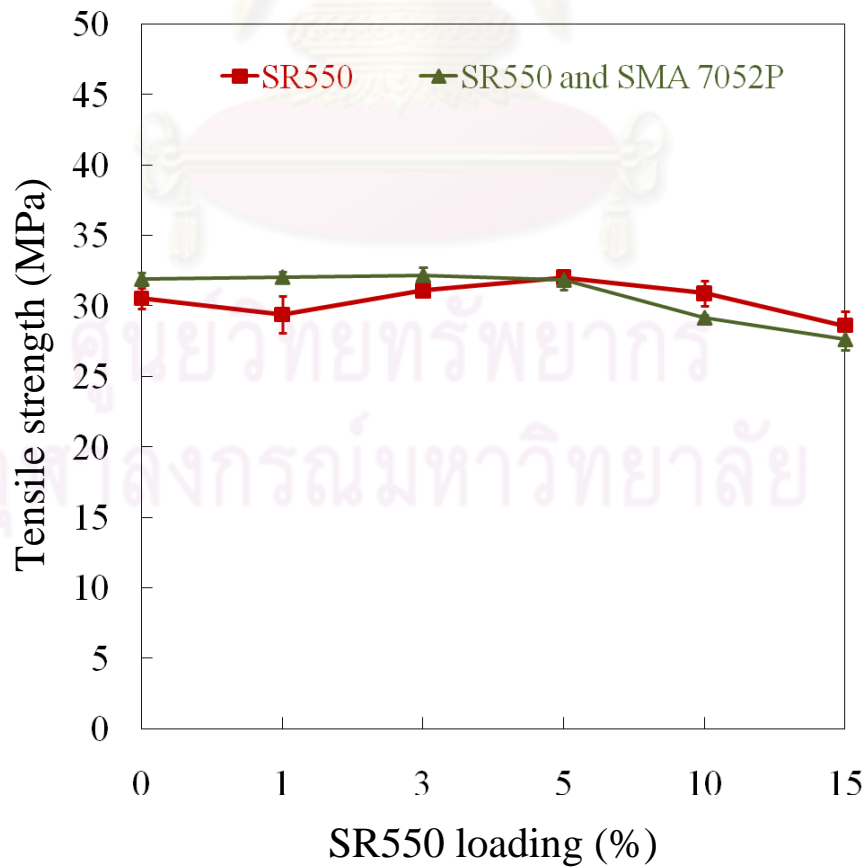
Figure 3.64 The effect of SR550 loading on tensile strength.
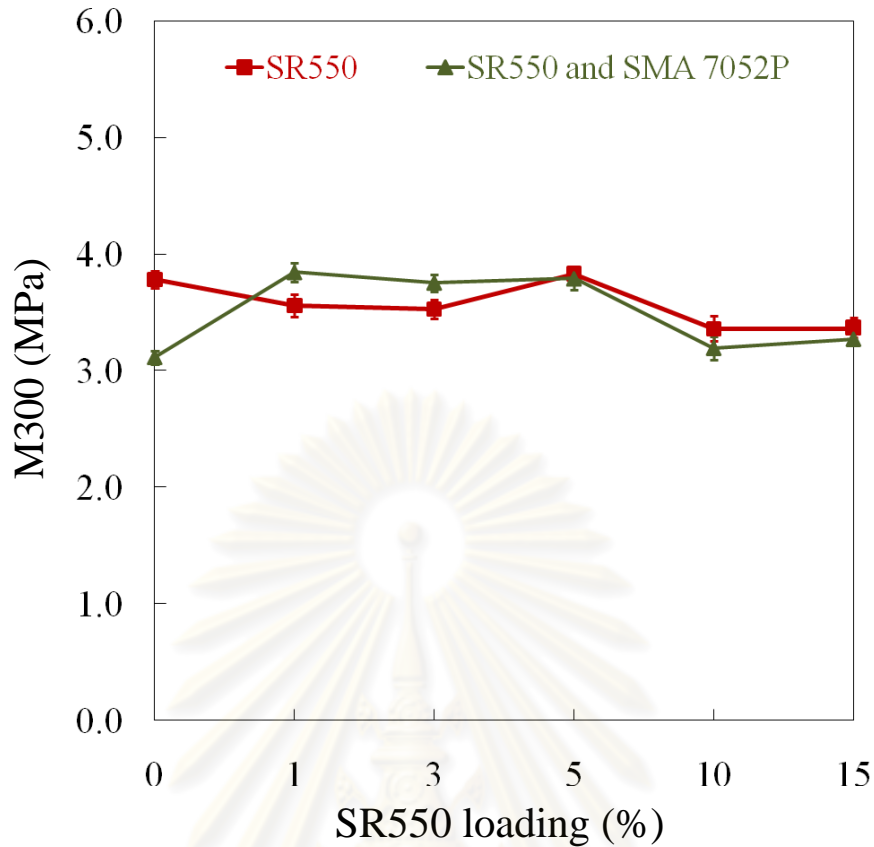
Figure 3.65 The effect of SR550 loading on M300.

Figure 3.66 exhibited the elongation at break. The results showed that the elongation at break had trend to increase which increasing SR550. Similarly to tensile strength and M300, when the SMA 7052P was presented, elongation at break was slightly increased below SR550 loading 5% by weight of silica and slightly decreased when SR550 loading was more than 5% by weight of silica. However, the presence of SMA 7052P also insignificantly affected on the elongation at break.

Tear strength had no affected by increasing SR550 loading as can be seen in Figure 3.67. In addition, the best tear strength was revealed presenting of SMA 7052P and SR550 loading 5%wt of silica. However, the presence of SMA 7052P had no relationship with increasing SR550 loading.

The abrasion resistance is displayed in Figure 3.68. It was shown that, the abrasion resistance had trend to reduce by increasing of SR550 loading. Similarly to tear strength, the abrasion resistance of the presence of SMA 7052P had no relationship with increasing SR550 loading.
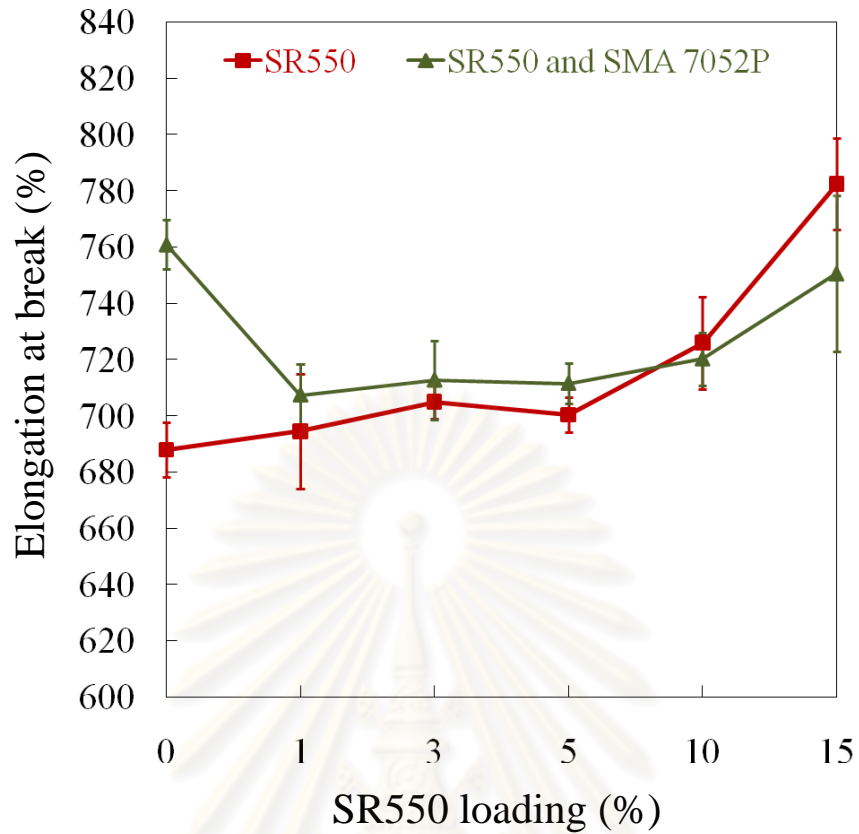
Figure 3.66 The effect of SR550 loading on elongation at break.
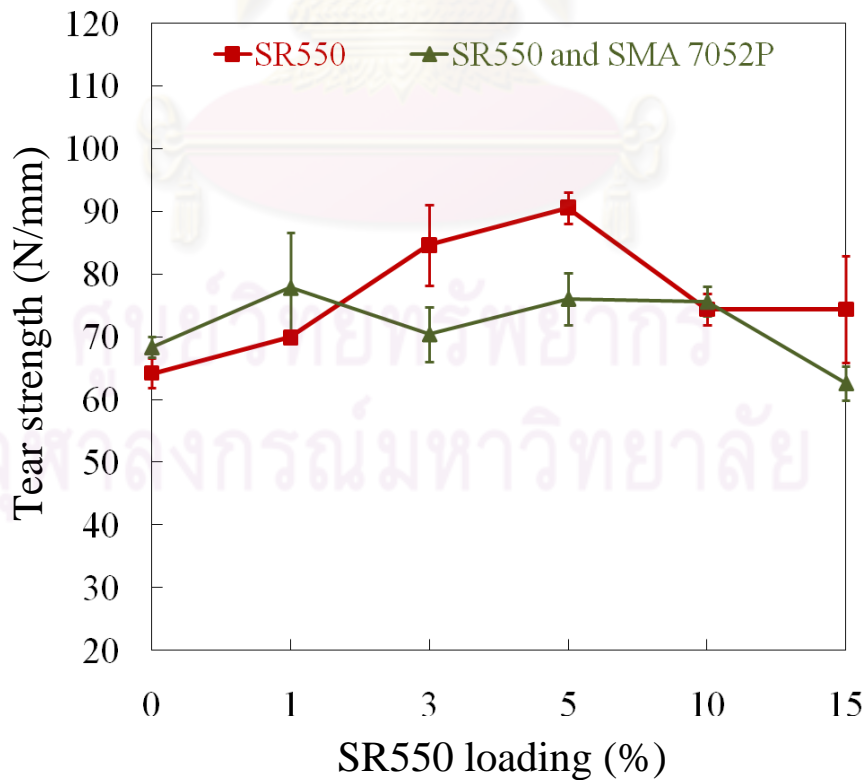
Figure 3.67 The effect of SR550 loading on tear strength.
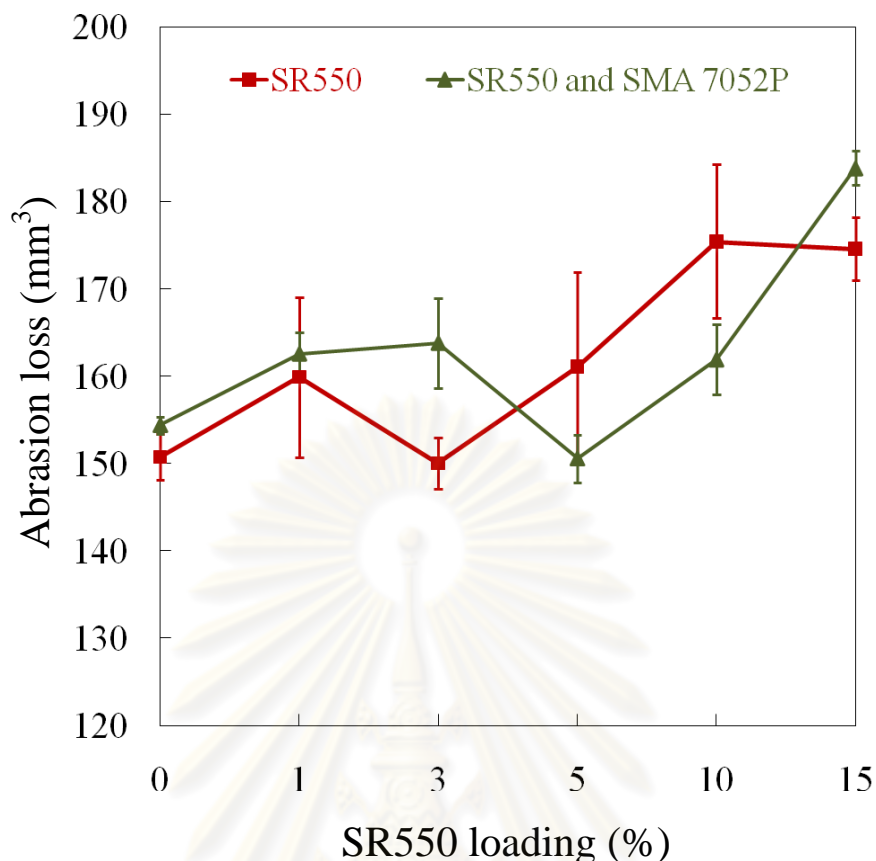
Figure 3.68 The effect of SR550 loading on abrasion resistance.

In summary, it could be presumed that the increasing of SR550 loading not affected to improve tensile strength, M300 and tear strength. The elongation at break was extended with increasing SR550 loading. In addition, abrasion resistance was diminished with increasing SR550 loading. Moreover, the presence of SMA 7052P was not affected to mechanical properties of nanosilica-filled NR vulcanizates.

3.5.3 Effect of SR550 and PEG 400 ratio

The study of SR550 and PEG 4000 ratio on the properties of vulcanized NR/silica nanocomposites was also surveyed to explore the relationship between SR550 and PEG 400. According to the study on the effect of the Si-69 and PEG 4000 ratio, the SR550 and PEG 4000 ratio was investigated at 10:0, 1:9, 3:7, 5:5 and 10:0. The numbers were corresponded to the amount of SR550 and PEG 4000, % by weight of silica, in rubber compounds. The curing behavior and hardness are exposed in Table C12 of Appendix C. Similarly to the study on the effect of Si69 and PEG 4000 ratio, the SR550 and PEG 4000 ratio at 10:0, with the absence of PEG 4000, disclosed

despicable properties on tensile strength, M300, tear strength and abrasion loss as demonstrated in Figures 3.69, 3.70, 3.72 and 3.73, respectively.

Figure 3.69 exhibited tensile strength. It was showed that the tensile strength was demonstrated the finest SR550 and PEG 4000 ratio at 9:1, %wt of silica. In addition, tensile strength was continuously subsided with decreasing PEG 4000 loading. Moreover, tensile strength was extremely diminished when PEG 4000 was absented. M300 results are displayed in Figure 3.70. The results showed that SR550 and PEG 4000 ratio at 7:3, %wt of silica, exhibited the highest M300. Figure 3.71 showed elongation at break result. It was found that elongation at break was stretched when SR550 or PEG 4000 was absented whereas other SR550 and PEG 4000 ratios provided the similar elongation at break. Similar tear strength was exhibited at all SR550 and PEG 4000, Figure 3.72. Figure 3.73 exposes abrasion resistance result. It was found that abrasion loss was diminished with decreasing of the amount of PEG 4000.
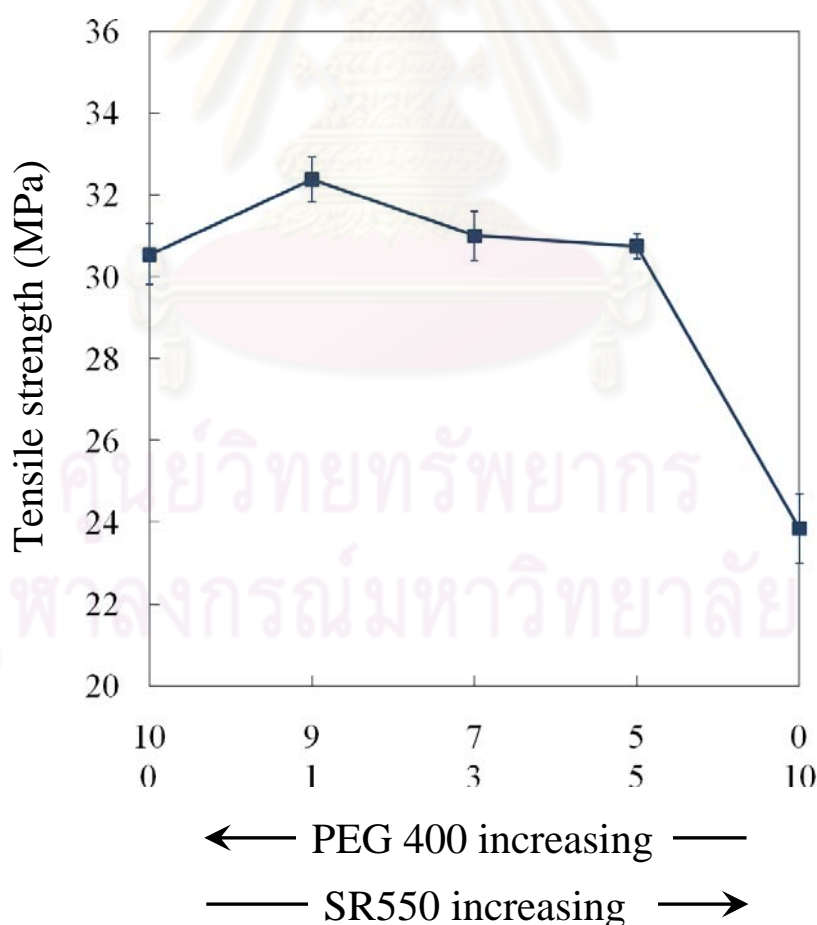
Figure 3.69 The effect of SR550 and PEG 4000 ratio on tensile strength.
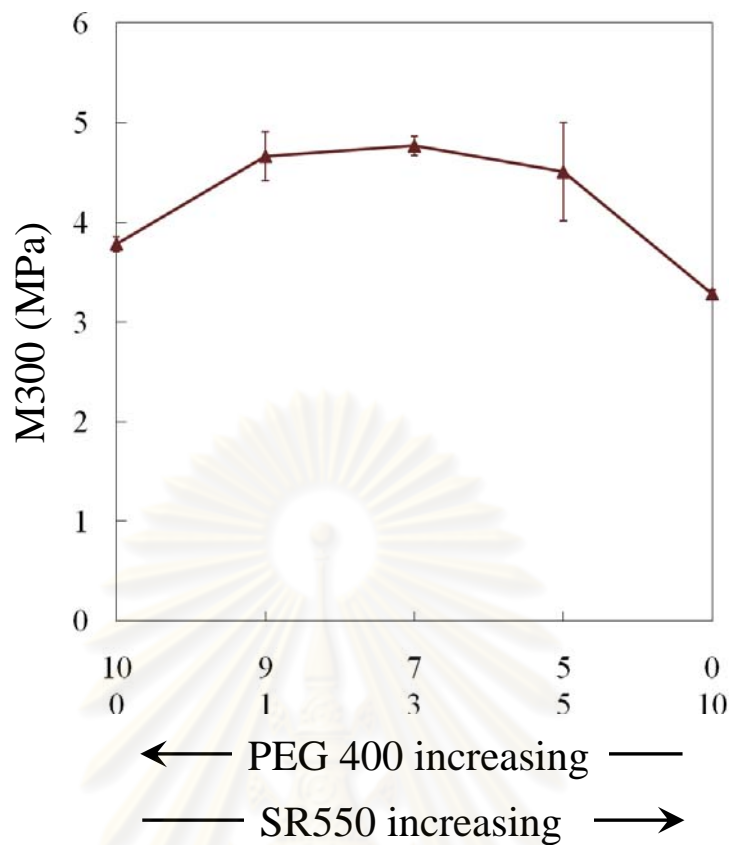
Figure 3.70 The effect of SR550 and PEG 4000 ratio on M300.
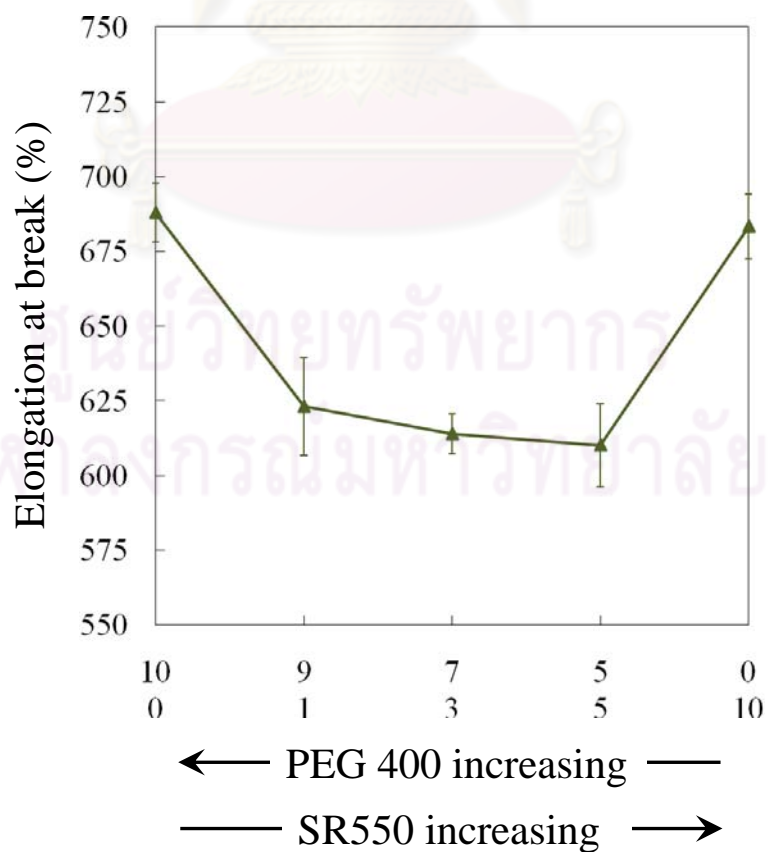
Figure 3.71 The effect of SR550 and PEG 4000 ratio on elongation at break.
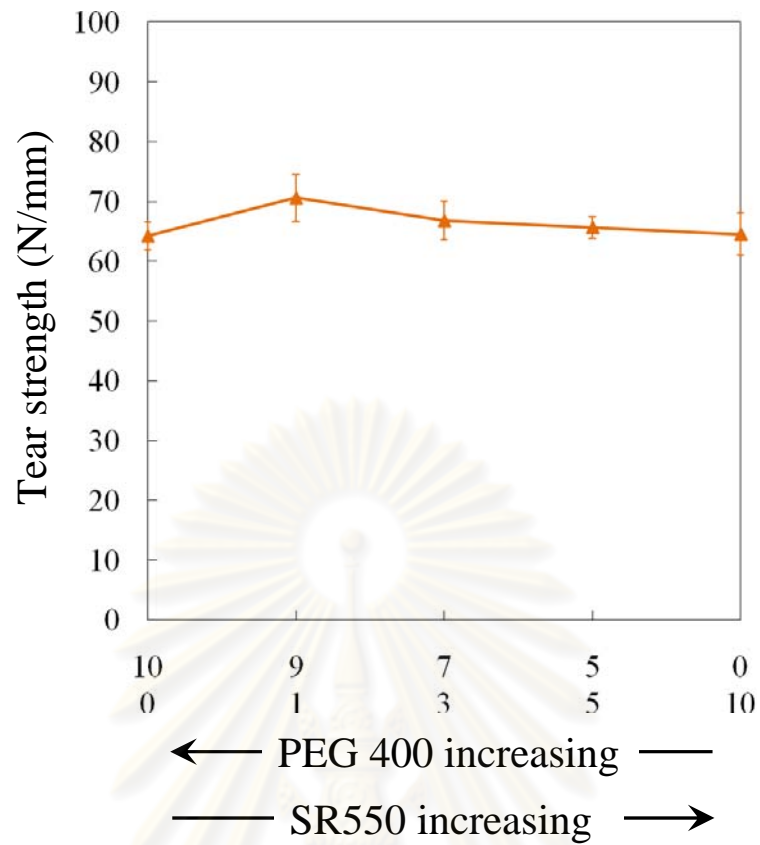
Figure 3.72 The effect of SR550 and PEG 4000 ratio on tear strength.
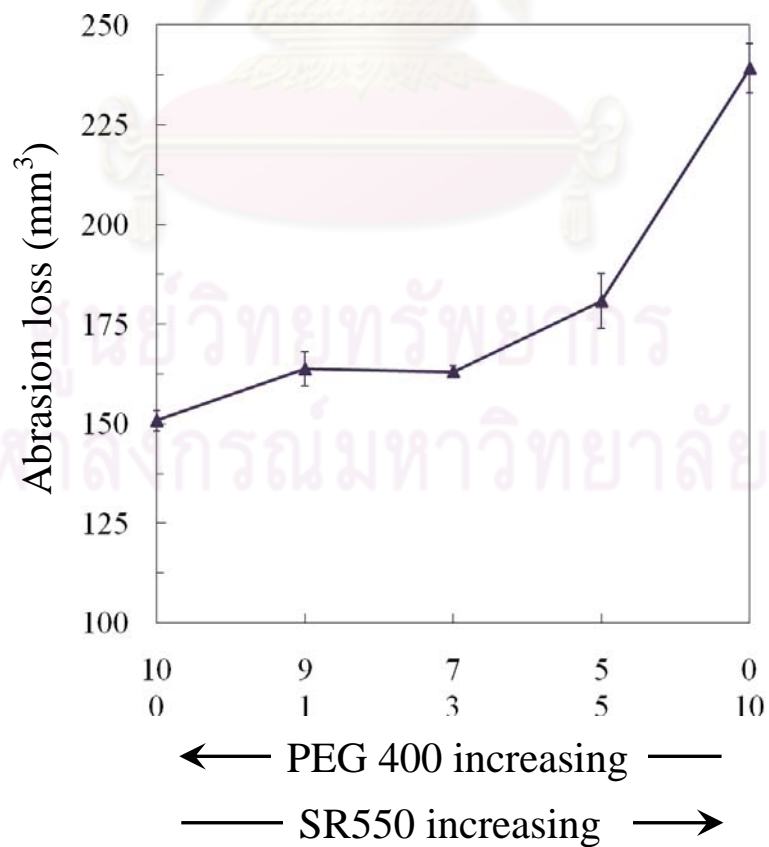
Figure 3.73 The effect of SR550 and PEG 4000 ratio on abrasion resistance.

Finally, similar to the study of the effects of Si-69 and PEG 4000 ratio, the absence PEG 4000 provided poor mechanical properties, especially, tensile strength, elongation at break and abrasion resistance. It was confirmed that PEG 4000 must be added to the recipe of silica reinforced rubber compound.

3.5.4 Effect of the types of PEG and PPG derivatives

The investigation on the types of PEG and PPG derivatives were focused on the effect of the length molecular chain, molecular structure and the functional group on molecules. The molecular chain lengthen of SR603 was as same as to that of SR 604 and longer than that of SR550 and SR256, respectively. In addition, the molecular skeleton of SR604, polypropylene glycol, was not similar to SR256, SR550 and SR603, polyethylene glycol. Moreover, SR256 and SR550 had borne one acrylate and methacrylate group at one molecular terminal, respectively. SR603 and SR604 contained two methacrylate groups at the end of molecules.
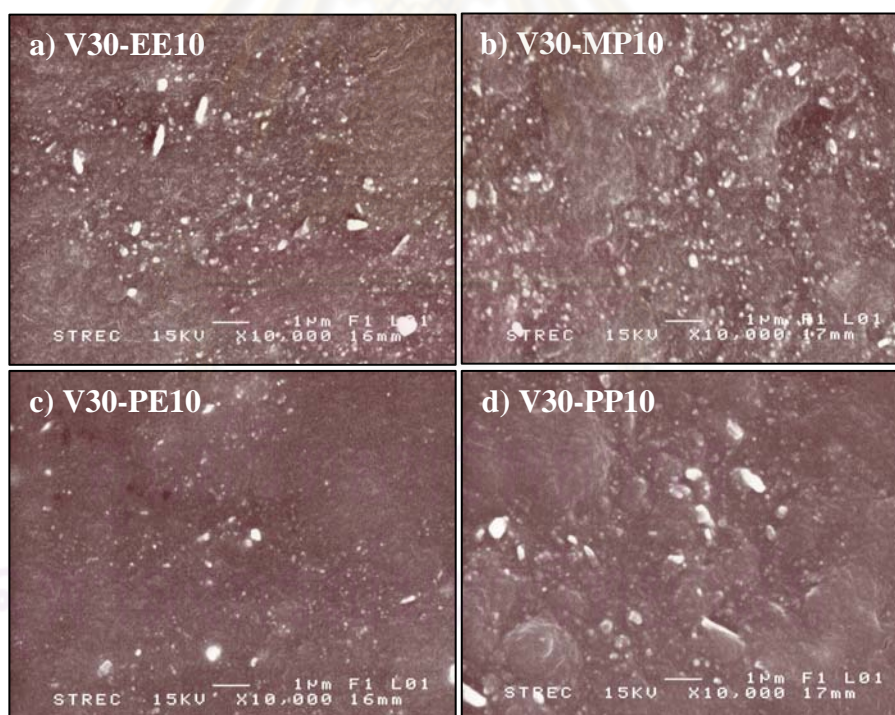
Figure 3.74 The SEM micrographs of the fractured surfaces of the nanosilica-filled NR vulcanizates with variable types of treating agent.

The SEM micrographs are exhibited in Figure 3.74. It was revealed that, SR603, Figure 3.74c, provided the best silica dispersion whereas SR604, Figure 3.74d,

showed very poor silica dispersion. Nevertheless, the silica aggregations were appeared in all samples.

The curing behavior and hardness of vulcanized NR are summarized in Table C13 of Appendix C. The effect of couple treating agents between "PEG and PPG derivatives" and SMA 7052P were also investigated. The properties of "PEG and PPG derivatives" and SMA 7052P treated nanosilica-filled NR vulcanizates were demonstrated in Table C14 of Appendix C.

Scorch time and optimum cured time are manifested in Figure 3.75. PG was referred to PEG and PPG derivatives. The results showed that the presence of SMA 7052P diminished both scorch time and optimum cured time. The results were similar to the outcome received from previous couple treating agents study. In addition, the longer molecular chain provided the deficient scorch time and optimum cured time, V30-PE10 and V30-PP10.
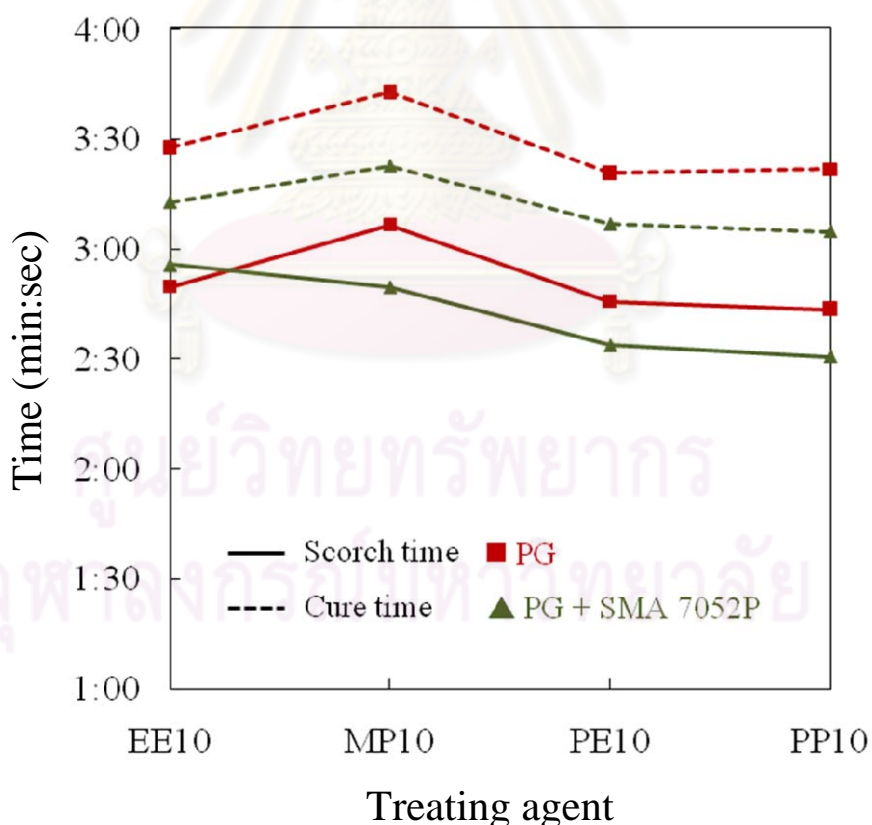
Figure 3.75 The effect of treating agent types on curing behavior.

The tensile strength gradually increased corresponding to the lengthen of molecular skeleton as can be seen in Figure 3.76. Whereas, the presence of SMA

7052P was insignificantly affected on tensile strength. The tensile strength in the presence of SMA 7052P was slightly developed in all vulcanized NR except for V30-EE10 when SR256 was used as treating agent. However, it could be concluded that types of treating agent was not affected to tensile strength of vulcanized NR/silica nanocomposites.
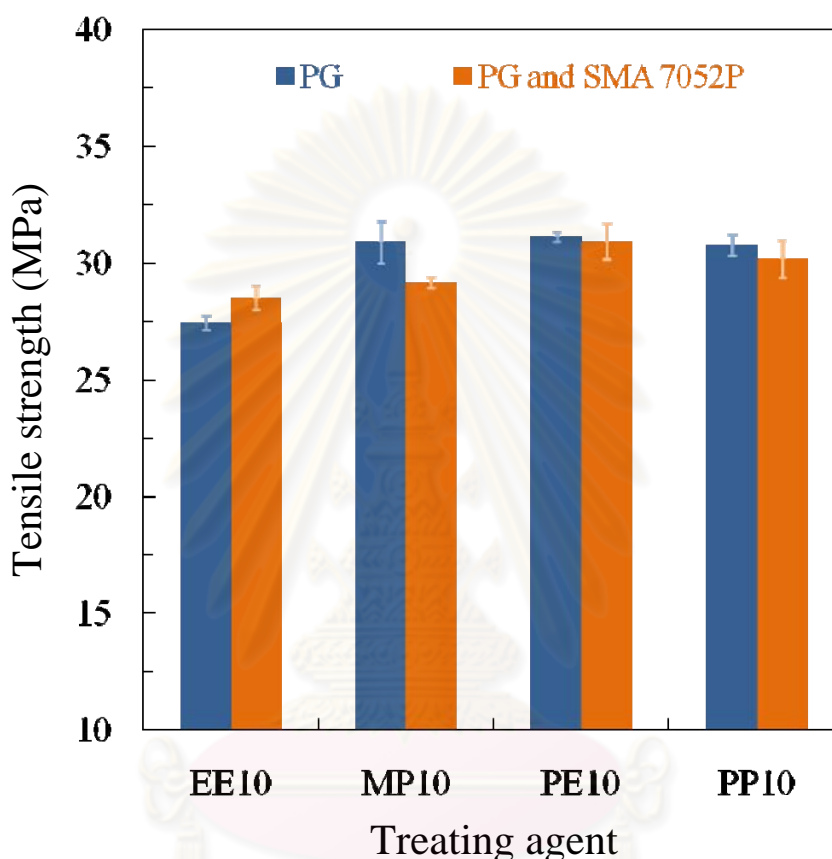
Figure 3.76 The effect of treating agent types on tensile strength.

Figure 3.77 exhibited the M300. The similar M300 results were received for all samples include the vulcanized NR that presence of SMA 7052P. It also could be concluded that types of treating agent was not affected to M300 of vulcanized NR/silica nanocomposites.

The elongations at break results are showed in Figure 3.78. It was found that elongation at break was stretched with presence SR603 and SR604. The results might be due to SR603 and SR604 had longer molecular chains, which the higher enable mobility molecular chain and longer extend under stress. In addition, elongation at break was not affected by presenting of SMA 7052P.
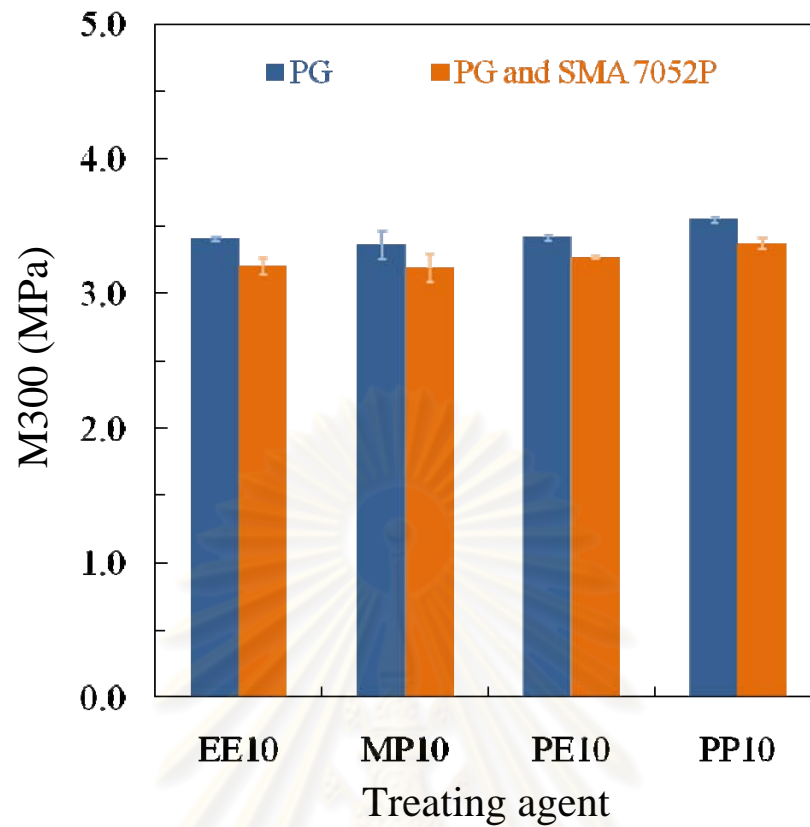
Figure 3.77 The effect of treating agent types on M300.
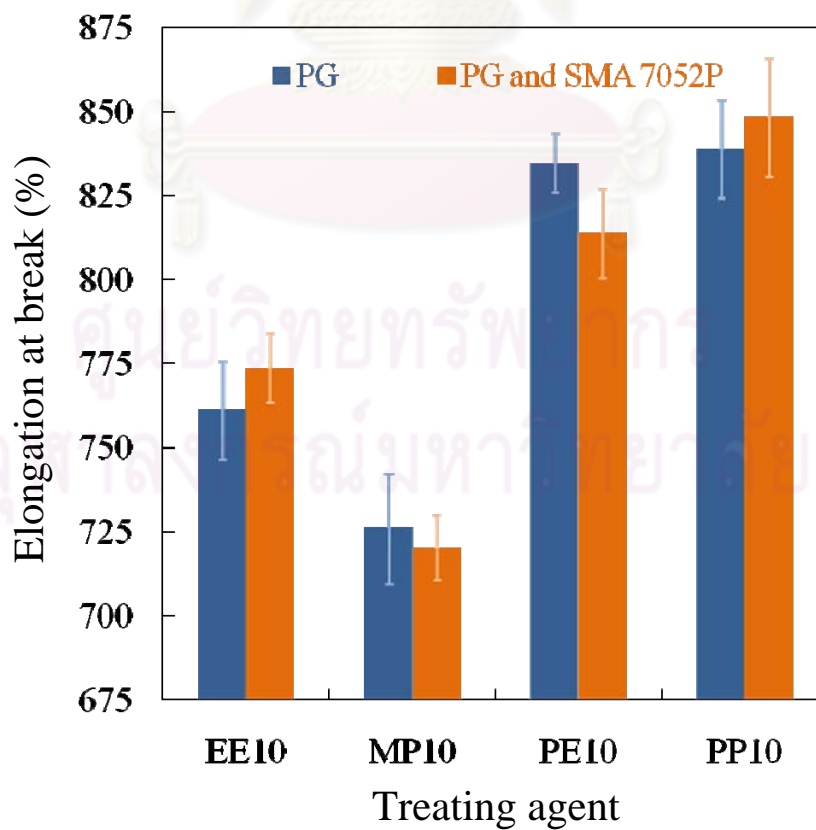
Figure 3.78 The effect of treating agent types on elongation at break.

The similar tear strength was obtained for all samples including the vulcanized NR in the presence of SMA 7052P, Figure 3.79. However, it could also be assumed that types of treating agent was not affected to tear strength of vulcanized NR/silica nanocomposites.

The abrasion resistance results showed in Figure 3.80. The good abrasion resistance was achieved with presence of SR550, SR603 and SR604. The results might be due to methacrylate group on SR550, SR603 and SR604 molecules had better precipitation in vulcanization reaction over acrylate group on SR256 molecules. However, the presence of SMA 7052P together with PG treated nanosilica-filled NR vulcanizates had no relationship on abrasion resistance when comparison with the presence only PG. The presence of SMA 7052P improved the abrasion resistance when SMA 7052P was presented together with SR256. Whereas the SMA 7052P was presented together with SR604, the abrasion resistance was diminished. Nevertheless, all abrasion resistance with presence of PEG and PPG derivatives were displayed lower that of untreated nanosilica-filled NR vulcanizates.
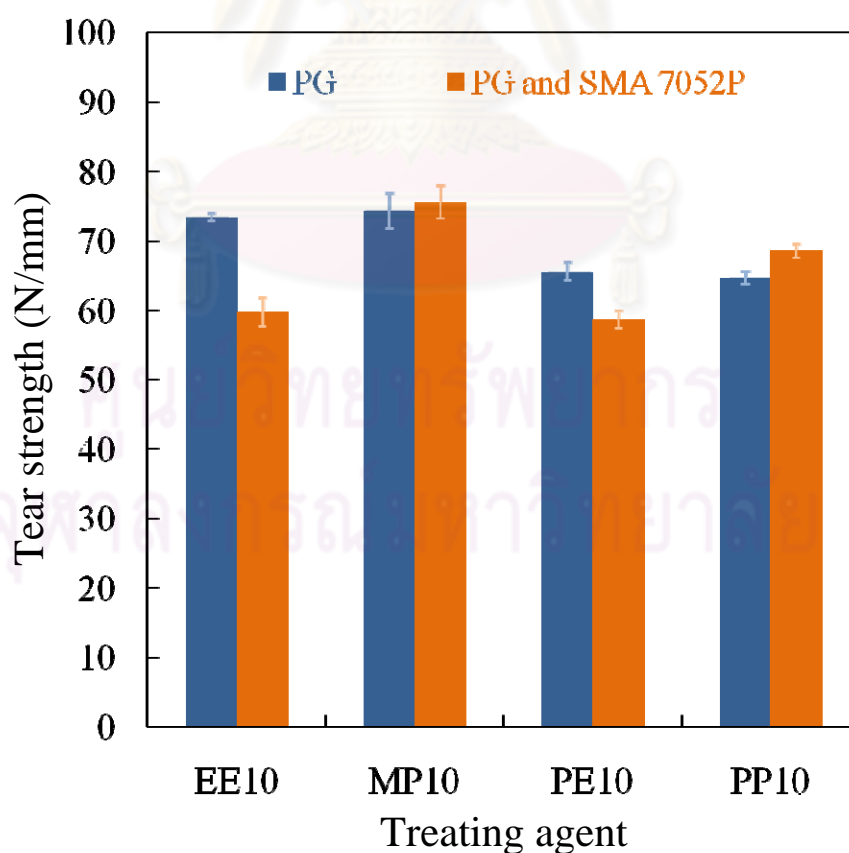
Figure 3.79 The effect of treating agent types on tear strength.
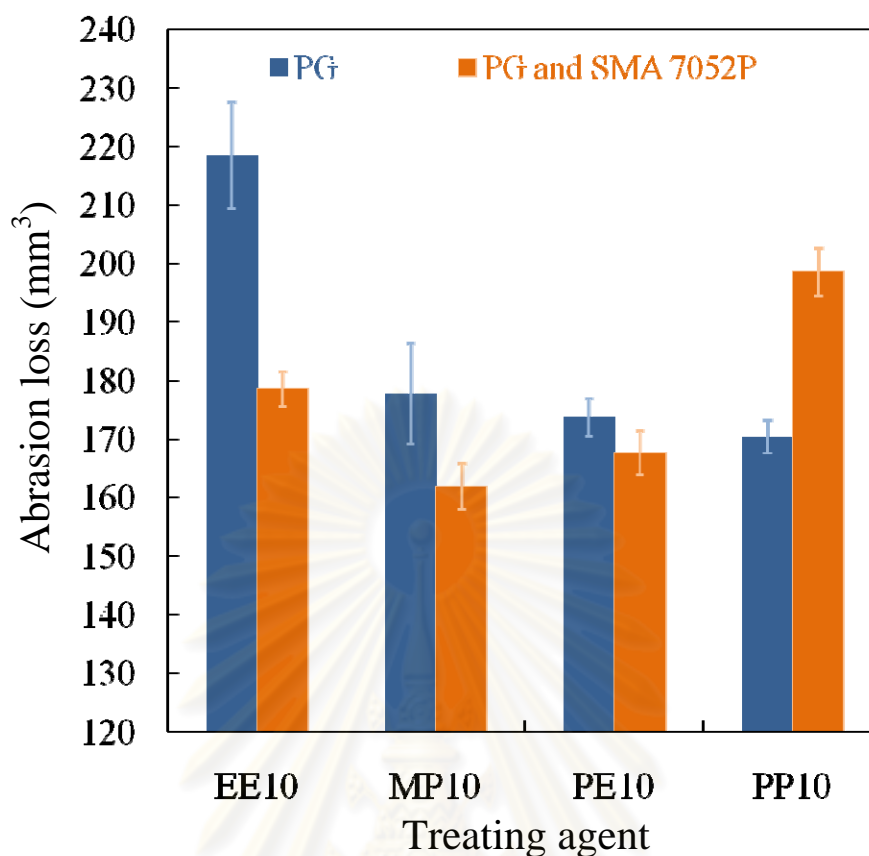
Figure 3.80 The effect of treating agent types on abrasion resistance.

In summary, it could assume that the length molecular chain, molecular structure and the functional group on molecules of PEG and PPG were not significantly affected to the mechanical properties of nanosilica-filled NR. Only the abrasion loss was declined when SR256 was presented. However, the PEG and PPG derivatives treated nanosilica-filled NR vulcanizates exhibited poor mechanical properties when comparing with untreated nanosilica-filled NR vulcaniizates.

CHAPTER IV

CONCLUSION

In the period of the course in this research, effects of modified silica nanoparticles on mechanical properties of natural rubber were studied. The nanosilica slurry was prepared by mechanical grinding of convention silica. The comminuting results showed that the mechanical grinding process provided ground silica with approximately particles size at 19.3 ± 3.4 nm. Furthermore, the mechanical grinding process also granted the good reproducibility and silica stability.

The nanosilica surface was treated by three types of treating agents including SMA, silane coupling agents and PEG derivatives. SMA modified silica surface, SMA 7052P was selected as treating model. The first one, SMA, the comparative study of three type of silica consisting of original silica (WL), untreated nanosilica (NS0) and treated nanosilica with SMA 7052P at constant loading at 1% by weight of silica (SC1) were investigated on mechanical properties on vulcanized NR at variable silica loadings. The resulting showed that SMA 7052P treated nanosilica-filled NR vulcanizates provided highest tensile strength by dominating filler-rubber interaction. The M300 was slightly increased with presence SMA 7052P while NS0 provided highest M300 at silica loading 30 phr by dominating filler-filler interaction. The elongation at break, tear strength and abrasion resistance were not affected by presenting SMA 7052P. The effects of SMA 7052P loading shown that, the increasing of SMA 7052P loading not improved mechanical properties of vulcanized NR/silica nanocomposites. In other word, the mechanical properties especially M300, elongation at break and abrasion resistance had trend to degrade when SMA 7052P loading was increased. Moreover, the mixture of nanosilica slurry and NRL was coagulated without adding formic acid when SMA 7052P was raised up to 3%wt of silica. The comparative study of SMA types, it can be conclude that tensile strength, M300 and abrasion resistance were not improved by changing SMA types. Elongation at break was stretched by presenting bulky molecular structure of SMA 1000I and SMA 1440F. Tear strength was increased by presenting SMA 1000F with providing best silica dispersion.

The second one, silane coupling agents, the untreated nanosilica-filled NR demonstrated the filler-filler interaction over the Si-69 treated nanosilica-filled NR. Whereas the Si-69 treated nanosilica-filled NR manifested filler-rubber interaction overpass the untreated nanosilica-filled NR. The study the effect of silica types and silica loadings on the properties of vulcanized NR/silica nanocomposites, the presence of Si-69 could be improve the mechanical properties of vulcanized NR/silica nanocomposites. The effects of Si-69 loading, it can be concluded that, the lowest filler-filler interaction and highest filler-rubber interaction were achieved which presented Si-69 at 10% by weight of silica. The mechanical properties of silica-reinforced NR vulcanizates were enhanced by increasing Si-69 loading. In addition, the presence of SMA 7052P had insignificantly affected on the mechanical properties of Si-69 treated nanosilica-filled NR vulcanizates. The study of Si-69 and PEG 4000 ratio showed that, the best Si-69 and PEG 4000 ratio was 1:1 weight ratio. The comparative study of silane coupling agent types, the thiol group on terminated of MTMO molecule could be precipitate in vulcanization reaction and reactive over other functional groups on other silane molecule, especially tetrasulfide group on Si-69 molecule. As a result of the high cross-linked density in vulcanized NR/silica nanocomposites, V20-MT10 and V20-MT10P, the lower tensile strength, higher M300, lower elongation at break, lower tear strength and better abrasion resistance were achieved. Similar to MTMO, AMEO had reactive amino group on terminated molecule. Resulting in good tensile strength and abrasion resistance were obtained. However, the presence of high polarity amino group on terminated of AMEO molecule affected to nanosilica slurry transform to cake form during treating process. Resulting in silica aggregation was established and low tear strength was appeared. In addition, the presence of silica aggregation could be enhancing the M300. The similar mechanical properties consisting of tensile strength, tear strength and abrasion resistance were achieved with presence of lower reactive functional groups including tetrasulfide, acrylate and glycidyl on Si-69, MEMO and Glyeo molecules, respectively. In addition, the presence of SMA 7052P had no affected on mechanical properties of silane treated nanosilica-filled NR vulcanizates. Therefore, it could be assume that the mechanical properties of V20-ME10 closely related to the mechanical properties of V20-ME10P.

The last one, PEG and PPG derivatives, the presence of SR550 was not influenced to improve the mechanical properties at all silica content, especially the reducing abrasion loss was found. In addition, the silica aggregation was presented which added SR550. Moreover, the extension of scorch time and optimum cured time were achieved when SR550 was present. The increasing of SR550 loading not affected to improve tensile strength, M300 and tear strength. The elongation at break was extended with increasing SR550 loading. In addition, abrasion resistance was diminished with increasing SR550 loading. Moreover, the presence of SMA 7052P was not affected to mechanical properties of nanosilica-filled NR vulcanizates. Similar to the study the effects of Si-69 and PEG 4000 ratio, the absence PEG 4000 provided poor mechanical properties, especially, tensile strength, elongation at break and abrasion resistance. It was confirmed that PEG 4000 must be added to the recipe of silica reinforced rubber compound. The length molecular chain, molecular structure and the functional group on molecules of PEG and PPG were not significantly affected to the mechanical properties of nanosilica-filled NR. Only the abrasion loss was declined when SR256 was presented. However, the PEG and PPG derivatives treated nanosilica-filled NR vulcanizates exhibited poor mechanical properties when comparing with untreated nanosilica-filled NR vulcaniizates.

The proposal for the future work

In this research, the nanosilica slurry and NR/silica naoncomposites were prepared by mechanical grinding and acid coagulation, respectively. It is interesting that the NR/silica nanocomposite can prepare in different ways. Therefore, the future works for this research are

1. Prepare the silica nanopartices from nanosilica slurry that achieved from this study by using spray dryer.

2. Prepare the NR/silica nanocomposites from the mixture of NRL and nanosilica slurry.

3. Prepare the nanosilica slurry from other methods, such as ultrasonic, and comparing the property of nanosilica slurry.

4. Prepare the nanosilica slurry from conventional silica slurry or cake.

REFERENCES

[1] Dick, J. S. *Rubber technology: Compounding and testing for performance.*
     Hanser publisher: Munich, 2001, 297-343.

[2] Dick, J. S. *How to improve rubber compounds. 1500 Experimental ideas for
     problem solving.* Ohio: Hanser Gardner Publications, Inc., 2004, 23-134.

[3] Hewitt, N. *Compounding precipitated silica in elastomers.* Norwich: William
     Andrew Publishing, 2007, 25-88.

[4] Poh, B. T.; and NG, C. C. Effecf of silane coupling agent on the mooney scorch
     time of silica-filled natural rubber compound. *Eur. Polym. J.* 34 (1998):
     975-979.

[5] Yan, H.; Tian, G.; Sun, K.; Zhang, Y.; and Zhang, Y. Effect of silane coupling
     agent on the polymer-filler interaction and mechanical properties of
     silica-filled NR. *J. Polym. Sci. Pol. Phys.* 43 (2005): 573–584.

[6] Sae-oui, P.; Sirisinha, C.; Thepsuwan, U.; and Hatthapanit, K. Role of silane
     coupling agent on properties of silica-filled polychloroprene. *Eur. Polym.
     J.* 42 (2006): 479-486.

[7] Arrighi, V.; McEwen, I. J.; Qian, H.; and Prieto, M. B. S. The glass transition
     and interfacial layer in styrene-butadiene rubber containing silica
     nanofiller. *Polymer.* 44 (2003): 6259-6266.

[8] Ansarifar, A.; Azhar, A.; Ibrahim, N.; Shiah, S. F.; and Lawton, J. M. D. The
     use of a silanised silica filler to reinforce and crosslink natural rubber.
     Int. J. Adhes. Adhes. 25 (2005): 77-86.

[9]   Peng, C.-C.; Göpfert, A.; Drechsler, M.; and Abetz, V. "Smart" silica-rubber nanocomposites in virture of hydrogen bonding interaction. *Polym. Adv. Technol.* 16 (2005): 771-782.

[10] Hashim, A. S.; Kawabata, N.; and Kohjiya, S. Silica reinforcement of epoxidized natural rubber by the sol-gel method. *J. Sol-Gel Sci. Technol.* 5 (1995): 211–218.

[11] Yoshikai, K.; Ohsaki, T.; and Furukawa, M. Silica reinforcement of synthetic diene rubber by sol-gel process in the latex. *J. Appl. Polym. Sci.* 85 (2002): 2053-2063.

[12] Messori, M.; Bignotti, F.; Santis, R. D.; and Taurino, R. Modification of isoprene rubber by in situ silica generation. *Polym. Int.* 5 (2009): 880-887.

[13] Poompradub, S.; Kohjiya, S.; and Ikeda, Y. Natural rubber/in situ silica nanocomposite of a high silica content. *Chem. Lett*. 34 (2005): 672-673.

[14] Tangpasuthadol, V.; Intasiri, A.; Nuntivanich, D.; Niyompanich, N.; and Kiatkamjornwong, S. Silica-reinforced natural rubber prepared by the sol-gel process of ethoxysilanes in rubber latex. *J. Appl. Polym. Sci.* 109 (2008): 424-433.

[15] Ikeda, Y.; Poompradub, S.; Morita, Y.; and Kohjiya, S. Preparation of high performance nanocomposite elastomer: effect of reaction conditions on in situ silica generation of high content in natural rubber. *J. Sol-Gel Sci. Technol*. 45 (2008): 299-306.

[16] Satraphan, P.; Intasiri, A.; Tangpasuthadol, V.; and Kiatkamjornwong, S. Effects of methyl methacrylate grafting and *in situ* silica particle formation on the morphology and mechanical properties of natural rubber composite films**.** *Polym. Adv. Technol.* 20 (2009): 473-486.

[17] Zhou, D.; and Mark, J. E. Preparation and characterization of *trans*-1,4-polybutadiene nanocomposites containing in situ generated silica *J. Macromol. Sci. Part A—Pure Appl. Polym.* Sci. 41 (2004): 1221-1232.

[18] Mende, S.; Stenger, F.; Peukert, W.; and Schwedes, J. Mechanical production and stabilization of submicron particles in stirred media mills. *Powder Technol. 132* (2003): 64-73.

[19] Stenger, F.; Mende, S.; Schwedes, J.; and Peukert, W. Nanomilling in stirred media mills. *Chem. Eng. Sci*. 60 (2005): 4557-4565.

[20] Wang, Y.; and Forssberg, E. Production of carbonate and silica nano-particles in stirred bead milling. *Int. J. Miner. Procress*. 81 (2006): 1-14.

[21] Pérez-Rodríguez, J. L.; Wiewiora, A.; Ramirez-Valle, V.; Durán, A.; and Pérez-Maqueda, L. A. Preparation of nano-pyrophyllite: Comparative study of sonication and grinding. *J. Phys. Chem. Solids*. 68 (2007): 1225-1229.

[22] Chen, Y.-C.; Chen, X.-L.; Liu, R. L.-H.; Shu, H.-J.; and Ger, M.-D. Preparation of villus-like PMMA/silica hybrids via surface modification and wet grinding. *J. Alloy Compd*. 507 (2010): 302-308.

[23] Bauer, F., et al. Trialkoxysilane grafting onto nanoparticles for the preparation of clear coat polyacrylate systems with excellent scratch performance. *Prog. Org. Coat.* 47 (2003):147-153.

[24] Park, S. J.; and Cho, K. S. Filler-elastomers: influence of silane coupling agent on crosslink density and thermal stability of silica/rubber composites. *J. Colloid Interf. Sci.* 267 (2003): 86-91.

[25] Weng, C.-C.; and Wei, K.-H. Selective distribution of surface-modified TiO_2 nanoparticles in polystyrene-*b*-poly(methyl methacrylate) diblock copolymer. *Chem. Mater.* 15 (2003): 2936-2941.

[26] Sun, Y.; Zhang, Z.; and Wong, C. P. Study on mono-dispersed nano-size silica by surface modification for underfill applications. *J. Colloid Interf. Sci.* 292 (2005): 436-444.

[27] Wada, T.; Inui, K.; and Uragami, T. Properties of organic-inorganic composite materials prepared from acrylic resin emulsions and colloidal silicas. *J. Appl. Polym. Sci.* 101 (2006): 2051-2056.

[28] Sun, S.; Li, C.; Zhang, L.; Du, H. L.; and Burnell-Gray, J. S. Effect of surface modification of fumed silica on interfacial structure and mechanical properties of poly(vinyl chloride) composites. *Eur. Polym. J.* 42 (2006): 1643-1652.

[29] Guo, Z.; Liang, X.; Pereira, T.; Scaffaro, R.; and Hahn, H. T. CuO nanoparticle filled vinyl-ester resin nanocomposutes: fabrication, characterization and property analysis. *Compos. Sci. Technol.* 67 (2007): 2036-2044.

[30] Hong, R. Y., et al. Surface-modified silica nanoparticles for reinforcement of PMMA. *J. Appl. Polym. Sci. 105*, (2007): 2176-2184.

[31] Song, R.; Yang, D. and He, L. Effect of surface modification of nanosilica on crystallization, thermal and mechanical properties of poly(vinylidene fluoride). *J. Mater. Sci.* 42 (2007): 8408-8417.

[32] Zou, W., et al. Effect of nano-SiO_2 on the performance of poly(MMA/BA/MAA)/EP. *Mater. Lett.* 61 (2007): 725-729.

[33] Ajayan, P. M.; Schadler, L. S.; Braun, P. V. *Nanocomposite science and technology.* Weinheim: Wiley-VCH GmbH & Co. KGaA, 2003, 1-75.

[34] Cao, G. *Nanostructures & nanomaterials. Synthesis, properties & applications.* London: Imperial College Press, 2004, 7-10.

[35] Zhang, Q., et al. In-situ, simultaneous milling and coating of particulates with nanoparticles. *Powder Technol.* 196 (2009): 292-297.

[36] Guojian, W.; Zehua, Q.; Lin, L.; Quan, S.; and Jianlong, G. Study of SMA graft modified MWNT/PVC composite materials. *Mater. Sci. Eng. A*. 472 (2008): 136-139.

[37] Spitalsky, Z.; Tasis, D.; Papagelis, K.; and Galiotis, C. Carbon nanotube–polymer composites: Chemistry, processing, mechanical and electrical properties. *Prog. Polym. Sci.* 35 (2010): 357-401.

[38] Dharmarajan, N.; Datta, S.; Ver Strate, G.; and Ban, L. Compatibilized polymer blends of isotatic polypropylene and strene-maleic anhydride copolymer. *Polymer.* 36 (1995): 3849-3861.

[39] Chiang, C.-R.; and Chang, F.-C. Polymer blends of polyamide (PA6) and poly(phenylene oxide) (PPO) compatibilized by styrene-maleic anhydride (SMA) copolymer. *Polymer.* 38 (1997): 4807-4817.

[40] Ju, M.-Y.; and Chang, F.-C. Compatibilization of PET/PS blends through SMA and PMPI dual compatibilizers. *Polymer.* 41 (2000): 1719-1730.

[41] Sae-oui, P.; Sirisinha, C.; Thepsuwan, U.; and Hatthapanit, K. Comparison of reinforcing efficiency between Si-69 and Si-264 in a conventional vulcanization system. *Polym. Test*. 23 (2004): 871-879.

[42] Sae-oui, P.; Sirisinha, C.; Hatthapanit, K.; and Thepsuwan, U. Comparison of reinforcing efficiency between Si-69 and Si-264 in an efficient vulcanization system. *Polym. Test*. 24 (2005): 439-446.

[43] Dick, J. S. *Rubber technology: Compounding and testing for performance.* Hanser publisher: Munich, 2001, 36-39.

[44] Peng, Z.; Kong, L. X.; Li, S-D.; Chen, Y.; and Huang M. F. Self-assembled natural rubber/silica nanocomposites: Its preparation and characterization *Compos. Sci. Technol.* 67 (2007): 3130-3139.

[45] Chen, Y.; Peng, Z.; Kong, L. X.; Huang, M. F.; and Li, P. W. Natural rubber nanocomposite reinforced with nano silica *Polym. Eng. Sci.* 48 (2008): 1674-1677.

[46] Mark, J. E.; Erman, B.; Eirich, F. R. *The science and technology of rubber.* Elsevier Academic Press, 2005, 388-395.

[47] Cassagnau, P. Payne effect and shear elasticity of silica-filled polymers in concentrated solutions and in molten state. *Polymer.* 44 (2003): 2455-2462.

[48] Wang, J.; Hamed, G. R.; Umetsu, K.; and Roland, C. M. The Payne effect in double network elastomers. *Rubber Chem. Technol.* 78 (2005): 76-83.

[49] Frohlich, J.; Niedermeier, W.; and Luginsland, H.-D. The effect of filler-filler and filler-elastomer interaction on rubber reinforcement. *Compos. Part A-Appl. S.* 36 (2005): 449-460.

[50] Ramier, J.; Gauthier, C.; Chazeau, L.; Stelandre, L.; and Guy, L. Payne effect in silica-filled styrene butadiene rubber: Influence of surface treatment. *J. Polym. Sci. Pol. Phys.* 45 (2007): 286-298.

[51] Sun, J., et al. Nonlinear rheological behavior of silica filled solution-polymerized styrene butadiene rubber. *J. Polym. Sci. Pol. Phys.* 45 (2007): 2594-2602.

[52] Cassagnau, P. Melt rheology of organoclay and fumed silica nanocomposites. *Polymer.* 49 (2008): 2183-2196.

[53] Gauthier, C.; Reynaud, E.; Vassoille, R.; and Stelandre, L. L. Analysis of the non-linear viscoelastic behaviour of silica filled styrene butadiene rubber. *Polymer.* 45 (2004): 2761-2771.

[54] Ouyang, G. B. Construction and simulation - modulus, hysteresis and the Payne effect. *Kautsch. Gummi. Kunstst.* 59 (2006): 332–343.

[55] Ouyang, G. B. Raw materials and applications - network junction model for carbon black reinforcement. *Kautsch. Gummi. Kunstst.* 59 (2006): 454–458.

[56] Merabia, S.; Sotta, P.; and Long, D. R. A microscopic model for the reinforcement and the nonlinear behavior of filled elastomers and thermoplastic elastomers (Payne and Mullins effects). *Macromolecules.* 41 (2008): 8252-8266.

[57] Katz, J. R. Röntgenspektrograpische untersuchungen am gedehnten kautschuk und ihre mögliche bedeutung für das problem der dehnungseigenschaften dieser substanz. *Naturwiss.* 19 (1925): 410-416.

[58] Mitchell, G. R. A wide-angle X-ray study of the development of molecular orientation in crosslinked natural rubber. *Polymer.* 25 (1984): 1562-1572.

[59] Ikeda, Y. et al. Mechanical characteristics of hydrogenated natural rubber vulcanizates. *Polym. Adv. Technol.* 19 (2008): 1608-1615.

[60] Dupres, S.; Long, D. R.; Albouy, P.-A.; and Sotta, P. Local deformation in carbon black-filled polyisoprene rubbers studied by NMR and x-ray diffraction. *Macromolecules.* 42 (2009): 2634-2644.

[61] Weng, G.; Huang, G.; Qu, L.; Nie, Y.; and Wu, J. Large-scale orientation in a vulcanized stretched natural rubber network: proved by in situ synchrotron x-ray diffraction characterization. *J. Phys. Chem. B.* 114 (2010): 7179-7188.

[62] Chenal, J.-M.; Gauthier, C.; Chazeau, L.; Guy, L.; and Bomal, Y. Parameters governing strain induced crystallization in filled natural rubber. *Polymer.* 48 (2007): 6893-6901.

[63] Chenal, J.-M.; Chazeau, L.; Guy, L.; Bomal, Y.; and Gauthier, C. Molecular weight between physical entanglements in natural rubber: A critical

parameter during strain-induced crystallization. *Polymer.* 48 (2007): 1042-1046.

[64] Poompradub, S. et al. Mechanism of strain-induced crystallization in filled and unfilled natural rubber vulcanizates. *J. Appl. Phys.* 97 (2005): 103529-103537.

[65] Ikeda, Y. et al. Strain-induced crystallization of peroxide-crosslinked natural rubber. *Polymer.* 48 (2007): 1171-1175.

[66] Ikeda, Y.; Yasuda, Y.; Hijikata, K.; Tosaka, M.; and Kohjiya, S. Comparative study on strain-induced crystallization behavior of peroxide cross-linked and sulfur cross-linked natural rubber. *Macromolecules.* 41 (2008): 5876-5884.

[67] Rattanasom, N.; Saowapark, T.; and Deeprasertkul, C. Reinforcement of natural rubber with silica/carbon black hybrid filler. *Polym. Test.* 26 (2007): 369-377.

APPENDICES
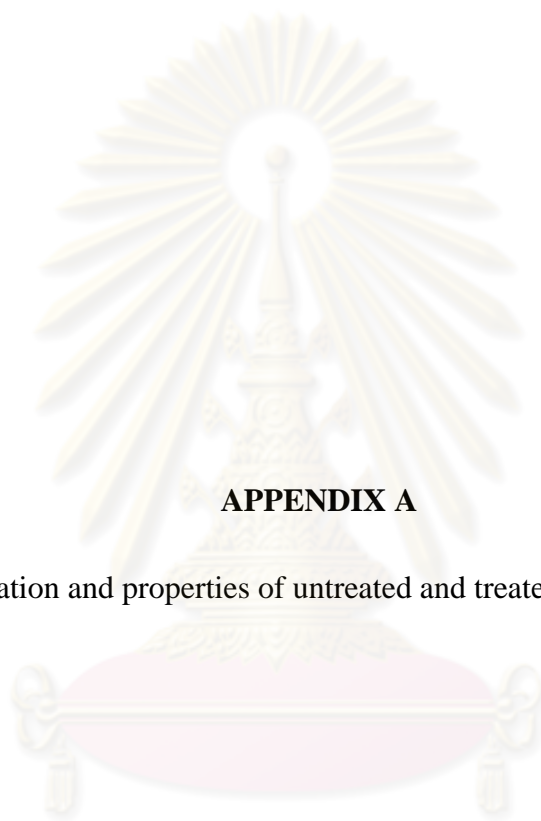
APPENDIX A

The preparation and properties of untreated and treated nanosilica slurry

Table A1 Preparation and properties of SMA treated nanosilica slurry

Sample code	Treating agent[a] (SMA)		Average size (nm)	Particle size distribution[b] (%)		
	Type	Amount[c] (%)		< 100 nm	0.1-1 μm	> 1 μm
NS0	-	-	68.14	90.07	9.44	0.48
SC0.1	Pro 7052P	0.1	68.14	90.07	9.44	0.48
SC1	Pro 7052P	1.0	68.14	90.07	9.44	0.48
SC2	Pro 7052P	2.0	68.14	90.07	9.44	0.48
SC3	Pro 7052P	3.0	68.14	90.07	9.44	0.48
SM1	1000F	1.0	68.14	90.07	9.44	0.48
SI1	1000I	1.0	68.14	90.07	9.44	0.48
AA1	1000MA	1.0	68.14	90.07	9.44	0.48
EA1	1440F	1.0	68.14	90.07	9.44	0.48

[a] Adding after nanosilica was collected and cooled down.

[b] Particle size distribution before treating with SMA.

[c] Percentage by weight of silica.

Table A2 Preparation and the effect of treating time on the properties of nanosilica slurry

Treating time[a] (min)	Average size[b] (nm)	Particle size distribution[b] (%)			Average size[c] (nm)	Particle size distribution[c] (%)		
		< 100 nm	0.1-1.0 μm	> 1 μm		< 100 nm	0.1-1.0 μm	> 1 μm
15	66.58	95.15	4.16	0.69	66.94	94.53	4.36	1.71
30	66.81	95.64	4.36	0	67.20	94.95	3.67	1.38
45	66.87	95.48	4.52	0	67.15	95.42	3.36	1.22
60	66.68	95.22	4.31	0.47	66.97	94.83	3.55	1.62

[a] Time after adding Si-69.　　　[b] Particle size distribution before adding Si-69.　　　[c] Particle size distribution after adding Si-69.

Table A3 Preparation and the effect of treating temperature on the properties of nanosilica slurry

Treating temperature[a] (°C)	Average size[c] (nm)	Particle size distribution[c] (%)			Average size[c] (nm)	Particle size distribution[c] (%)		
		< 100 nm	0.1-1.0 μm	> 1 μm		< 100 nm	0.1-1.0 μm	> 1 μm
60	66.81	95.64	4.36	0	67.20	94.95	3.67	1.38
70	66.54	95.02	4.16	0.82	66.82	94.46	3.57	1.97
80	66.59	94.88	4.25	0.87	66.90	94.08	3.75	2.17
90	66.75	94.48	4.74	0.78	67.09	93.90	4.12	1.98

[a] Temperature after adding Si-69.　　　[b] Particle size distribution before adding Si-69.　　　[c] Particle size distribution after adding Si-69.

Table A4 Preparation and properties of silane coupling agents treated nanosilica slurry

Sample code	Silane coupling agent		Size[a,c] (nm)	Particle size distribution[a] (%)			Size[b,c] (nm)	Particle size distribution[b] (%)		
	Type	Amount[d]		< 100 nm	0.1-1 μm	> 1 μm		< 100 nm	0.1-1 μm	> 1 μm
TS1	Si-69	1.0	66.67	95.47	4.13	0.48	66.72	95.41	3.19	1.40
TS3	Si-69	3.0	66.60	95.24	4.23	0.53	66.79	94.93	3.59	1.48
TS5	Si-69	5.0	66.55	95.44	4.03	0.53	66.96	94.19	3.71	2.10
TS10	Si-69	10.0	66.81	95.64	4.36	0	67.20	94.95	3.67	1.38
TS15	Si-69	15.0	66.53	95.37	3.96	0.67	66.90	94.85	3.36	1.79
ME10	MEMO	10.0	65.53	99.82	0.18	0	65.56	99.82	0.18	0
MT10	MTMO	10.0	65.50	99.83	0.17	0	65.69	99.58	0.21	0.21
GL10	Glyeo	10.0	65.42	99.84	0.16	0	65.43	99.84	0.16	0
AM10	AMEO	10.0	65.34	99.86	0.14	0	-	-	-	-

[a] Particle size before adding silane coupling agents.

[b] Particle size after adding silane coupling agents.

[c] Average particle size.

[d] Percent by weight of silica.

Table A5 Preparation and properties of PEG and PPG derivatives treated nanosilica slurry

Sample code	PEG or PPG derivatives		Size[a,c] (nm)	Particle size distribution[a] (%)			Size[b,c] (nm)	Particle size distribution[b] (%)		
	Type	Amount[d]		< 100 nm	0.1-1 μm	> 1 μm		< 100 nm	0.1-1 μm	> 1 μm
MP1	SR550	1.0	67.92	90.54	8.62	0.84	67.73	91.52	7.76	0.72
MP3	SR550	3.0	67.80	91.29	8.02	0.69	67.53	92.71	6.78	0.51
MP5	SR550	5.0	67.81	91.25	8.08	0.67	67.63	92.15	7.32	0.53
MP10	SR550	10.0	68.00	90.30	9.13	0.57	67.60	92.53	7.08	0.39
MP15	SR550	15.0	68.12	89.78	9.40	0.82	67.67	92.05	7.41	0.54
EE10	SR256	10.0	68.03	90.44	8.94	0.62	67.72	91.99	7.48	0.53
PE10	SR603	10.0	68.04	90.22	9.09	0.69	67.70	92.00	7.46	0.54
PP10	SR604	10.0	68.09	90.00	9.19	0.81	67.74	91.73	7.67	0.60

[a] Particle size before adding PEG and PPG derivatives.

[b] Particle size after adding PEG and PPG derivatives.

[c] Average particle size.

[d] Percent by weight of silica.
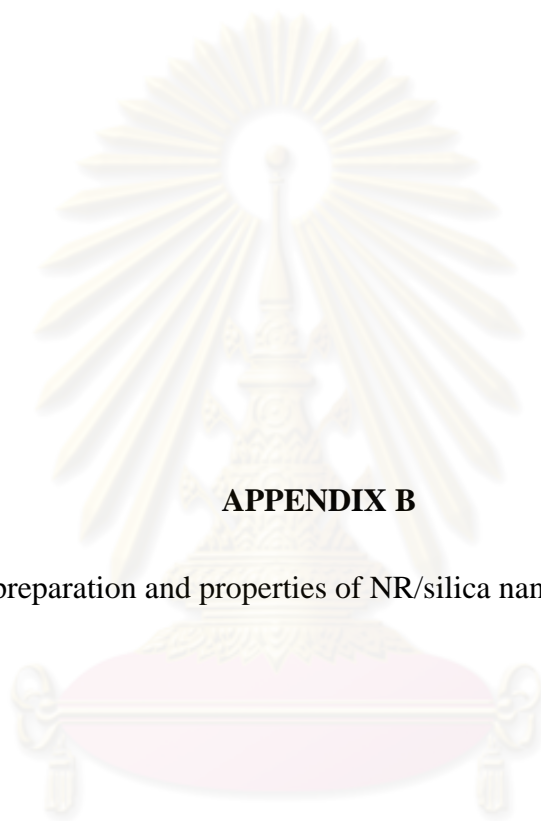
APPENDIX B

The preparation and properties of NR/silica nanocomposites

Table B1 Preparation and properties of untreated and SMA treated nanosilica-filled NR

Sample name	Nanoilica slurry[a]		NR/silica nanocomposites[b]		Weight loss (%)		
	Code	Amount (g)	Silica content (phr)	Weight (g)	Rubber	Silica	Total
NC13-NS0	NS0	300	13.17	334.8	1.39	14.81	2.96
NC21-NS0	NS0	500	21.42	361.3	0.81	15.03	3.65
NC34-NS0	NS0	700	33.54	389.9	2.67	6.74	3.73
NC13-SC1	SC1	300	12.86	331.1	2.33	16.24	4.15
NC22-SC1	SC1	500	21.65	342.3	6.37	19.91	8.90
NC31-SC1	SC1	700	31.34	363.0	8.10	17.70	10.60
NC36-SC1	SC1	900	35.63	390.5	4.20	24.73	10.51
NC40-SC1	SC1	1100	39.98	389.0	7.63	32.85	16.64
NC31-SC0.1	SC0.1	700	31.02	380.7	3.17	14.18	6.02
NC30-SC2	SC2	700	30.43	387.7	1.15	14.90	4.77
NC30-SC3	SC3	700	29.95	382.4	1.81	18.79	6.31
NC31-SM1	SM1	700	31.34	363.0	8.10	17.70	10.60
NC31-SI1	SI1	700	31.02	373.5	5.20	15.97	8.02
NC30-AA1	AA1	700	29.62	325.0	16.61	29.43	19.96
NC32-EA1	EA1	700	31.95	374.6	5.60	25.03	12.10

[a] Nanosilica slurry (pH 6.0) 15% by weight was used.

[b] NR/silica nanocomposites after drying.

Table B2 The effect of treating time and temperature on properties of Si-69 treated nanosilica-filled NR

Treating conditions		NR/silica nanocomposites[a]		Weight loss (%)		
		Silica content (phr)	Weight (g)	Rubber	Silica	Total
Time[b] (min)	15	31.08	370	8.09	18.38	10.95
	30	33.41	384.0	6.40	10.65	7.58
	45	32.44	313.0	23.11	28.73	24.67
	60	32.74	327.5	19.74	24.92	21.18
Temperature[c] (°C)	60	33.41	384.0	6.40	10.65	7.58
	70	31.61	375.0	7.25	16.23	9.75
	80	31.52	375.0	7.18	16.41	9.75
	90	30.05	393.3	1.47	15.40	5.34

[a] NR/silica nanocomposites after drying.

[c] Time after adding Si-69.

[b] Temperature after adding Si-69.

Table B3 Preparation and properties of Si-69 treated nanosilica-filled NR

Sample name	Nanoilica slurry[a]		NR/silica nanocomposites[b]		Weight loss (%)		
	Code	Amount (g)	Silica content (phr)	Weight (g)	Rubber	Silica	Total
NC13-TS10	TS10	300	12.79	340.7	0.45	15.08	2.52
NC21-TS10	TS10	500	20.82	350.0	5.08	20.93	8.50
NC33-TS10	TS10	700	33.41	384.0	6.40	10.65	7.58
NC34-TS1	TS1	700	33.70	388.0	3.51	14.70	4.45
NC34-TS3	TS3	700	33.83	400.0	1.12	4.43	2.00
NC40-TS5	TS5	700	32.15	385.4	3.96	11.77	6.06
NC32-TS15	TS15	700	31.98	380.8	7.20	15.20	9.49
NC31-TS1P	TS1	700[c]	31.20	372.7	5.76	15.98	8.45
NC32-TS3P	TS3	700[c]	31.69	393.7	1.30	10.64	3.79
NC33-TS5P	TS5	700[c]	32.50	401.0	0.58	7.68	2.50
NC30-TS10P	TS10	700[c]	30.34	387.5	3.38	16.24	6.97
NC30-TS15P	TS15	700[c]	30.16	400.0	1.22	14.90	5.17

[a] Nanosilica slurry (pH 6.0) 15% by weight was used.

[b] NR/silica nanocomposites after drying.

[c] SMA 7052P (1% by weight of silica) solution was added before mixing with NRL.

Table B4 Preparation and properties of Silane treated nanosilica-filled NR

Sample name	Nanoilica slurry[a]		NR/silica nanocomposites[b]		Weight loss (%)		
	Code	Amount (g)	Silica content (phr)	Weight (g)	Rubber	Silica	Total
NC30-ME10[c]	ME10	700	-	-	-	-	-
NC25-MT10	MT10	700	24.53	374.0	1.83	31.18	9.99
NC25-GL10	GL10	700	25.40	318.3	17.07	39.82	23.39
NC23-AM10	AM10	700	23.02	353.7	5.93	38.11	14.87
NC20-TS10P	TS10	500[d]	19.83	350.0	3.99	25.57	8.68
NC26-ME10P	ME10	700[d]	26.45	338.0	12.90	34.18	18.65
NC24-MT10P	MT10	700[d]	24.01	306.7	19.28	44.63	26.19
NC28-GL10P	GL10	700[d]	27.65	385.0	1.80	22.43	7.34
NC22-AM10P	AM10	700[d]	22.34	345.7	7.66	41.06	16.80

[a] Nanosilica slurry (pH 6.0) 15% by weight was used.

[b] NR/silica nanocomposites after drying.

[c] Not coagulated.

[d] SMA 7052P (1% by weight of silica) solution was added before mixing with NRL.

Table B5 Preparation and properties of SR550 treated nanosilica-filled NR

Sample name	Nanoilica slurry[a]		NR/silica nanocomposites[b]		Weight loss (%)		
	Code	Amount (g)	Silica content (phr)	Weight (g)	Rubber	Silica	Total
NC13-MP10	MP10	300	13.16	342.0	0.40	12.65	2.15
NC21-MP10	MP10	500	20.65	354.7	3.66	20.40	7.27
NC30-MP10	MP10	700	30.44	367.8	8.16	20.11	11.48
NC34-MP1	MP1	700	33.98	374.5	6.76	10.63	7.77
NC31-MP3	MP3	700	31.03	375.0	5.28	16.01	8.12
NC33-MP5	MP5	700	32.95	344.3	14.73	19.73	16.08
NC31-MP15	MP15	700	31.31	336.0	17.65	26.33	20.14
NC31-MP1P	MP1	700[c]	30.72	391.0	0.76	12.91	3.95
NC32-MP2P	MP3	700[c]	31.56	398.0	0.12	9.93	2.74
NC33-MP3P	MP5	700[c]	32.58	401.0	0.65	7.51	2.50
NC31-MP4P	MP10	700[c]	31.25	393.0	2.74	13.16	5.42
NC32-MP5P	MP15	700[c]	32.31	377.3	8.52	15.55	10.55

[a] Nanosilica slurry (pH 6.0) 15% by weight was used.

[b] NR/silica nanocomposites after drying.

[c] SMA 7052P (1% by weight of silica) solution was added before mixing with NRL.

Table B6 Preparation and properties of PEG and PPG derivatives treated nanosilica-filled NR

Sample name	Nanoilica slurry[a]		NR/silica nanocomposites[b]		Weight loss (%)		
	Code	Amount (g)	Silica content (phr)	Weight (g)	Rubber	Silica	Total
NC34-EE10	EE10	700	33.86	357.0	13.30	16.11	14.08
NC31-PE10	PE10	700	30.93	344.5	14.32	24.28	17.03
NC33-PP10	PP10	700	32.88	399.7	2.15	8.09	3.80
NC31-MP10P	MP10	700[c]	31.25	393.0	2.74	13.16	5.42
NC30-EE10P	EE10	700[c]	30.18	339.2	15.31	26.97	18.57
NC30-PE10P	PE10	700[c]	29.92	368.7	7.74	21.14	11.49
NC32-PP10P	PP10	700[c]	32.44	396.8	2.75	9.87	4.74

[a] Nanosilica slurry (pH 6.0) 15% by weight was used.

[b] NR/silica nanocomposites after drying.

[c] SMA 7052P (1% by weight of silica) solution was added before mixing with NRL.
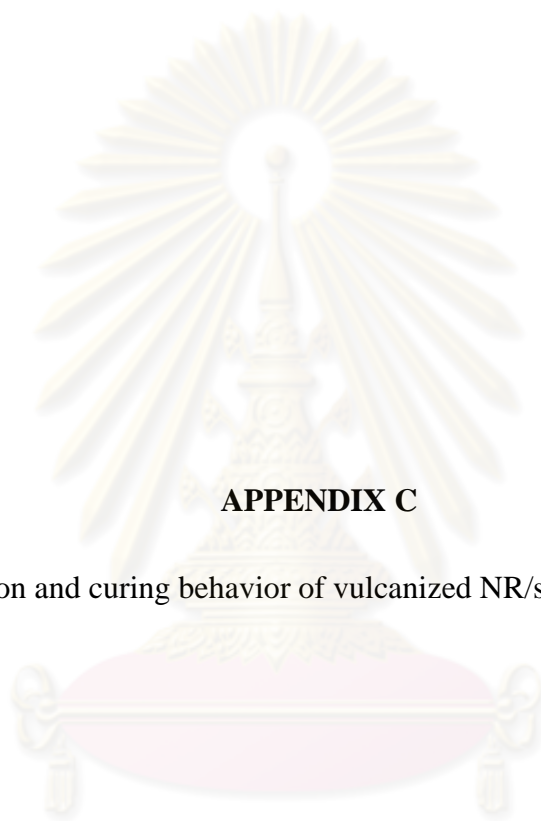
APPENDIX C

The preparation and curing behavior of vulcanized NR/silica nanocomposites

Table C1 The properties of sulfur cross-linking of original silica-filled NR at variable silica loading

Ingredients (phr)	Sample name of vulcanized NR/silica nanocomosites					
	VNR	V10-WL	V20-WL	V30-WL	V35-WL	V40-WL
NR (TTR 5L)	100	100	100	100	100	100
Silica powder (WL180)	0	10	20	30	35	40
Properties						
t_s2 (min:sec)	1:21	2:01	2:13	1:55	1:57	2:04
t_c90 (min:sec)	1:54	2:29	2:41	2:35	2:32	2:39
CRI^a (sec^{-1})	3.03	3.57	3.57	2.50	2.86	2.86
Toque (dN/m)						
ML	2.14	2.52	2.87	3.60	5.67	6.74
MH	10.09	11.00	12.24	17.44	21.15	21.19
Hardness (Shore A)	36	40	46	57	60	64

[a] Cure rate index.

Table C2 The effect of untreated and SMA 7052P treated nanosilica on the properties of vulcanized NR/silica nanocomposites with variable silica loading

Ingredients (phr)	Sample name of vulcanized NR/silica nanocomposites							
	V10-NS0	**V20-NS0**	**V30-NS0**	**V10-SC1**	**V20-SC1**	**V30-SC1**	**V35-SC1**	**V40-SC1**
NR/silica nanocomposite	NC13-NS0	NC21-NS0	NC34-NS0	NC13-SC1	NC22-SC1	NC31-SC1	NC36-SC1	NC40-SC1
Silica content	10	20	30	10	20	30	35	40
SMA 7052P (phr)	-	-	-	0.10	0.20	0.30	0.35	0.40
SMA 7052P (%[a])	-	-	-	1	1	1	1	1
Properties								
t_s2 (min:sec)	2:32	3:05	1:59	2:01	2:21	2:27	2:16	2:13
t_c90 (min:sec)	2:54	3:32	2:27	2:24	2:53	2:57	2:50	2:44
CRI^{b} (sec^{-1})	4.55	3.70	3.57	4.35	3.12	3.33	2.94	3.23
Toque (dN/m)								
ML	2.12	2.28	3.87	2.62	2.69	4.29	5.07	7.50
MH	11.29	12.60	17.63	11.33	12.71	17.03	17.71	20.81
Hardness (Shore A)	39	46	57	39	43	55	57	62

[a] Percentage by weight of silica.　　　　[b] Cure rate index.

Table C3 The effect of SMA 7052P treated nanosilica on the properties of vulcanized NR/silica nanocomposites with
variable SMA 7052P loading

Ingredients (phr)	Sample name of vulcanized NR/silica nanocomposites				
	V30-NS0	V30-SC0.1	V30-SC1	V30-SC2	V30-SC3
NR/silica nanocomposite	NC34-NS0	NC31-SC0.1	NC31-SC1	NC30-SC2	NC30-SC3
Silica content	30	30	30	30	30
SMA 7052P (phr)	-	0.03	0.30	0.60	0.90
SMA 7052P (%[a])	-	0.1	1	2	3
Properties					
t_s2 (min:sec)	1:59	2:47	2:27	2:19	1:31
t_c90 (min:sec)	2:27	3:20	2:57	2:52	1:59
CRI^b (sec^{-1})	3.57	3.03	3.33	3.03	3.57
Toque (dN/m)					
ML	3.87	4.46	4.29	4.30	4.25
MH	17.63	17.08	17.03	16.84	16.43
Hardness (Shore A)	57	54	55	55	54

[a] Percentage by weight of silica.   [b] Cure rate index.

Table C4 The effect of SMA treated nanosilica on the properties of vulcanized NR/silica nanocomposites with variable SMA types

Ingredients (phr)	Sample name of vulcanized NR/silica nanocomposites				
	V30-SC1	**V30-SM1**	**V30-SI1**	**V30-AA1**	**V30-EA1**
NR/silica nanocomposite	NC31-SC1	NC31-SM1	NC31-SI1	NC30-AA1	NC32-EA1
Silica content	30	30	30	30	30
SMA (phr)	0.30	0.30	0.30	0.30	0.30
SMA (%[a])	1	1	1	1	1
Properties					
t_s2 (min:sec)	2:27	2:51	2:50	3:00	2:55
t_c90 (min:sec)	2:57	3:08	3:05	3:16	3:09
CRI[b] (sec^{-1})	3.33	5.88	6.67	6.25	7.14
Toque (dN/m)					
ML	4.29	3.26	4.19	2.70	3.59
MH	17.03	14.77	15.80	13.56	14.71
Hardness (Shore A)	55	54	54	52	52

[a] Percentage by weight of silica.   [b] Cure rate index.

Table C5 The effect of Si-69 treated nanosilica on the properties of vulcanized NR/silica nanocomposites with variables Si-69 content and silica loading

Ingredients (phr)	Sample name of vulcanized NR/silica nanocomposites						
	V10-TS10	V20-TS10	V30-TS10	V30-TS1	V30-TS3	V30-TS5	V30-TS15
NR/silica nanocomposite	NC13-TS10	NC21-TS10	NC33-TS10	NC34-TS1	NC34-TS3	NC40-TS5	NC32-TS15
Silica content	10	20	30	30	30	30	30
Si-69 (phr)	1.0	2.0	3.0	0.3	0.9	1.5	4.5
Si-69 (%[a])	10	10	10	1	3	5	15
Properties							
t_s2 (min:sec)	2:52	2:41	2:25	2:38	2:36	2:29	2:17
t_c90 (min:sec)	3:15	3:06	2:54	3:15	3:07	3:01	2:46
CRI[b] (sec^{-1})	4.35	4.00	3.45	2.70	3.23	3.12	3.45
Toque (dN/m)							
ML	2.35	2.85	3.59	3.48	3.24	3.37	3.75
MH	10.87	13.08	16.46	16.41	15.63	16.21	17.16
Hardness (Shore A)	43	49	58	55	55	56	58

[a] Percentage by weight of silica.   [b] Cure rate index.

Table C6 The effect of couple treating agent between Si-69 and SMA 7052P on the properties of vulcanized NR/silica nanocomposites

Ingredients (phr)	Sample name of vulcanized NR/silica nanocomposites					
	V30-SC1	**V30-TS1P**	**V30-TS3P**	**V30-TS5P**	**V30-TS10P**	**V30-TS15P**
NR/silica nanocomposite	NC31-SC1	NC31-TS1P	NC32-TS3P	NC33-TS5P	NC30-TS10P	NC30-TS15P
Silica content	30	30	30	30	30	30
Si-69 (phr)	-	0.3	0.9	1.5	3.0	4.5
Si-69 (%[a])	-	1	3	5	10	15
SMA 7052P (phr)	0.30	0.30	0.30	0.30	0.30	0.30
SMA 7052P (%[a])	1	1	1	1	1	1
Properties						
t_s2 (min:sec)	2:27	2:32	2:32	2:18	2:09	2:09
t_c90 (min:sec)	2:57	3:02	2:48	2:46	2:35	2:40
CRI[b] (sec^{-1})	3.33	3.33	6.25	3.57	3.85	3.23
Toque (dN/m)						
ML	4.29	3.67	4.04	3.75	3.93	3.73
MH	17.03	16.18	17.26	16.72	17.01	17.60
Hardness (Shore A)	55	53	56	56	57	58

[a] Percentage by weight of silica.   [b] Cure rate index.

Table C7 The effect of Si-69 and PEG 4000 ratio on the properties of vulcanized NR/silica nanocomposites

Ingredients (phr)	Si-69 and PEG 4000 ratio				
	0 : 10	**1 : 9**	**3 : 7**	**5 : 5**	**10 : 0**
NR/silica nanocomposite	NC34-NS0	NC34-TS1	NC34-TS3	NC32-TS5	NC33-TS10
Silica content	30	30	30	30	30
Si-69 (phr)	-	0.3	0.9	1.5	3.0
Si-69 (%[a])	**0**	**1**	**3**	**5**	**10**
PEG 4000 (phr)	3.0	2.7	2.1	1.5	-
PEG 4000 (%[a])	**10**	**9**	**7**	**5**	**0**
Properties					
t_s2 (min:sec)	1:59	2:36	2:37	2:35	2:12
t_c90 (min:sec)	2:27	3:15	3:07	3:06	2:45
CRI[b] (sec^{-1})	3.57	2.56	3.33	3.23	3.03
Toque (dN/m)					
ML	3.87	3.61	3.41	3.46	4.28
MH	17.63	16.63	15.54	15.73	15.07
Hardness (Shore A)	57	56	55	56	51

[a] Percentage by weight of silica. [b] Cure rate index.

Table C8 The effect of silane treated nanosilica on the properties of vulcanized NR/silica nanocomposites with variable silane types

Ingredients (phr)	Sample name of vulcanized NR/silica nanocomposites				
	V20-TS10	**V20-ME10**	**V20-MT10**	**V20-GL10**	**V20-AM10**
NR/silica nanocomposite	NC21-TS10	NC30-ME10	NC25-MT10	NC25-GL10	NC23-AM10
Silica content	20	-	20	20	20
Silane (phr)	2	-	2	2	2
Silane (%[a])	10	-	10	10	10
Properties					
t_s2 (min:sec)	2:41	-	0:17	153	1:39
t_c90 (min:sec)	3:06	-	1:08	178	2:04
CRI[b] (sec^{-1})	4.00	-	1.96	4.00	4.00
Toque (dN/m)					
ML	2.85	-	8.64	2.73	4.18
MH	13.08	-	26.13	13.21	13.63
Hardness (Shore A)	49	-	46	49	45

[a] Percentage by weight of silica.   [b] Cure rate index.

Table C9 The effect of couple treating agent between silane and SMA 7052P on the properties of vulcanized NR/silica nanocomposites
with variable silane types

Ingredients (phr)	Sample name of vulcanized NR/silica nanocomposites				
	V20-TS10P	**V20-ME10P**	**V20-MT10P**	**V20-GL10P**	**V20-AM10P**
NR/silica nanocomposite	NC20-TS10P	NC26-ME10P	NC24-MT10P	NC28-GL10P	NC22-AM10P
Silica content	20	20	20	20	20
Silane (phr)	2	2	2	2	2
Silane (%[a])	10	10	10	10	10
SMA 7052P (phr)	0.20	0.20	0.20	0.20	0.20
SMA 7052P (%[a])	1	1	1	1	1
Properties					
t_s2 (min:sec)	2:41	2:31	0:18	2:13	1:24
t_c90 (min:sec)	3:04	2:55	1:07	2:39	1:53
CRI[b] (sec^{-1})	4.35	4.17	2.04	3.85	3.45
Toque (dN/m)					
ML	2.74	2.67	9.37	3.31	5.27
MH	12.83	13.37	27.76	14.56	13.76
Hardness (Shore A)	48	48	45	51	44

[a] Percentage by weight of silica. [b] Cure rate index.

Table C10 The effect of SR550 treated nanosilica on the properties of vulcanized NR/silica nanocomposites with variables silica content and SR550 loading

Ingredients (phr)	Sample name of vulcanized NR/silica nanocomposites						
	V10-MP10	**V20-MP10**	**V30-MP10**	**V30-MP1**	**V30-MP3**	**V30-MP5**	**V30-MP15**
NR/silica nanocomposite	NC13-MP10	NC21-MP10	NC30-MP10	NC34-MP1	NC31-MP3	NC33-MP5	NC31-MP15
Silica content	10	20	30	30	30	30	30
SR550 (phr)	1.0	2.0	3.0	0.3	0.9	1.5	4.5
SR550 (%[a])	10	10	10	1	3	5	15
Properties							
t_s2 (min:sec)	3:08	3:15	3:07	3:02	3:00	2:55	2:51
t_c90 (min:sec)	3:32	3:46	3:43	3:39	3:35	3:29	3:31
CRI[b] (sec^{-1})	4.17	3.23	2.78	2.70	2.86	2.94	2.50
Toque (dN/m)							
ML	2.80	3.15	3.61	3.48	4.00	4.09	4.15
MH	11.30	12.75	15.36	15.68	15.92	16.01	17.31
Hardness (Shore A)	40	46	53	53	55	56	55

[a] Percentage by weight of silica.   [b] Cure rate index.

Table C11 The effect of couple treating agent between SR550 and SMA 7052P on the properties of vulcanized NR/silica nanocomposites

Ingredients (phr)	Sample name of vulcanized NR/silica nanocomposites					
	V30-SC1	V30-MP1P	V30-MP3P	V30-MP5P	V30-MP10P	V30-MP15P
NR/silica nanocomposite	NC31-SC1	NC31-MP1P	NC32-MP3P	NC33-MP5P	NC31-MP10P	NC32-MP15P
Silica content	30	30	30	30	30	30
SR550 (phr)	-	0.3	0.9	1.5	3.0	4.5
SR550 (%[a])	-	1	3	5	10	15
SMA 7052P (phr)	0.30	0.30	0.30	0.30	0.30	0.30
SMA 7052P (%[a])	1	1	1	1	1	1
Properties						
t_s2 (min:sec)	2:27	2:46	2:42	2:42	2:50	2:42
t_c90 (min:sec)	2:57	3:18	3:15	3:16	3:23	3:16
CRI[b] (sec^{-1})	3.33	3.15	3.03	2.94	3.03	2.94
Toque (dN/m)						
ML	4.29	4.04	4.50	4.12	3.84	4.00
MH	17.03	15.75	16.68	16.00	15.78	16.09
Hardness (Shore A)	55	53	56	56	54	58

[a] Percentage by weight of silica. [b] Cure rate index.

Table C12 The effect of SR550 and PEG 4000 ratio on the properties of vulcanized NR/silica nanocomposites

Ingredients (phr)	Si-69 and PEG 4000 ratio				
	0 : 100	10 : 90	30 : 70	50 : 50	100 : 0
NR/silica nanocomposite	NC34-NS0	NC34-MP1	NC31-MP3	NC33-MP5	NC30-MP10
Silica content	30	30	30	30	30
SR550 (phr)	-	0.3	0.9	1.5	3.0
SR550 (%[a])	**0**	**1**	**3**	**5**	**10**
PEG 4000 (phr)	3.0	2.7	2.1	1.5	-
PEG 4000 (%[a])	**10**	**9**	**7**	**5**	**0**
Properties					
t_s2 (min:sec)	1:59	2:43	2:54	3:02	2:21
t_c90 (min:sec)	2:27	3:20	3:30	3:39	3:03
CRI^b (sec^{-1})	3.57	2.70	2.78	2.70	2.38
Toque (dN/m)					
ML	3.87	3.60	3.32	3.75	3.89
MH	17.63	15.38	14.13	13.92	13.43
Hardness (Shore A)	57	55	56	54	51

[a] Percentage by weight of silica.　　　　　　　　　　[b] Cure rate index.

Table C13 The effect of PEG and PPG derivatives treated nanosilica on the properties of vulcanized NR/silica nanocomposites with variable treating agent types

Ingredients (phr)	Sample name of vulcanized NR/silica nanocomposites				
	V30-NS0	**V30-MP10**	**V30-EE10**	**V30-PE10**	**V30-PP10**
NR/silica nanocomposite	NC34-NS0	NC30-MP10	NC34-EE10	NC31-PE10	NC33-PP10
Silica content	30	30	30	30	30
PEG and PPG derivatives (phr)	-	3	3	3	3
PEG and PPG derivatives (%[a])	-	10	10	10	10
Properties					
t_s2 (min:sec)	1:59	3:07	2:50	2:46	2:44
t_c90 (min:sec)	2:27	3:43	3:28	3:21	3:22
CRI^b (sec^{-1})	3.57	2.78	2.63	2.88	2.63
Toque (dN/m)					
ML	3.87	3.61	4.29	5.22	6.01
MH	17.63	15.36	16.73	17.23	19.31
Hardness (Shore A)	57	53	56	55	56

[a] Percentage by weight of silica.　　　　　　　　　　[b] Cure rate index.

Table C14 The effect of couple treating agent between PEG/PPG derivatives and SMA 7052P on the properties of vulcanized NR/silica nanocomposites

Ingredients (phr)	Sample name of vulcanized NR/silica nanocomposites				
	V30-SC1	**V30-MP10P**	**V30-EE10P**	**V30-PE10P**	**V30-PP10P**
NR/silica nanocomposite	NC31-SC1	NC31-MP10P	NC30-EE10P	NC30-PE10P	NC30-PP10P
Silica content	30	30	30	30	30
PEG and PPG derivatives (phr)	-	3	3	3	3
PEG and PPG derivatives (%[a])	-	10	10	10	10
SMA 7052P (phr)	0.30	0.30	0.30	0.30	0.30
SMA 7052P (%[a])	1	1	1	1	1
Properties					
t_s2 (sec)	2:27	2:50	2:56	2:34	2:31
t_c90 (sec)	2:57	3:23	3:13	3:07	3:05
CRI[b] (sec^{-1})	3.33	3.03	5.88	3.03	2.94
Toque (dN/m)					
ML	4.29	3.84	3.93	5.07	5.06
MH	17.03	15.78	16.03	17.62	18.53
Hardness (Shore A)	55	54	52	55	55

[a] Percentage by weight of silica.   [b] Cure rate index.

VITA

Mr. Adisak Chaitanee was born on October 7, 1980 in Mahasarakham, Thailand. He graduated with Bachelor Degree of Science in Chemistry from Mahidol University in 2003 and Master Degree of Petrochemistry and Polymer Science from Chulalongkorn University in 2006. Since then, he has been a graduate student studying Doctor of Philosophy in Chemistry at Chulalongkorn University. He was supported by research grant for this thesis from the Royal Golden Jubilee Ph.d. Program, the Thailand Research Fund (TRF) and the Graduate School, Chulalongkorn University. He presented his research in a poster presentation topic, "Styrene maleic anhydride copolymer (SMA) treated silica nanoparticles: Its effect on NR/silica nanocomposites", at the 238th American Chemical Society National Meeting & Exposition at Washington DC, USA on August 16-20, 2009.

His present address is 111 Moo 26, Nongseang, Wapipathum, Mahasarakham, 44120, Thailand.